Didar Yeskermessov (diko090@gmail.com)
IGI Global Platform
Downloaded: 10/3/2023 3:42:03 AM
IP Address: 91.185.25.163

Chapter 2
Study of the Influence of Electrolytic-Plasma Treatment on the Tribological Properties of High-Speed Steel:
High Temperature Testing of Nitrided Layers High-Speed Steel

Zarina Aringozhina
https://orcid.org/0009-0001-8428-4033
D. Serikbayev East Kazakhstan Technical University, Kazakhstan

Yerkezhan Tabiyeva
https://orcid.org/0000-0002-9726-7187
D. Serikbayev East Kazakhstan Technical University, Kazakhstan

Bauyrzhan Rakhadilov
PlasmaScience LLP, Kazakhstan

Waqar Ahmed
University of Lincoln, UK

Didar Yeskermessov
https://orcid.org/0000-0002-2206-8132
D. Serikbayev East Kazakhstan Technical University, Kazakhstan

ABSTRACT

This chapter is devoted to experimental studies of changes in structural-phase blocks and tribological properties of combustion of layers of high-speed steels R6M5, R9, and R18 during electrolytic-plasma nitriding. Systematized experimental data on the effect of electrolytic-plasma nitriding on the structure, phase composition, and tribological properties of the surface layer of high-speed steels have been obtained. In addition, the patterns of formation of modified layers in high-speed steels during electrolytic-plasma nitriding, revealed in this work, can be used by researchers when choosing the modes of electrolytic-plasma treatment of alloyed steels, as well as when analyzing structural transformations of high-speed steels.

DOI: 10.4018/978-1-6684-6830-2.ch002

Copyright © 2023, IGI Global. Copying or distributing in print or electronic forms without written permission of IGI Global is prohibited.

Didar Yeskermessov (diko090@gmail.com)
IGI Global Platform
Downloaded: 10/3/2023 3:42:03 AM
IP Address: 91.185.25.163

INTRODUCTION

The development of engineering technologies largely depends on the technical level of tool production. Thus, one of the problems of environmental protection in mechanical engineering is the high wear resistance of metalworking tools under various conditions of the loading process when machining parts by cutting. The durability of the tool depends not only on the properties of the material, implemented by the technology of formation and volumetric hardening, but also in the manifestation of the degree of surface properties. Its role in ensuring the performance properties of products is constantly increasing, which, along with the widespread use of traditional methods of chemical-thermal treatment, has contributed to the emergence and development of a new direction-surface engineering by methods of energy and physical-chemical effects. The implementation of this concept when choosing a material will improve the performance properties of the tool, and in some cases reduce the consumption of expensive materials. So, recently, due to the use of protective coatings and surface hardening, high-speed steels are increasingly being used and produced, which has made it possible to reduce the cost of expensive hard alloys. At the same time, an important role in the application of protective coatings and surface hardening is played by the use of resource-saving technologies that help reduce resource and energy costs and increase labor productivity.

The most promising method of surface hardening is the method of chemical-thermal treatment in an electrolyte plasma, which makes it possible to intensify the saturation process. Reducing the duration of the saturation process is one of the important directions for the further development of this process. As is known, nitriding is the most common process of chemical-thermal treatment, which makes it possible to increase the tool life of high-speed steels. At present, a large number of technological processes of nitriding based on liquid nitriding in cyanide baths, gas nitriding and ion-plasma nitriding have been developed. However, despite the many advantages of these processes, they have significant drawbacks - a long process time, high cost and environmental hazard. Since nitriding consumes a large amount of energy and technological materials, and in many cases ammonia is used as a saturating medium, which is harmful to the environment. Therefore, it is advisable to use the electrolytic-plasma method for nitriding tools made of high-speed steels, which makes it possible to intensify the process of surface saturation, reduce processing time, reduce energy costs, improve the environmental performance of the process and reduce the consumption of the saturating medium.

Recently, quite intensive research has been carried out on the effect of electrolytic-plasma treatment on the structure and properties of steels and alloys, work is underway to develop and implement an electrolytic-plasma heating process for surface treatment, in particular, surface chemical-thermal treatment of various products. At the same time, research in this direction is limited to surface carburizing, nitrocarburizing, boriding, sulfiding, and nitriding of low-carbon and low-alloyed structural steels, carbon tool steels, and stainless steels. Literature analysis showed that there is no information about the chemical-thermal treatment of high-speed steels in an electrolyte plasma. This may be due to the laboriousness of electrolytic plasma treatment at relatively low temperatures, which does not allow the use of this method as a finishing treatment, which is an important condition for some alloyed steels, in particular, for high-speed steels. In addition, there is very little information about the structural-phase states and tribological characteristics of steels nitrided in electrolytic plasma, as well as about the physical processes that determine the formation of the composition, structure, and properties of the nitrided layer during electrolytic-plasma nitriding. Moreover, the experimental data are not sufficiently systematized in the literature and are often very contradictory. It should also be noted the insufficient level of

Didar Yeskermessov (diko090@gmail.com)
IGI Global Platform
Downloaded: 10/3/2023 3:42:03 AM
IP Address: 91.185.25.163

development of the metallurgical approach to the tribological properties of nitrided steels, structural criteria responsible for the tribological characteristics of nitrided steels, which hinders the possibility of a reasonable choice of processing technology and the full implementation of the existing hidden reserves of this effective method of chemical-thermal treatment.

1. ANALYSIS OF THE CURRENT STATE OF THE PROBLEM

This section presents a literature analysis of the main methods for modifying the surface layers of high-speed steels based on chemical-thermal treatment, which have been implemented over the past 10–20 years, as well as recent data on the formation of structural-phase states and properties of modified layers of structural and tool steels in as a result of electrolytic-plasma nitriding. Attention was paid to the features of hardening and changes in the structural-phase states of high-speed steels during nitriding.

1.1 Modification of Surface Layers of High-Speed Steels by Chemical-Thermal Treatment Methods

At present, high-speed steels, which combine high strength, hardness, wear resistance and sufficiently high ductility, are a universal material for the manufacture of metal-cutting tools. High-speed steel and the method of its hardening have been known for more than 100 years, and it should be noted that during this time no material has been found that can replace it. Such tool materials as hard alloys, superhard materials and ceramic-metal composites have limited applications and cannot compete with high-speed steels in the mass production of tools for metal processing. The production of cutting tools from high-speed steels goes through a large number of technological operations. At the same time, one of the most important is various types of heat treatments. This includes pre-heat treatment and final heat treatment. Preliminary heat treatment involves reducing the hardness of workpieces, improving their machinability and preparation for subsequent heat treatment. The final heat treatment in the classic version, depending on the type of steel used, includes stepped heating for hardening to reduce internal stresses and prevent deformations. After the final heating, the tool is subjected to hardening and tempering according to individual modes, taking into account a specific type of steel (Kremnev, 1985). Over the past 20 years, special attention has been paid to the development and research of methods for additional surface treatment, which are the final stage in the technological chain for the manufacture of high-speed tools and are designed to additionally increase hardness, create useful compressive stresses, increase tensile strength, reduce frictional interaction between the processed and tool materials. during the cutting process. All methods of hardening surface treatment of high-speed tools can be divided into two large groups, which are fundamentally different from each other. The first group of methods is aimed at modifying the surface properties of a high-speed tool. The second group of methods involves applying additional coatings with improved physical and mechanical properties to the surface of the tool. The first group of methods is more promising.

Methods of surface modification of a high-speed tool can be conditionally divided into 3 groups (Grigoriev et al., 2011): mechanical, physical, and chemical-thermal. Each of these methods has its advantages and disadvantages, however, for economic reasons and due to technological simplicity and efficiency, chemical-thermal methods for modifying the surface of tools made of high-speed steels have found the widest application. Cutting tools, first of all, must be wear-resistant, hard, durable, have high

Didar Yeskermessov (diko090@gmail.com)
IGI Global Platform
Downloaded: 10/3/2023 3:42:03 AM
IP Address: 91.185.25.163

heat resistance and corrosion resistance. The most acceptable and providing these requirements are the processes of nitriding, carbonitriding (cyanidation), boriding and sulfiding. Diffusion saturation of the metal surface with boron compounds in the form of iron borides Fe_2B and FeB is used to increase the wear resistance and heat resistance of products, including those operating at elevated or low temperatures, alternating and shock loads, or in aggressive and abrasive media. Boriding is mainly used to harden metal surfaces that work on abrasion: cutting tools made of high-speed steels, stamping tools, molds, crushing machine parts, screen troughs, coke pusher shoes and parts operating at 500-850 ° C. Boriding is carried out in a mixture of boron-containing powders, pastes, gases or in molten salts. As a result of boriding, a change in the dimensions of the part is possible. Therefore, in the manufacture of precise and high-precision parts, it is advisable to process them in the following sequence: preliminary machining (peeling); improvement (hardening and low tempering according to modes corresponding to steel grades); machining with a finishing allowance, boriding, heat treatment to ensure the required set of properties of the base metal; final fine-tuning of the dimensions of hardened parts by mechanical processing methods (grinding, polishing). As a result of boriding, the durability of a die tool made of carbon steels reaches up to 10 times, of alloyed tool steels - 3-4 times (Guriev et al., 2009; Guryev et al., 2001; Guryev et al., 2007). General disadvantages of the surface boriding process: chipping at operating temperatures above 800°C, punching and chipping of high-hardness boride layers based on a softer base, difficulty in restoring a worn surface due to the high hardness of boride layer residues. Sulfiding is applied to technological equipment and tools made of high-speed steels of all grades and steels of the 105WCr6 and 90CrSi types in order to improve the anti-friction properties of surfaces. As the analysis showed, the sulfiding of cutting tools gives conflicting results: in some cases (Zubtsov & Korsakov, 1971), an increase in wear resistance by 1.5–2 times is achieved, in others (Loladze, 1982) it is not detected. Therefore, in the factory, to increase the durability of cutting tools, sulfiding has so far found very little use. Most often, in the practice of tool production, to harden tools made of high-speed steels, methods are used to jointly saturate their surface layers with nitrogen and carbon (cyanidation, carbonitration, nitrocarburizing).

Cyaniding is a process of surface saturation of steel with nitrogen and carbon from melts of cyanide salts. Cyanides and cyanates of alkali and alkaline earth metals, their mixtures, urea, cyanamides, and other compounds are used as components of saturating media (Chatterjee-Fisher, & Supova,, 1990; Lakhtin, et al., 1973). Cyanidation of high-speed steels is constantly being improved, mainly in the direction of intensifying the process, for which baths with accelerating additives to cyanide salts are offered, molten salts are blown with ammonia (Novikov, 1986), bath compositions with urea have been developed (Minkevich, & Suchevyanu,, 1968), carbonitration of steels at elevated temperatures has been developed - so called "tenifer process". This process also has some disadvantages. Maintaining the activity of saturating media during cyanidation requires periodic introduction of highly toxic compounds (KCN, etc.) into their composition (Neustroyev et al., 1972; Solntseva, 1988). In the case of using non-toxic starting components of the bath, based on carbamide, cyanide compounds are formed in the melt as a result of chemical reactions, the amount of which is about 20% of the total volume of the melt (Lakhtin, & Kogan, 1982). In addition, as a result of the interaction of the melt with the tool material and the crucible, their dissolution is observed. This shortcoming forces the use of crucibles made of special alloys, which leads to an increase in the cost of technology. Currently, cyanidation is gradually being phased out of production, as it is considered unpromising due to the extremely high toxicity of cyanide salts and their decay products and the ensuing environmental problems.

Didar Yeskermessov (diko090@gmail.com)
IGI Global Platform
Downloaded: 10/3/2023 3:42:03 AM
IP Address: 91.185.25.163

Along with cyanidation in tool production, the saturation of high-speed steels in gaseous media is widely used – low-temperature nitrocarburizing. Low-temperature nitrocarburizing is more convenient in mass production, and its results are close in hardening effect to those obtained in cyanide baths. Tool processing during gas nitrocarburizing is carried out in an atmosphere consisting of a mixture of ammonia with carbon-containing gases such as methane, pyrolysis products of liquid hydrocarbons (synthine, kerosene, etc.). The process is carried out at a temperature of 570-580°C for 2-5 hours in sealed shaft chamber or continuous furnaces. Intense forced circulation of the gas atmosphere is used to uniformly saturate all surfaces of the instruments. As a result of nitrocarburizing, carbonitride zones 7–25 mm thick are formed on the surface of cutting tools (Chatterjee-Fisher, & Supova,, 1990). Nitrocarburizing is very effective for hardening cutting tools made of high speed steels. It is shown that nitrocarburizing of steels R9, R18, R9K5, R6M5, etc. at temperatures of 550-580°C for 1-1.5 hours, allows you to increase their wear resistance by 1.5-3 times.

There are quite a few examples of the positive experience of using nitrocarburizing to improve the physical and mechanical properties of tool steels in the literature, but it is necessary to mention the disadvantages of this process. Firstly, nitrocarburizing treatment noticeably embrittles tool steels, which are already not very tough. The mechanism of such embrittlement has not yet been sufficiently studied, although it is believed that the reason for the reduced impact strength of nitrocarburized steels is the presence of hard and brittle carbonitride crusts on their surfaces (Przhenosil, 1969). There is another explanation for this phenomenon associated with the presence of hydrogen in diffusion layers (Astaf'yev, 1997). The second disadvantage is associated with environmental problems, since during nitrocarburizing, the exhaust gas atmosphere contains such harmful substances as ammonia, carbon monoxide, carbonic and hydrocyanic (hydrogen cyanide) acids. In order to protect the environment during carbonitriding, intensive ventilation (extraction of gases) and neutralization or disposal of harmful substances before they are released into the atmosphere are necessary. Solving environmental problems associated with nitrocarburizing significantly (several times) increases the cost of its implementation. Nitriding of high-speed tools, i.e. saturation of its surface with pure nitrogen can have a significant effect of increasing tool life without changing the structure of the tool core. The low temperature of the process allows nitriding the finished tool, which has undergone preliminary mechanical and thermal processing. The nitrided steel surface has a reduced coefficient of friction and improved anti-friction properties, which ensures easy chip removal, reduces tool heating and reduces tool wear. All this makes it possible to increase the feed and cutting speed, and, consequently, the speed of metalworking. As reported in (Rakhshtadt et al., 2005), as a result of nitriding, the durability of cutters, drills, and other tools increases from 2 to 8 times. In its traditional form, nitriding is rarely used to increase the tool life of high-speed and other tool steels. This is due to the fact that when nitriding by traditional methods such as gas nitriding, the reactions of nitrogen with iron and alloying elements present in steel occur at a low temperature quite slowly, therefore, in order to obtain a sufficient depth of a nitrided layer on the surface of the part, a long exposure of about 15 -20 hours or more. The need for long exposure during nitriding is the main disadvantage of this process. In order to intensify the process of saturation of the treated surface, in recent years, high-temperature ion nitriding has been increasingly used to improve the performance properties of tool steels, especially for cutting (R6M5, R18, R9, etc.) and stamping (Kh 2, Kh12F1, Kh6VF, etc.) tool (Arzamasov, et al., 1999). The process of high-temperature nitriding is carried out in a nitrogen-containing environment, in the temperature range from 600 to 1200°C, i.e. above the eutectoid transformation temperature of Al in the Fe-N system, when the γ-phase is formed in the diffusion layer (Arzamasov, et al., 1999; Lakhtin, & Arzamasov, 1985; Lakhtin, et al., 1991). As

Didar Yeskermessov (diko090@gmail.com)
IGI Global Platform
Downloaded: 10/3/2023 3:42:03 AM
IP Address: 91.185.25.163

a result of high-temperature nitriding, a structure is formed in structural steels and alloys, consisting of dispersed nitride particles distributed in a solid solution. Thus obtained finely dispersed stable nitride particles in steels and alloys provide high performance (Petrova, 2001; Petrova, 2004). The authors of (Budilov, Agzamov, & Ramazanov, 2004; Budilov, Agzamov, & Ramazanov, 2004) proposed to carry out high-temperature nitriding of tool steels with a glow discharge plasma with a hollow cathode at temperatures of 700–720°C, when the diffusion mobility of the elements increases sharply, and the nitriding time is reduced to 1–2 hours, as well as combined treatment, consisting of high-temperature nitriding and subsequent bright quenching under vacuum conditions in one technological cycle. Under such conditions of nitriding, a significant increase in microhardness occurs on the surface of specimens of R6M5 high-speed steel (Ramazanov et al., 2010). In world practice, the most widely used cutting tool nitriding is treatment in glow discharge plasma (ion nitriding) (Budilov et al., 2007). The energy of a glow discharge in a rarefied gas is used to transport nitrogen ions to the surface of the workpiece, which serves as the cathode. In this case, the moving ions provide the cathode with sufficient energy to heat it up to the nitriding temperature. Ionic nitriding provides a high rate of saturation, obtaining diffusion layers of a given composition and minor deformations during processing. Ion nitriding at 560°C for 10–30 hours makes it possible to noticeably increase the tool life of high speed steel tools in s-6–5–2 (R6M5 type) (Lakhtin, 1993). Nitriding in the plasma of a two-stage vacuum arc discharge has become a new stage in the development of ion nitriding of high-speed steels (Sablev et al., 2000). Such a discharge can exist in various gaseous media, i.e. it is possible to carry out nitriding in various saturating gases and their mixtures. The nitriding temperature is controlled by the value of the potential on the tool or the value of the arc discharge current. The main advantage is that the rate of nitriding at the initial stage is 3 times higher than in glow discharge nitriding.

Thus, it can be established that nitriding is the most effective method of chemical-thermal treatment, which provides a high range of operational properties of machined cutting tools made of high-speed steels: hardness, wear resistance, extreme pressure properties, heat resistance, corrosion resistance, fatigue strength. Recently, various methods and methods of plasma nitriding have been increasingly developed and used, which allow not only to get rid of the shortcomings of traditional nitriding methods. Plasma nitriding methods ensure the formation of a nitrided layer with a given structure on the surface of workpieces. This increases the wear resistance of the tool and its heat resistance. The nitrided surface of the tool, which has a reduced coefficient of friction and improved antifriction properties, provides easier chip removal, and also prevents chip sticking to the cutting edges and the formation of wear holes, which makes it possible to increase the feed and cutting speed (Sal'nikova & Rudman, 1987).

1.2 Analysis of Existing Methods of Nitriding High-Speed Steels

Nitriding is widely used to harden various steels and alloys, machine parts and tools operating under various operating conditions. At present, many technological variants of the process have been developed. Nitriding processes are classified according to (Lakhtin, & Arzamasov,, 1985; Prokoshkin, 1984):

- the composition of the medium - nitriding in gases, liquid and solid media (in pastes or powders);
- process temperature t - low-temperature, medium-temperature and high-temperature;
- diffusing element - nitriding, carbonitriding, hydroxynitriding, oxycarbonitriding, sulfonitriding;
- pressure in the reactor - nitriding at high, low and pulsating pressure;

Didar Yeskermessov (diko090@gmail.com)
IGI Global Platform
Downloaded: 10/3/2023 3:42:03 AM
IP Address: 91.185.25.163

- method of energy supply - heating due to convection, radiation, low-temperature plasma, induction electronic and laser heating;
- type of furnace device - nitriding in chamber, shaft, crucible and other furnaces;
- the structure of the resulting layers on iron and steel - nitriding to obtain a composite layer (nitride zone ε - and γ'-phases and a diffusion sublayer consisting of α-phase, excess γ'-phase of special nitrides and carbides (carbonitrides) - zone of internal nitriding ; internal nitriding (only diffusion sublayer - α + γ' + MN(M_2N) phases + carbides (carbonitrides); anticorrosion nitriding (non-porous dense surface nitride ε-phase or oxycarbonitride zone (Fe, M) (N, C, O);
- combinations of technological processes - nitriding + hardening (nitriding, carbonitriding); nitriding + hardening when heated Current high frequency, laser emitter; nitriding + mechanical hardening surface plastic deformation; nitriding + oxidation; carburizing + nitriding.

Liquid nitriding in cyanide baths has the highest productivity of the saturation process, however, it is expensive and environmentally harmful, therefore, at present, they are trying to replace it with gas nitriding. The prospects for the development of gas nitriding are also due to the fact that it is a more economical and more environmentally friendly process than nitriding in salt baths, and also allows you to control the process, i.e. makes it possible to obtain hardened layers with a given thickness and composition (Lakhtin, & Arzamasov, 1985). However, gas nitriding has the following disadvantages:

- long duration of the technological cycle. The main reason for the slow flow of the process is the low efficiency of the use of the saturating medium;
- formation on the surface of hardened tools (parts) of a developed nitride zone, which requires mandatory subsequent grinding, which reduces the strength properties of the surface. The search for ways to eliminate the above disadvantages led to the development of a fundamentally new method - nitriding using an electric discharge in a gas as an intensifier, both glow and arc (ion or ion-plasma nitriding). The use of these processes made it possible to significantly reduce the duration of nitriding, reduce the consumption of electricity and gas, and obtain a high-quality nitrided layer even on parts of complex configuration. The process is easily automated and provides the possibility of nitriding steels without special surface preparation. Nitriding in a glow discharge is realized in a gaseous medium (ammonia or a mixture of nitrogen and hydrogen) of reduced pressure when an electric field between the anode and cathode is applied to the gas gap. In general, the workpiece can be either a cathode (predominantly occurring) or an anode, or alternating this function. Active particles generated by a glow discharge in the working gas form various compounds or solid solutions with the metal components of the surface. Application of the glow discharge nitriding process in practice has revealed the following advantages. Firstly, the consumption of energy, working gas and processing time are reduced by one or two orders of magnitude. However, the process of nitriding in a glow discharge has its own significant drawback. This is due to the use of hydrogen-containing gas media (ammonia or a mixture of nitrogen and hydrogen) in the technology. The presence of hydrogen in a glow discharge stimulates hydrogen embrittlement. For cutting tools, gear wheels, as well as friction pairs operating at significant stresses in the surface layer, not only high hardness values, but also plasticity characteristics are essential. A fragile tool will not work at the slightest dynamic loads, and they are inevitable in real cutting processes. The lack of plastic properties at the root of the tooth leads to breakage of the gears. The chipping off of particles of high hardness from a nitrided surface subjected to significant contact stresses is essen-

Didar Yeskermessov (diko090@gmail.com)
IGI Global Platform
Downloaded: 10/3/2023 3:42:03 AM
IP Address: 91.185.25.163

tially the process of generating an abrasive that destroys the surface of metal parts (Pastukh,, 2006; Pastukh & Zdybel', 2008). In order to eliminate hydrogen embrittlement during nitriding, a new glow discharge nitriding technology has been developed using working gaseous media that do not contain hydrogen. This process is called "hydrogen-free glow-discharge nitriding". Recently, methods of ion-plasma (ion) nitriding have been increasingly developed and used, which make it possible to get rid of the shortcomings of traditional nitriding methods. At present, a number of technological processes of ion-plasma nitriding have been developed, such as hydrogen-free nitriding in a glow discharge and nitriding of a vacuum-arc discharge, etc. However, ion-plasma (ion) nitriding, along with advantages over conventional furnace nitriding, also has some disadvantages, namely: high cost of equipment, difficulty in processing parts of complex geometric shapes, the need for individual connection of each large-sized part with a high-voltage electric generator, and also the fact that the loading of parts into the nitriding container is carried out taking into account mutual shielding. Thus, the literature analysis showed that the existing nitriding processes used to harden cutting tools, despite a lot of advantages, have significant drawbacks - a long process time, high cost, labor intensity and environmental hazard of the process. Since nitriding consumes a large amount of energy and technological materials, and in many cases ammonia is used as a saturating medium, which is harmful to the environment. Therefore, at present, an urgent task is to develop resource-saving methods for nitriding high-speed steels, which make it possible to intensify the process of surface saturation, reduce processing time, reduce energy consumption, improve the environmental performance of the process, and reduce the consumption of saturating gas. One of the promising methods of nitriding, which practically does not have the above disadvantages, is the method of nitriding in electrolyte plasma. However, this method of nitriding is still not well understood. In addition, the literature does not provide information on the nitriding of high-speed steels in electrolytic plasma. In this regard, research and development of resource-saving methods of electrolytic-plasma nitriding for hardening high-speed steels seems to be an urgent and timely task.

1.3 Electrolyte-Plasma Nitriding as a Promising Direction of the Nitriding Process

One of the promising methods of nitriding is nitriding by electrolytic-plasma heating in an electrolyte. This method is based on the features of the flow of an electric current of high density (several amperes per square centimeter) at the metal-electrolyte interface. Over the past 15 years, an environmentally friendly method of electrolytic-plasma processing of metal products has been intensively introduced into production. New ways of implementing this method are being improved and developed. Electrolyte-plasma hardening is one of the methods of high-speed heating, in which the workpiece is a cathode or anode relative to an aqueous electrolyte (Gupta, Tenhundfeld, Daigle, & Ryabkov, 2007). Depending on the heating mode, electrolyte composition, design parameters of the equipment, it is possible to perform hardening, chemical-thermal and thermocyclic processing of materials. Chemical-thermal treatment by electrolytic-plasma heating is carried out by heating and holding in a saturating medium due to a change in the electric potential in the plasma layer created between the electrolyte and the sample surface. The closure of the electrical circuit between the electrodes occurs through the electrolyte (aqueous salt solution). The conversion of electrical energy into thermal energy takes place mainly in the layer adjacent to the product. As a result of heating, this layer passes into a vapor-gas state, and microarcs are

Didar Yeskermessov (diko090@gmail.com)
IGI Global Platform
Downloaded: 10/3/2023 3:42:03 AM
IP Address: 91.185.25.163

excited in it under the influence of an applied voltage. The power density reaches up to $3 \cdot 10^3 W/cm^2$. To increase productivity, the processing is performed by several electrolyte heaters. The technology makes it possible to vary the rate of heating and cooling and the thickness of the hardened layer within a wide range. By controlling the temperature-speed modes of plasma surface heating and cooling, as well as by using various electrolytes, it is possible to change the structural-phase state of the surface, creating an optimal set of microstructures that provide high mechanical properties (Gupta, Tenhundfeld, Daigle, & Ryabkov, 2007; Yerokhin et al., 1999).

The specific features of heating metals in an electrolyte plasma are:

- the possibility of surface and local hardening, while you can freely adjust the degree and depth of hardening;
- the possibility of high-speed heating, reducing the time of heat treatment;
- exclusion of oxidation of the heating surface of the part and improvement of the quality of its surface;
- the possibility of using an aqueous solution in which heating is carried out as a quenching medium;
- the presence of electroerosive phenomena that contribute to an increase in the efficiency of heating metals in an electrolyte plasma;
- the possibility of local hardening of products with such shapes that do not allow for high-frequency hardening.

The heating of metals in an electrolyte plasma during the anode process as a result of a favorable combination of high temperature of the active electrode, the flow of electrical discharges in the vapor-gas shell between the metal and electrolyte electrodes allows a number of processes of local accelerated thermal and chemical-thermal treatment of steel parts to be carried out. These processes include: heat treatment followed by cooling in the same electrolyte (i.e., to carry out the hardening process), nitriding, carburizing, carburizing, tungstening, molybdenation, and other types of complex diffusion saturation (Suminov et al., 2011). Many parts of machines and mechanisms subjected to bulk heat and chemical-thermal treatment require local surface hardening: hardening or chemical-thermal treatment. The traditional technology of local chemical-thermal treatment with heating in furnaces followed by volumetric hardening is characterized not only by the long duration of the diffusion saturation process (tens of hours during nitriding or hours during carburization and nitrocarburizing), but also the need to perform many additional operations (applying protective coatings, intermediate mechanical processing, etc.), which causes an increase in inter-shop transportation, a significant consumption of electricity, additional labor and other unproductive costs (Arzamasov, et al., 1999). One of the most important advantages of thermal and chemical-thermal treatment with heating in an electrolyte plasma during the anode process is the possibility of local treatment without applying protective coatings to the workpiece, which can significantly simplify technological processes and improve the quality of products (Bakovets, Polyakov, & Dolgovesova, 1991). Among the many methods of chemical-thermal treatment for strengthening various steels and alloys, nitriding has been widely used for more than 60 years. The main advantage of nitriding is the ability to control the composition and structure of the diffusion layer by controlling the saturating atmosphere; this makes it possible to strengthen a whole range of machine parts and tools operating in various operating conditions (Petrova & Zyuzin, 2005). In industry, both furnace and ion nitriding (nitriding in a glow discharge) are actively used. These processes, with all their advantages, have a common drawback - a long saturation time (tens of hours), which requires solving the problem of intensifying

Didar Yeskermessov (diko090@gmail.com)
IGI Global Platform
Downloaded: 10/3/2023 3:42:03 AM
IP Address: 91.185.25.163

the technological process (Lakhtin, 1995; Petrova et al., 2003). The approach to solving the problem of intensifying the processes of chemical-thermal treatment (carburizing, nitriding, carbonitriding, etc.) is to activate elementary processes that occur during the formation of a diffusion layer: dissociation and formation of an active element in the gas phase, adsorption of atoms of a diffusing element on a metal surface, diffusion element to metal. One of the promising methods for accelerating nitrogen saturation during nitriding is the use of a glow-spark discharge, which is both a powerful source of energy and a good surface activator. The use of a glow-spark discharge makes it possible to form active nitrogen in the gas phase with an elevated temperature.

Electrolyte-plasma nitriding consists in processing products in a glow-spark discharge (low-temperature plasma) created between the electrolyte and the surface of the product. To create and maintain a low-temperature plasma, an electrolyte is used, which is a source of ions for the nitriding process: an aqueous solution of salts containing nitrogen ions, an aqueous solution of ammonia and other nitrogen-containing media. During the nitriding process, the workpiece is immersed in an open reactor filled with electrolyte. A rectified voltage is applied to the part (cathode) and the solid electrode (anode). Near the surface of the part, a gas-vapor jacket approximately 50–120 μm thick (Suminov et al., 2011) is created, consisting of electrolyte vapors in which water and salts interact to form ions. The gas-vapor shell enveloping the workpiece contains electrolyte ions, and, accordingly, nitrogen ions. It is a low-temperature plasma and is an active saturating atmosphere for nitriding. This saturating medium is dense; the pressure in the reactor corresponds to atmospheric pressure (Slovetskiy, 1991). In low-temperature plasma, microdischarges occur on the surface of the product, and a possibility is created for the flow of a stationary electric current. For efficient plasma combustion, the area of the cathode must be five times smaller than the area of the solid anode (Bakovets, Polyakov, & Dolgovesova, 1991). It was known from the literature analysis that electrolytic-plasma nitriding is possible in both anodic and cathodic processes.

Anode processes have recently been used much more frequently (Belkin & Pasinkovskiy, 1989; Plotnikov et al., 2016). Anode heating differs from cathode heating in the absence of erosion and the impossibility of melting the part. However, anodic thermal or chemical-thermal treatment processes are accompanied by the inevitable formation of an oxide layer. This layer, which significantly affects the processes of dissolution and diffusion saturation, does not allow increasing the hardness and wear resistance of the material at a sufficient level (Belkin & Ganchar, 1988). In addition, during anodic processes, anodic dissolution of the surface takes place, which leads to a change in the size of the processed material. Traditional cathodic processes are characterized by erosion of the surface of the workpiece, temperature control in the range of 400–700°C is difficult, there is a danger of edge melting (Suminov et al., 2011; Yasnorodskiy, 1971), and low reproducibility of results (Slovetskiy et al., 1986) prevents the widespread use of this process even when machining simple-shaped parts. low accuracy. However, the cathodic process favorably differs from the anodic one in the absence of an oxide layer, as well as in the high wear resistance and hardness of the processed products (Duradzhi & Bryantsev, 1979; Lazarenko, et al., 1979). It is assumed that a deeper study and development of a more efficient cathodic heating process allows the widespread application of the cathodic chemical-thermal treatment process. Nitriding in electrolyte plasma accelerates the process so much that it exceeds liquid cyanidation in baths in speed, and at the same efficiency ensures high environmental cleanliness. In this regard, it is advisable to use the method of electrolytic-plasma nitriding to harden the working surface of a tool made of high-speed steels. On the other hand, it should be noted that there is no information in the literature about the electrolytic-plasma nitriding of high-speed steels, so this issue requires a special study. Perhaps this is due to the fact that the known methods of electrolytic-plasma modification do not allow the processing

Didar Yeskermessov (diko090@gmail.com)
IGI Global Platform
Downloaded: 10/3/2023 3:42:03 AM
IP Address: 91.185.25.163

process to be carried out at a relatively low temperature, which does not allow it to be used as a finishing treatment for heat-treated high-speed steels. In connection with the foregoing, one of the main tasks in the application of electrolytic-plasma technology for surface hardening of high-speed steels is to improve the cathodic heating process and develop a highly efficient method of electrolytic-plasma nitriding, which does not have the above disadvantages. An important direction in improving the cathodic process of electrolytic-plasma nitriding is the development of a new environmentally friendly electrolyte and an energy-saving heating method that allows you to control the temperature in the range of 400–700°C and does not lead to edge melting. This must be taken into account when developing resource-saving technologies, the main task of which is to obtain modified layers with desired properties.

2. MATERIALS, EQUIPMENT, AND METHODS OF EXPERIMENTAL STUDIES

2.1 Study Materials

In accordance with the tasks set, R6M5, R9 and R18 tool high-speed steels were chosen as the research material. The use of high-speed steels for cutting tools makes it possible to increase the cutting speed by several times, and tool life by dozens of times (Poznyak, et al., 1977). The main distinguishing feature of high speed steels is their high heat resistance or red hardness (600-700°C) in the presence of high hardness (63-70 HRC) and tool wear resistance. The unique properties of high-speed steels are achieved through special alloying and complex heat treatment, providing a certain phase composition (Gol'dshteyn et al., 1985). Table 1 shows the chemical composition of high speed steels R6M5, R9 and R18.

The choice of research materials is also justified by the fact that high-speed steels R6M5, R9, R18 are the most common in metalworking, typical high-speed steels of moderate heat resistance (Gol'dshteyn et al., 1985). Table 2 shows data on the use of selected research materials. At present, in order to reduce the consumption of expensive and scarce elements, especially tungsten, economically alloyed steels are mainly used. Of these, R6M5 steel has the widest application (Anel'nik et al., 1981), so a more detailed study was carried out on high-speed tool steel R6M5. The main alloying elements of high-speed steels R6M5, R9, R18, providing high red hardness, are tungsten, molybdenum, vanadium. In addition, these steels are alloyed with chromium. An important component is carbon (Gol'dshteyn et al., 1985).

Sample blanks for research in the form of parallelepipeds with dimensions of 10x20x20 mm^3 were cut from cutting tools (disc cutters) from steels R6M5, R9 and R18 of steels R6M5, R12 and R18 with a

Table 1. Chemical composition of high-speed steel R6M5, R9 and R18 (State standard 19265-73)

Steel Grade	C	Mn	Si	Cr	W	V	Co	Mo	Ni	Cu	S	P
R9	0.85 - 0.95	up to 0.50	up to 0.50	3.80 - 4.40	8.50 - 9.50	2.30-2.70	up to 0.50	up to 1.00	up to 0.40	-	up to 0.03	up to 0.03
R6M5	0.82-0.9	0,20 - 0.50	0,20 - 0.50	3.80 - 4.40	5.50 - 6.50	1.70-2.10	up to 0.50	4.80-5.30	up to 0.60	up to 0.25	up to 0.025	up to 0.03
R18	0.73-0.83	0,20 - 0.50	0,20 - 0.50	3.80 - 4.40	17.00 - 18.50	1.00 - 1.40	up to 0.50	up to 1.00	up to 0.60	up to 0.25	up to 0.03	up to 0.03

Didar Yeskermessov (diko090@gmail.com)
IGI Global Platform
Downloaded: 10/3/2023 3:42:03 AM
IP Address: 91.185.25.163

Table 2. Data on the use of selected research materials

Steel Grade	Application
R9	For simple shaped tools that do not require a large amount of grinding operations; it is applied to processing of usual constructional materials; has increased plasticity and can be used for the manufacture of tools by plastic deformation methods; reduced grindability.
R6M5	It can be used for all types of cutting tools, especially those subjected to increased grinding, when processing common structural materials. Has high technology.
R18	Steel for all kinds of cutting tools. Used for tools working with shock loads; increased tendency to decarburization.

diamond disk (thickness 1 mm), which was previously immersed in a coolant. At low cutting speeds n = 350 rpm and low load m = 250 g, the sample does not experience deformation and thermal effects. High service properties of high-speed steel tools are achieved by heat treatment. Therefore, sample blanks for electrolytic plasma treatment were cut from tools made of R6M5, R9, and R18 steels subjected to heat treatment common for these steels (Arshinger, 1982) (Table 3).

A prerequisite for all metallographic examinations is the preparation of sections that can be used for microscopic examination using light and electron microscopes, for determining microhardness, as well as for quantitative measurement of structural components. The correct preparation of thin sections is extremely important, since the correct interpretation of microstructures depends on this. The main point in the manufacture of metallographic sections is to prevent damage to the surface of the section, which consists in changing the microstructure of the surface layer of the material as a result of deformation or heating. Grinding of metallographic samples by mechanical means is carried out on special grinding machines. The grinding machine is one or more metal wheels driven by an electric motor. On metal circles impose or stick twists cut out of sanding paper. Sometimes carborundum wheels are used instead of coarse sanding paper. During mechanical grinding, as well as during manual grinding, grinding skins are changed, successively moving from coarse-grained to fine-grained. During mechanical grinding, samples often heat up; in this case, they are periodically cooled in water. Grinding of metallographic samples was carried out on a LaboPol-5 grinding and polishing machine with a device for automatic grinding and polishing of samples LaboForce-3 manufactured by Struers (Denmark). Electrolytic-plasma nitriding of high-speed steel specimens was carried out on a setup at LLP PlasmaScience.

Table 3. Modes of preliminary heat treatment of high-speed steels

Steel Grade	Types of Heat Treatment	
	Hardening	Vacation
R9	from 1240°C into oil	560°C (three times: duration of each vacation 1 hour, cooling in air)
R6M5	from 1230°C into oil	560°C (three times: duration of each vacation 1 hour, cooling in air)
R18	from 1270°C to oil	560°C (three times: duration of each vacation 1 hour, cooling in air)

Didar Yeskermessov (diko090@gmail.com)
IGI Global Platform
Downloaded: 10/3/2023 3:42:03 AM
IP Address: 91.185.25.163

2.2 Methods for Studying the Nitrided Layer

2.2.1 Metallographic Analysis

Optical metallography was used for the structure of natural materials. Metallographic researches were conducted on optical microscope "ALTAMI-MET-1M". Sections for research were prepared according to the standard technique, including mechanical grinding and mechanical polishing (Skakov & Rakhadilov, 2013). Grinding is carried out on sandpaper (sandpaper) of different grain sizes, successively moving from paper with large abrasive grains to papers of ever smaller grain sizes. Grinding is done manually or on a mechanical machine with rotating discs covered with sandpaper, to which the surface of the sample is gently pressed. When switching from coarse-grained sandpaper to fine-grained sandpaper, the sample is cleaned of emery dust, rotated 90° relative to the original grinding direction, and continue to grind until the scratches (scratches) from the previous processing completely disappear. Polishing was carried out on a grinding disk covered with felt, pre-washed and soaked in water for 1-2 hours. Further, in order to reveal the structure, sections were subjected to etching. A 4% alcohol solution of nitric acid was used for etching. Qualitative and quantitative metallographic analysis was carried out according to the recommendations given in (Baranova & Demina, 1986; Veynberga, 1973; Yelyutina, 1979).

2.2.2 X-Ray Diffraction Phase Analysis

X-ray diffraction studies of steel samples were performed using known methods of X-ray diffraction analysis on X'PertPRO and D8 ADVANCE diffractometers. Diffraction patterns were taken using CuK_{α} radiation (λ=2.2897 Å) at a voltage of 35 kV. In the D8 ADVANCE diffractometer, reflection from a flat pyrographite monochromator was used in front of the detector to isolate a narrow portion of the spectrum (monochromatization), as a result of which Kα radiation with certain wavelengths was selected into the detection unit. The method of X-ray diffraction analysis used in this work made it possible to analyze the following important parameters of the structure of the samples under study: determination of the crystal structure (unit cell type); accurate determination of unit cell parameters; determination of the phase composition of the material under study; determination of fine crystal structure parameters (sizes of coherent scattering regions). The interpretation of the diffraction patterns was carried out manually using standard methods and the PDF-4 database, and the quantitative analysis was performed using the Powder Cell program. Qualitative phase analysis was carried out by the X-ray diffraction method based on the comparison of the relative integrated intensity of diffraction lines and experimental values of interplanar spacings with reference interplanar spacings (Chernyavskiy, 1977; Gorelik, Skakov, and Rastorguyev, 2002; Mirkin, 1961). Quantitative phase analysis is based on the fact that the intensity of the lines of a given phase is proportional, apart from all intensity factors, to the volume fraction of the given phase in the mixture. The sizes of crystallites and microdistortions of the crystal lattice were determined from the broadening of the profiles of the Bragg maxima (Chernyavskiy, 1977).

The fact of detection of one or another phase was recorded if the two most intense lines of this phase were found on the diffraction patterns. X-ray diffraction is a common technique that determine a sample's composition or crystalline structure. For larger crystals such as macromolecules and inorganic compounds, it can be used to determine the structure of atoms within the sample. If the crystal size is too small, it can determine sample composition, crystallinity, and phase purity. This technique sends x-ray beams through it. X-ray beams are chosen because their wavelength is similar to the spacing be-

Didar Yeskermessov (diko090@gmail.com)
IGI Global Platform
Downloaded: 10/3/2023 3:42:03 AM
IP Address: 91.185.25.163

tween atoms in the sample, so the angle of diffraction will be affected by the spacing of the atoms in the molecule, as opposed to using much larger wavelengths, which would be unaltered by the spacing between atoms. The x-rays then pass through the sample, "bouncing" off of the atoms in the structure, and changing the direction of the beam at some different angle, theta, from the original beam. This is the angle of diffraction. Some of these diffracted beams cancel each other out, but if the beams have similar wavelengths, then constructive interference occurs. Constructive interference is when the x-ray beams that are whole number integers of the same wavelength add together to create a new beam with a higher amplitude. The greater amplitude of the wave translates into a greater signal for this specific angle of diffraction. The angle of diffraction can then be used to determine the difference between atomic planes using Bragg's law $\sin\theta = n\lambda/2d$, where lambda is the wavelength added, theta is the angle of diffraction, and d is the distance between atomic planes. The distance between atomic plates can then be used to determine composition or crystalline structure.

An X-ray incident upon a sample will either be transmitted, in which case it will continue along its original direction, or it will be scattered by the electrons of the atoms in the material. All the atoms in the path of the X-ray beam scatter X-rays. We are primarily interested in the peaks formed when scattered X-rays constructively interfere. Constructive interference occurs when two X-ray waves with phases separated by an integer number of wavelengths add to make a new wave with a larger amplitude.When two parallel X-rays from a coherent source scatter from two adjacent planes their path difference must be an integer number of wavelengths for constructive interference to occur.

Path difference = n λ

Therefore:

$2d_{hkl}\sin\theta = n\lambda$

(Popilov & Zaytseva, 1963) or dh_{kl} - interplanar spacing, θ - diffraction beam reflection angle, n- is the diffraction order, λ- *w*avelength added.

2.2.3 Electron Microscopic Research Methods

The morphology and elemental composition of the sample treated in electrolyte plasma was studied using a JSM-6390LV scanning electron microscope (JEOL, Japan) with an INCAEnergy energy dispersive microanalysis attachment from "OXFORD Instruments". The phase composition of the carbide phases and their sizes were studied by electron backscatter diffraction analysis on a system with electron and focused ion beams Quanta 200 3D. The principle of operation of electron backscatter diffraction analysis is as follows: the sample, tilted at an angle of 70°, is placed in the microscope column (system), and the surface under study is subjected to automatic step-by-step scanning "from point to point". The diffracted electrons backscattered from each scan point form a diffraction (Kikuchi) pattern on the fluorescent screen of a digital video camera mounted inside the microscope. These diffraction patterns are digitized and automatically displayed. Before the study, the samples were ground and polished. To identify the boundaries of grains and particles of carbide phases, chemical etching of thin sections in a 4% alcohol solution of nitric acid was used (etching time 5-7 s.). An EM-125 transmission electron microscope was used to study the fine structure of the nitrided layer in order to reveal the morphology,

Didar Yeskermessov (diko090@gmail.com)
IGI Global Platform
Downloaded: 10/3/2023 3:42:03 AM
IP Address: 91.185.25.163

phase composition, and sizes of the second phases. The studies were carried out by diffraction electron microscopy of thin foils at an accelerating voltage of 125 kV. The working magnification in the microscope column was chosen from 10,000 to 80,000 times. To prepare a foil for studying the treated sample surface by the electrospark method, plates ~ 0.2–0.3 mm thick were cut out. The resulting plates were electrolytically drowned in an electrolyte of 90% phosphoric acid (H_3PO_4) and 10% chromic anhydride (CrO_3) at a voltage of 15–20 V and a current density of 3–4 A/cm^2. Subsequent electropolishing was carried out in a solution of 22% perchloric acid ($HClO_4$) + 78% acetic acid ($C_2H_4O_22$). To preserve the surface under study, polishing was performed only on the non-nitrided side. Microdiffraction analysis was used to identify the phases present in the material. The phases were identified according to the procedures described in (Endryus et al., 1971; Kheyker & Zevin, 1963). To do this, we used schemes of microdiffraction patterns calculated from the tabular values of the parameters of the corresponding crystal lattices. For each specific place under study on the sample, a large area of the foil was examined and up to 20–30 micrographs and microdiffraction patterns for them were taken.

2.3 Methods for Conducting Physical and Mechanical Tests

2.3.1 Method for Determining Microhardness

Microhardness, along with fatigue strength and wear resistance, is one of the most widely used mechanical characteristics of metals and alloys (Grigorevich, 1976; Utevskiy, 1973). At the same time, the microhardness test differs from other methods for determining the mechanical properties of materials by its high sensitivity and short testing time. It is carried out without destruction of samples, requires a minimum of costs in their preparation. Measurement of the microhardness of steel samples, carried out on the device PMT-3M in accordance with GOST 9450–76, with a load on the indenter P = 1 N and a holding time at this load of 10 sec. A regular tetrahedral diamond pyramid with an apex angle between opposite faces of 136° was used as an indenter for measuring microhardness, similarly to the determination of Vickers hardness. The number of measurements per sample was at least 20. The microhardness Hμ was determined in accordance with GOST 9450-76 using the formula:

$$H_{\mu} = \frac{P}{S} = \frac{1854P}{d^2}\left(kgf\ /\ mm^2\right) = \frac{18,2\times10^6 P\left(kg\right)}{d^2\left(\mu m\right)}$$

or d – is the arithmetic mean of the pyramid indentation diagonals, (mm); P – is the value of the load acting on the pyramid, N (kgf); S=(s^2/1854) – the area of the lateral surface of the resulting pyramidal imprint.

When testing in accordance with the recommendations of GOST 9450-76, the following rules were observed:

- the distance from the center of the imprint to the edge of the object must be at least twice the size of the imprint;
- the distance between the centers of adjacent prints should exceed the size of the print by more than 3 times;

Didar Yeskermessov (diko090@gmail.com)
IGI Global Platform
Downloaded: 10/3/2023 3:42:03 AM
IP Address: 91.185.25.163

- the minimum thickness of the object or layer must exceed the depth of the imprint by at least 10 times.

2.3.2 Tribological Testing Methods

Tribological tests for sliding friction were carried out on a high-temperature tribometer THT-S-BE-0000 using the standard «ball-disk» technique (Figure 1 a) (international standards ASTM G 133-95 and ASTM G 99). As a counterbody, a ball with a diameter of 6.0 mm was used, from a certified material – Al_2O_3. The tests were carried out at a load of 1 N and a linear velocity of 2 cm/sec, a wear curvature radius of 5 mm, and a friction path of 31.4 m. Tribological tests were carried out at room temperature, as well as at high temperatures at 500, 550, and 600°C. The tribological characteristics of the modified layer were characterized by wear intensity and friction coefficient (Boyarskaya et al., 1986). Tribological tests of samples of high-speed steel were carried out under conditions of dry sliding friction on a tribometer (friction machine) CETR UMT-3 using the "scratch-testing" method at the Institute of Materials Science and Connecting Technologies of the University. Otto-von-Guerike (Magdeburg, Germany). The CETR UMT-3 tribometer is designed to determine the coefficients of friction of flat and cylindrical specimens when varying the level of the contact load, the trajectory of the relative motion of the specimens, the temperature, and the medium. Тестирование соответствует международному стандарту ASTM G 99. The tribometer makes it possible to test specimens for friction in the range of contact loads from 1 to 100 N at a rate of longitudinal displacement of specimens from 0.001 to 1 mm/s at temperatures up to 350°C. Tests of flat samples of high-speed steel were carried out with their translational movement along the X axis at a speed of 0.2 mm / s with a uniform increase in the contact load from 0 to 32 N (Figure 1b). The length of the friction path along the X axis was 8 mm. In order to study the friction coefficient at a constant load, tribological tests were carried out using the "Pin-disk" method on the "Pin-on-DiscTribotester" tribometer (Figure 1c). A pin with a contact size of 100 μm was used as a counterbody, made of a certified material – Al_2O_3. The tests were carried out in air at room temperature with a load of 10 N and a linear speed of 20 mm/sec, a wear curvature radius of 4 mm, a friction path of 60 m. Testing complies with the international standard ASTM G 99-95a and ASTM G 133-95.

Figure 1. Tribological tests according to the "ball-disk" scheme (a), according to the "scratch-testing" method (b), according to the "pin-disk" scheme (c)

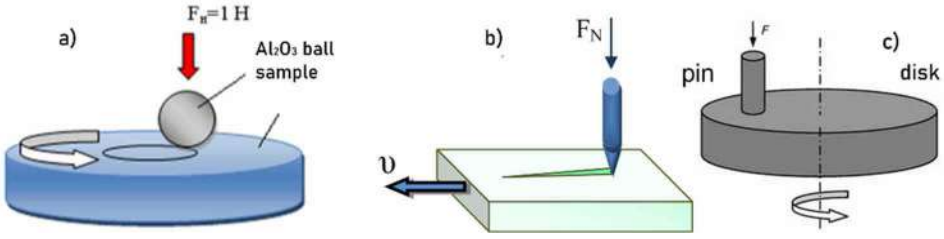

Didar Yeskermessov (diko090@gmail.com)
IGI Global Platform
Downloaded: 10/3/2023 3:42:03 AM
IP Address: 91.185.25.163

2.3.3 Test Method for Abrasion

Tests of samples for abrasive wear were carried out on an experimental setup for testing abrasive wear during friction against non-rigidly fixed abrasive particles according to the "rotating roller - flat surface" scheme in accordance with GOST 23.208-79, which coincides with the American standard ASTM C 6568. For testing abrasion on a rubber wheel, the surfaces of the samples were ground and polished, they were also cleaned with acetone and dried (Fillipov et al., 2009). A cylindrical rubber roller, pressed with a radial surface to a flat surface of the test sample with a force of 22 N, rotated at a frequency of 1 s^{-1}. The appearance and scheme of the device is shown in Figure 2. The rate of entry of abrasive particles between the rubber wheel and the sample, that is, into the test area, was 41-42 g/min. Electrocorundum with a grain size of 200–250 μm was used as abrasive particles. The wear resistance of the tested nitrided sample was evaluated by comparing its wear with the wear of the reference sample (not nitrided sample). Wear was measured by the gravimetric method on an ADV-200 analytical balance with an accuracy of 0.0001 g. The samples were weighed every minute and tested for three minutes, the total wear length was 28.8 m. Before weighing, the samples were burned with compressed air to remove the remaining sand particles on the samples. The wear resistance of the tested material was evaluated by comparing its wear with the wear of the reference sample (steel 45) by the weight loss of the samples during the test according to GOST-23.208-79. The relative wear resistance was calculated by the formula

$$\kappa_{wr} = \frac{g_r \rho_{wr} N_{wr}}{g_{wr} \rho_r N_r}$$

or g_r, g_{wr} – values of mass loss during testing of the reference sample and samples of the test material; ρ_r, ρ_{wr} – density of reference and test material, g/cm^2; N_r, N_{wr} – the number of revolutions of the roller when testing the reference and test materials.

Figure 2. Scheme for testing samples for abrasive wear

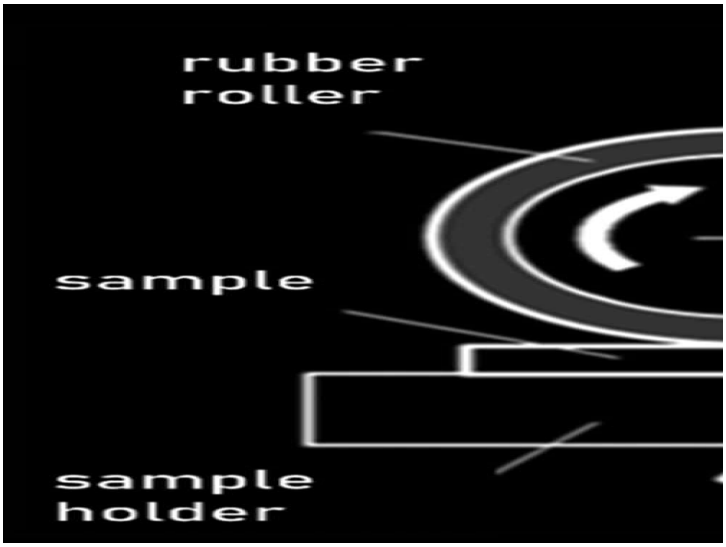

Didar Yeskermessov (diko090@gmail.com)
IGI Global Platform
Downloaded: 10/3/2023 3:42:03 AM
IP Address: 91.185.25.163

3. EFFECT OF ELECTROLYTIC-PLASMA NITRIDING ON THE TRIBOLOGICAL PROPERTIES OF THE SURFACE OF HIGH-SPEED STEELS

Ensuring maximum wear resistance of a metalworking tool under various loading conditions when machining parts by cutting is one of the most important problems of modern mechanical engineering. Since the working surfaces of the cutting tool wear out both from the mechanical impact of the material being processed on it, and as a result of molecular-thermal processes occurring in the cutting zone on the contact surfaces of the tool with the material being processed. In addition, the wear resistance of metallic materials is a structurally sensitive characteristic. For the technological support of the process of forming a wear-resistant structure during nitriding, a necessary condition is the knowledge of the laws that describe the relationship between the microstructure of the surface layer and the tribotechnical characteristics of the interface. Therefore, a relevant and promising direction in the development and improvement of the technology of electrolytic-plasma nitriding is the tribological approach to assessing the quality of the nitrided layer and developing structural criteria for the wear resistance of surface layers to improve the performance of nitrided high-speed steels under friction and wear conditions (Khrushchov & Babichev, 1970; Poznyak, 1996).

3.1 Influence of Electrolyte-Plasma Nitriding Modes on Tribological Characteristics and Microhardness of High-Speed Steels

The treatment process was carried out in an electrolyte from an aqueous solution containing 20% carbamide, 10% sodium carbonate in the following mode: the temperature of the nitriding of the samples is 450-550°C, the applied voltage between the anode and the sample when heated to the nitriding temperature of -320 V, 450-550°C-180-200 V, nitriding time varied from 3 to 12 minutes. As you know, the wear resistance of high-speed steel is one of its most important characteristics, since it determines the tool life and associated features of metalworking technology. Increased tool life reduces the time required to reinstall and regrind the tool, thereby increasing productivity and reducing the consumption of expensive cutting tools, which is most beneficial for the economy. It should be noted that wear resistance is a very complex property. It depends not only on the structure and properties of tool steel, but also on the properties of the material being processed, as well as on the coefficient of friction and the external conditions under which wear occurs: temperature in the friction zone and mechanical influences. When changing some of these conditions, the wear resistance of tool steel changes in turn (Baranchikov et al., 1990).

In this work, the tribological characteristics of high-speed steels before and after nitriding in an electrolyte plasma are studied. Figure 3 shows the wear rate (mm^3/Hm) of samples of R6M5 high-speed steel after testing according to the "ball-disk" scheme. It can be seen from the figure that the wear intensity of nitrided samples varies significantly depending on the nitriding time. All nitrided samples show a significant reduction in wear rate compared to the original state. It was determined that the wear intensity of samples nitrided for 7 min is 5 orders of magnitude less than that of the original. Figure 4 shows changes in the wear intensity of samples of high-speed steels R6M5, R9 and R18 depending on the nitriding temperature at a constant process duration of 7 minutes. All nitrided samples show a significant decrease in wear intensity compared to the original. It is known that wear resistance is affected not only by microstructure and hardness, but also by surface roughness, which depends on the nitriding temperature.Thus, we can conclude that the wear intensity of high-speed steels depends on the nitriding

Didar Yeskermessov (diko090@gmail.com)
IGI Global Platform
Downloaded: 10/3/2023 3:42:03 AM
IP Address: 91.185.25.163

Figure 3. Wear intensity of samples of high-speed steels before and after nitriding at a temperature of 550° C

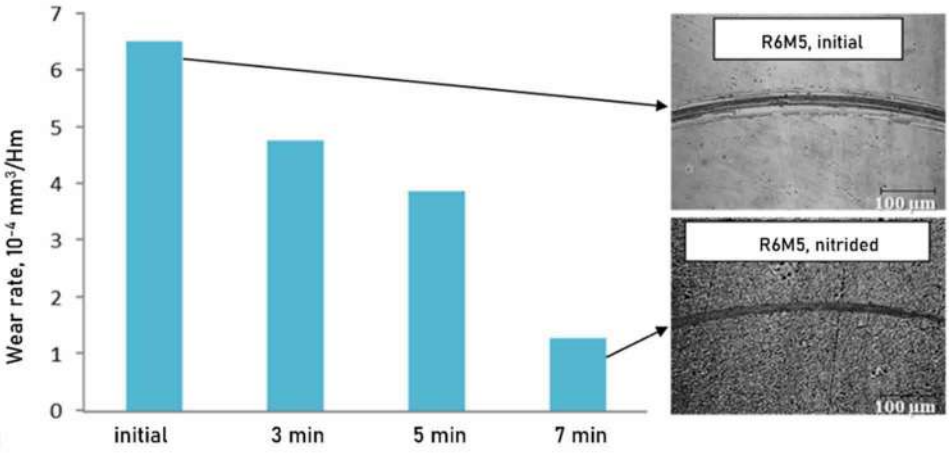

Figure 4. Dependence of wear intensity of high-speed steel specimens on nitriding temperature

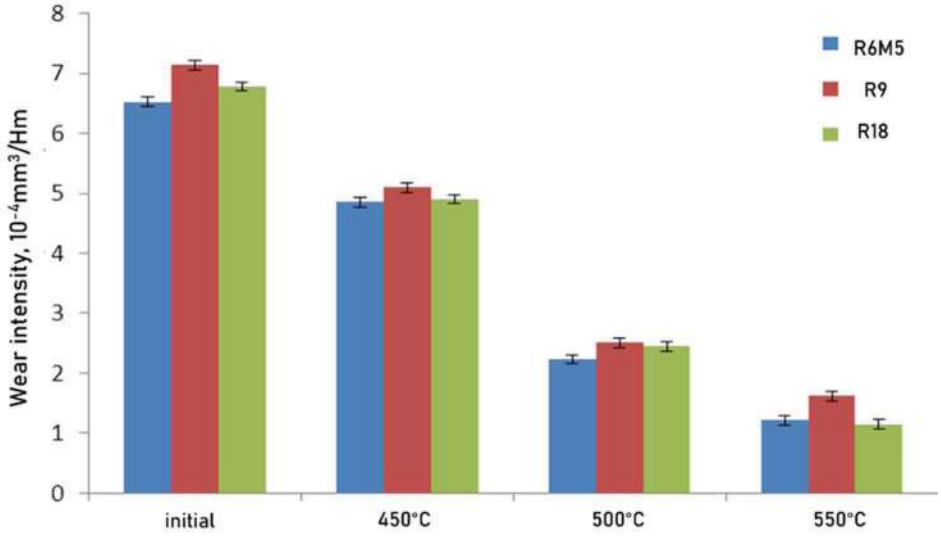

temperature. At a nitriding temperature of 550°C, the wear intensity of nitrided specimens of R9, R6M5, and R18 high-speed steels decreases by 77%, 81%, and 83%, respectively, which indicates a significant increase in the wear resistance of high-speed steels after surface nitriding (Geller, 1983; Rakhadilov and Skakov, 2012; Skakov et al., 2014). This may be due to with the formation of finely dispersed nitrides. Since, it is known (Badisch & Mitterer, 2003; Rakhadilov & Skakov, 2014; Ustinovshchikov, 1988) that dispersed precipitates, such as finely dispersed nitrides of alloying elements, protect the grain volume of a relatively soft matrix from abrasion.

Didar Yeskermessov (diko090@gmail.com)
IGI Global Platform
Downloaded: 10/3/2023 3:42:03 AM
IP Address: 91.185.25.163

As is known, in practice, the acting loads leading to wear are in most cases very complex and diverse, it is impossible to give a universal recipe for choosing steel, for the most optimal state of the structure and nitriding parameters. In this regard, in the work the tribological characteristics of samples of high-speed steels are also a certain method of scratch testing (method of controlled scratching), which is one of the modern methods of testing materials for wear resistance. The method is based on controlled scratching with a diamond indenter on a selected area of the sample (product).

Friction tests of R6M5 steel samples were carried out according to the procedure described in Section 3, with the translational movement of the sample along the X axis at a speed of 0.2 mm/s and a stroke length of 8 mm. In this case, the indenter tip moved over the sample surface with increasing load. Typical graphs of the friction coefficient, wear depth and contact load versus time (friction) of the translational motion of R6M5 steel specimens in the initial state and after nitriding are shown in Figure 5. It can be seen from the figure that the maximum depth of the scar on the surface of the R6M5 steel sample formed during friction is 9.4 μm before nitriding, and 4.4 μm after nitriding, which shows a significant increase in the hardness and wear resistance of the steel surface after nitriding. The graph shown in Figure 5 shows a decrease in the coefficient of friction after nitriding. The decrease in the friction coefficient is possibly associated with an increase in wear resistance (Chaus, 2008). Since, an increase in the wear resistance of the surface layer of steel during nitriding is manifested in a decrease in the coefficient of friction.

Thus, tests carried out by the scratch testing method showed that after nitriding, the friction coefficient decreases. However, this test method does not accurately determine the coefficient of friction, as by constantly increasing the load, the coefficient of friction is greater. In this regard, to study the coefficient of friction of nitrided samples, tests were carried out according to the "pin-disk" scheme on a tribometer TRIBO tester. Figure 6 shows the change in the coefficient of friction of the samples over time before and after nitriding at different temperatures. The figure shows that the coefficient of

Figure 5. Graphs of friction coefficient f, scar depth h and load P versus friction time τ:
a – before, b – after nitriding of R6M5 steel

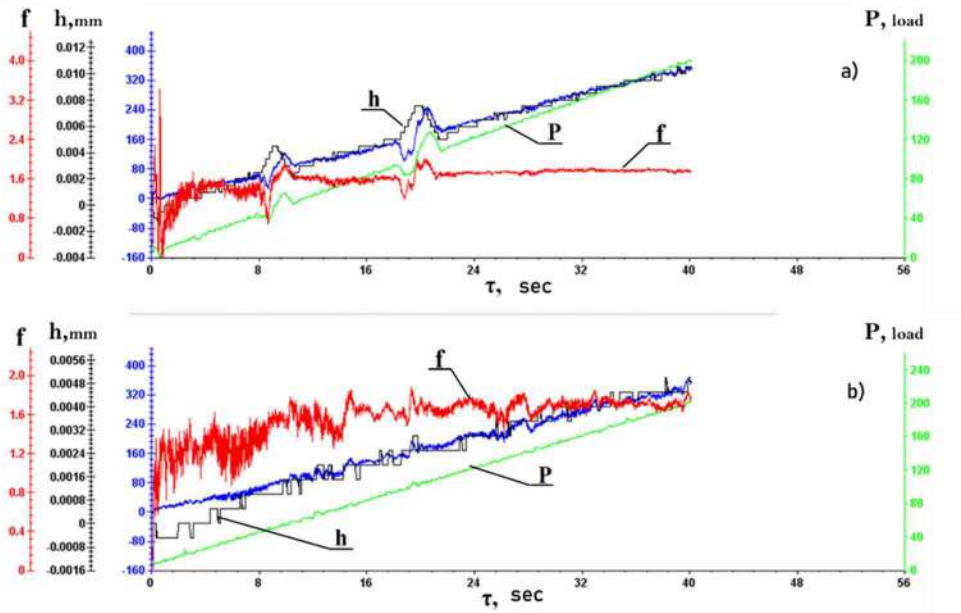

Didar Yeskermessov (diko090@gmail.com)
IGI Global Platform
Downloaded: 10/3/2023 3:42:03 AM
IP Address: 91.185.25.163

friction after nitriding decreases depending on the nitriding temperature. The friction coefficient of the original sample was 6.8±0.4. After electrolytic-plasma nitriding at 450 and 500°C, the friction coefficient decreases to 5.5±0.5 and 5.3±0.2, respectively. And after electrolytic-plasma nitriding at 550°C, there is a significant decrease in the coefficient of friction of the surface of the steel sample to 4.1 ± 0.2.

The decrease in the friction coefficient is explained by an increase in the wear resistance of the sample surface with the formation of particles of iron nitrides and alloying elements.As is known (Braun, Bushe, & Buyanovsky, 2001), with a decrease in the coefficient of friction during sliding (in the form of friction, which is most typical for the operation of most tools), their durability increases due to the less intense heat release during cutting and deformation, a decrease in the intensity of adhesion and sticking of the material being processed, especially soft, on the work surface. In addition, it is known (Belyy et al., 1991) that an increase in the amount and hardness of carbides and nitrides is accompanied by a more significant decrease in the friction coefficient. It is known (Belyy et al., 1991) that an important criterion for the wear resistance of nitrided steels is the high hardness of the surface layer. It is believed that with a higher hardness of the layer, its wear resistance increases. This principle underlies the choice of the chemical composition of steels and nitriding regimes.

At the same time, the analysis of works (Belyy et al., 1991; Braun, Bushe, & Buyanovsky, 2001; Chaus, 2008) devoted to the issues of friction and wear of various materials shows that it is not always necessary to strive for obtaining high hardness to ensure maximum wear resistance, since the structure of the material corresponding to maximum hardness and maximum wear resistance may be different. Considering that one of the most important properties of the nitrided layer, which largely affects wear resistance, is hardness, in this section, changes in the microhardness of the surface layer of high-speed steels during electrolytic-plasma nitriding are studied. Figure 7 shows the dependence of the microhardness of the surface layer of R6M5 steel on the nitriding temperature. Measurements of the microhardness of alloy samples were carried out on the PMT-3M device in accordance with GOST 9450-76, with loads on the indenter P = 1H (100g) and the holding time at this load of 10 seconds. One can see a significant increase in the microhardness of the surface of the steel samples after nitriding. In this case, the microhardness increases depending on the nitriding temperature. This is apparently due to the structural-phase state of the modified surface layer.

Figure 8 shows the distribution of microhardness over the depth of the nitrided layer of high-speed steels R6M5, R9 and R18 after nitriding at 550°C for 7 minutes. One can see a significant increase in microhardness near the surface of the treated steel samples. The nature of the transition zone has a smooth transition from the hardened layer to the base, while the microhardness of the base does not change significantly. After nitriding, the microhardness of the surface of steels R6M5, R9 and R18 increases up to 1.6 times.

According to the nature of the distribution of microhardness, it was revealed that electrolytic-plasma nitriding has an important advantage over the conventional gas nitriding process. Thus, during saturation in an electrolyte plasma, there is no sharp decrease in hardness, which is characteristic of ordinary saturation in ammonia. Since, during nitriding in ammonia, a sharp decrease in hardness is observed upon transition from the nitrided layer to the base (Lakhtin, & Silina, 1977). Figure 8 shows that the microhardness of the nitrided layer of steels R9, R6M5 and R18 differs from each other. This is due to the fact that alloying elements are present in these steels in various concentrations. The high hardness of the nitrided layer of steel R18 compared with steels R6M5 and R9 is due to the fact that alloying elements are present in greater amounts in steel R18. Since, the more alloying elements in the steel, the greater will be the hardness of the nitrided layer (Belyy et al., 1991). As a result of electrolytic-plasma nitriding

Didar Yeskermessov (diko090@gmail.com)
IGI Global Platform

Downloaded: 10/3/2023 3:42:03 AM
IP Address: 91.185.25.163

Figure 6. Changes in the coefficient of friction f of samples of R6M5 steel over time, before (a) and after nitriding at 450°C (b), 500°C (c) and 550°C (d) for 7 min

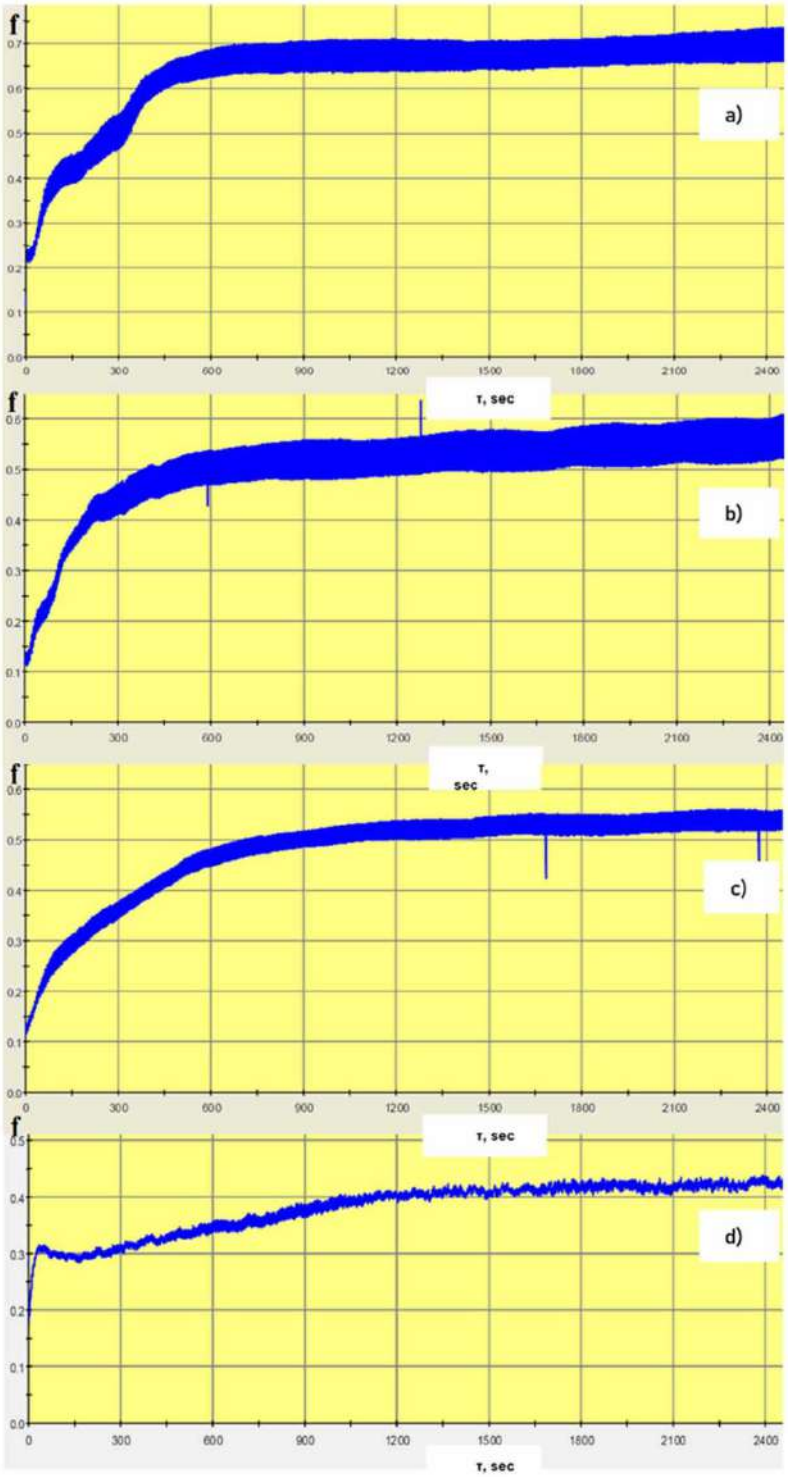

Didar Yeskermessov (diko090@gmail.com)
IGI Global Platform
Downloaded: 10/3/2023 3:42:03 AM
IP Address: 91.185.25.163

Figure 7. Dependence of the microhardness of the surface layer of R6M5 steel on the nitriding temperature

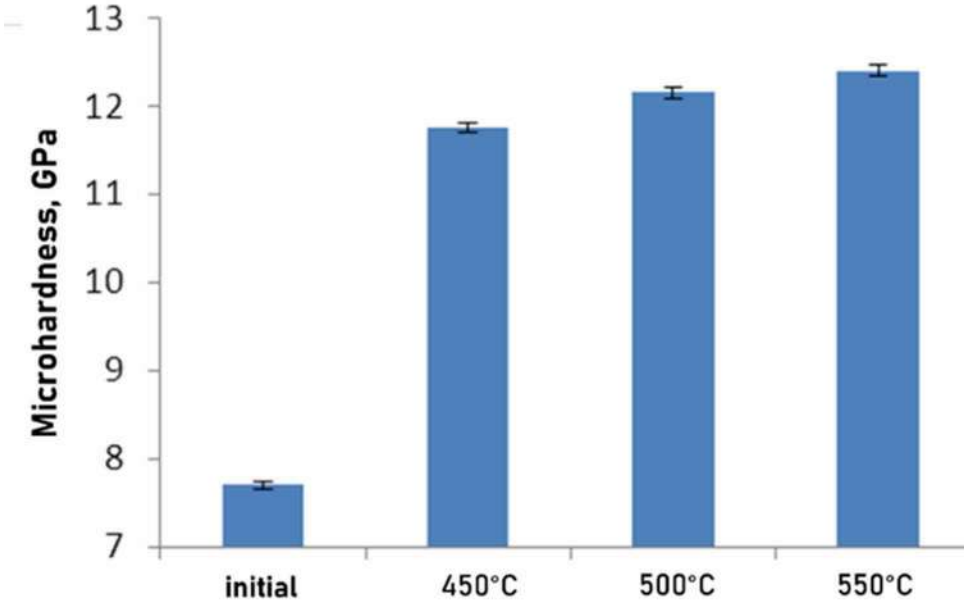

Figure 8. Distribution of microhardness over the depth of the nitrided layer of high-speed steels

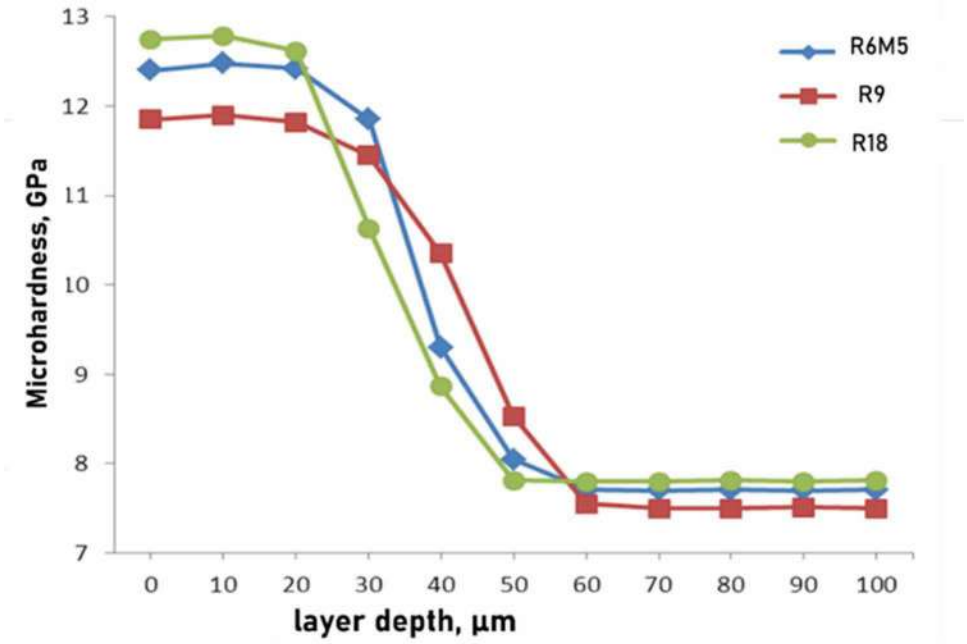

Didar Yeskermessov (diko090@gmail.com)
IGI Global Platform
Downloaded: 10/3/2023 3:42:03 AM
IP Address: 91.185.25.163

at 550°C, samples from high-speed steels, there was an increase in surface microhardness by 1.6 times. It has been experimentally established that the main increase in the microhardness of the diffusion layer occurs after nitriding at 550°C, which may be the result of the precipitation of finely dispersed, fully or partially coherent with the matrix, nitrides in the supersaturated α phase, which distort the crystal lattice of the matrix. Since it is known from (Belotskiy & Permyakov, 1972; Du et al., 2002; Kardonina et al., 2010; Lakhtin,, 1995) that the high hardness of the nitrided layer on steels alloyed with nitride-forming elements (Al, Cr, Mo, B, V) is the result of the total hardening effect:

a) the formation of nitrides of alloying elements in the process of nitriding;
b) separation and pre-isolation of dispersed nitrides of alloying elements in the process of intermediate γ®α-transformation;
c) isolation or pre-isolation of nitrides of alloying elements due to a decrease in solubility with decreasing temperature.

3.2 High-Temperature Testing of Nitrided Samples of High-Speed Steel for Wear Resistance

Modern mechanical engineering is characterized by difficult operating conditions for cutting tools associated with a high level of operating stresses, a wide temperature range, aggressive media, etc. Therefore, it is necessary to comply with special requirements for materials, in particular, high wear resistance at high temperatures and durability of the cutting tools from which they are made. In this regard, in this section, the wear resistance of nitrided samples of high-speed steel at high test temperatures is studied.

Figure 9. Dependence of the wear intensity of high-speed steel specimens on the test temperature

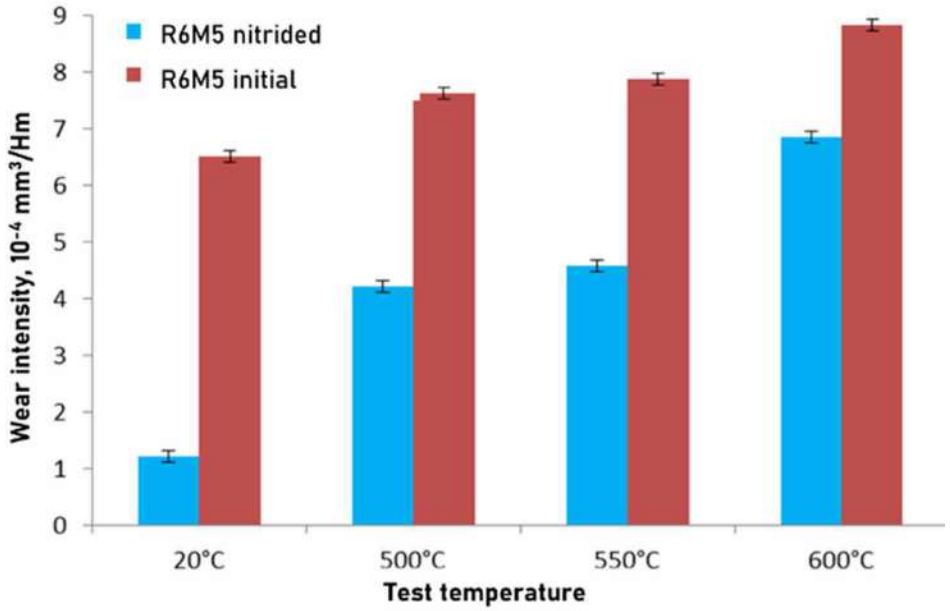

Didar Yeskermessov (diko090@gmail.com)
IGI Global Platform
Downloaded: 10/3/2023 3:42:03 AM
IP Address: 91.185.25.163

Figure 10. Graphs of friction coefficient f, counterbody penetration depth h, sample temperatures t1 and furnace t2 versus friction time τ during tests at temperatures of 20°C (a), 500°C (b), 550°C (c) of nitrided R6M5 steel specimens

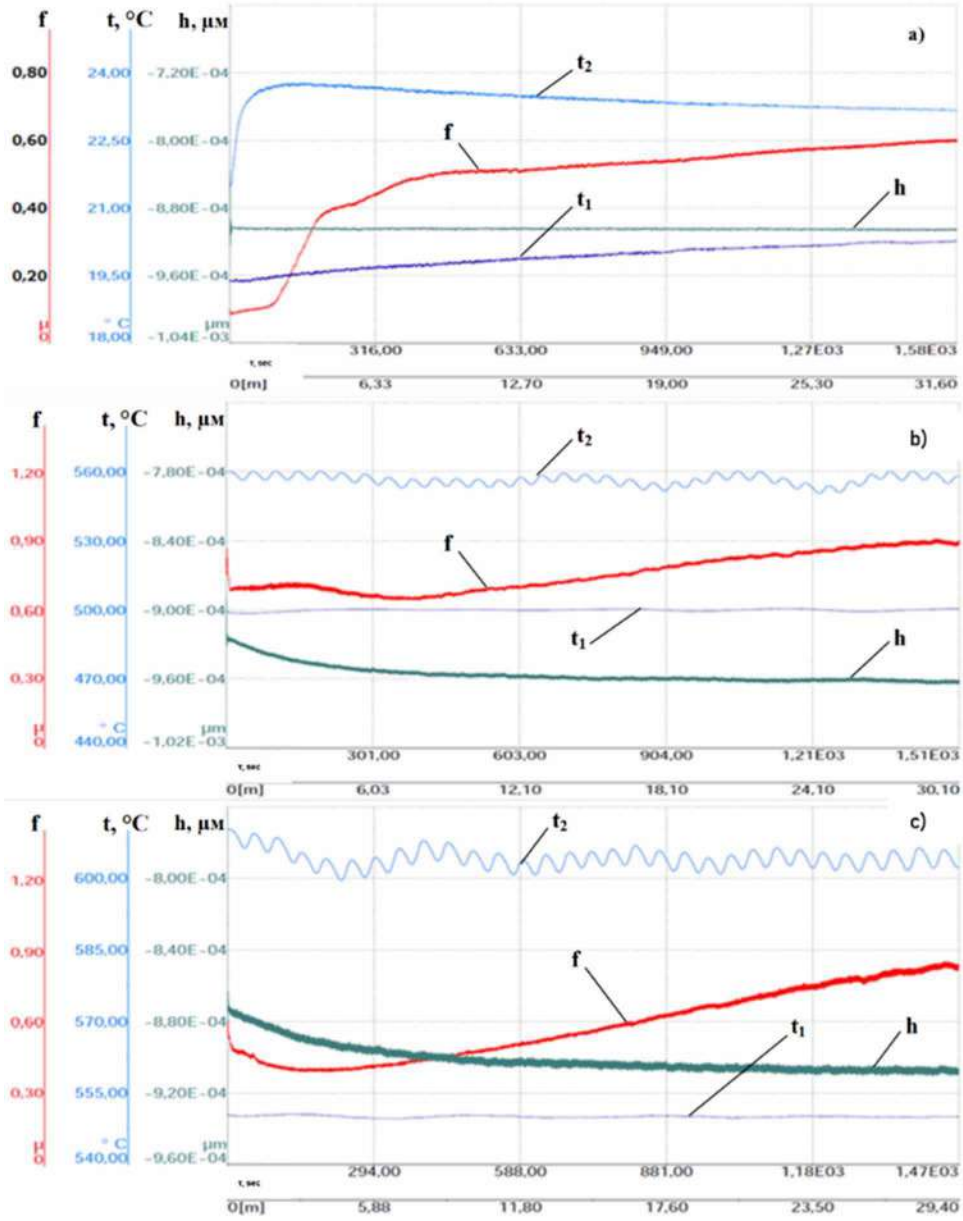

High-temperature tests were carried out according to the procedure described in section 2 of this work. The tests were carried out at temperatures of 500°C, 550°C and 600°C according to the "ball-disk" scheme. Wear resistance was evaluated by wear intensity and friction coefficient. The wear intensity values in each position are averaged over the results of testing three samples. Figure 9 shows the dependence of the wear intensity of the initial and nitrided samples of R6M5 steel on the test temperature. When tested

Didar Yeskermessov (diko090@gmail.com)
IGI Global Platform
Downloaded: 10/3/2023 3:42:03 AM
IP Address: 91.185.25.163

at room temperature, the wear intensity of nitrided samples of R6M5 steel turned out to be significantly lower than that of non-nitrided samples. The wear intensity of nitrided specimens when tested at 500^0C and 550^0C averages $3.1*10^{-4}$ and $3.5*10^{-4}$ mm^3/Hm, and when tested at 600^0C - $6.7*10^{-4}$ mm^3/ Hm. At test temperatures of 500^0C and 550^0C, there is a noticeable increase in the wear intensity value for nitrided and non-nitrided samples. And at the test temperature at 600^0C, a more significant increase in the wear intensity value is observed. Perhaps this is due to the coagulation of carbides, which reduces hardness. Since it is known (Younesi, Bahrololoom, and Fooladfar, 2010; Grigor'yev, 2004; Badisch and Mitterer, 2003) that dispersed precipitates, such as finely dispersed nitrides of alloying elements, protect the grain volume of a relatively soft matrix from abrasion.

The results of tribological tests at high temperatures of R6M5 steel specimens that have undergone nitriding at a temperature of 550°C are shown in Figures 10 and 11. Figure 10 shows the curves of the change in the coefficient of friction, the depth of penetration of the counterbodies depending on the friction time during tests at temperatures of 20°C, 500°C and 550°C of nitrided samples of R6M5 steel. At high temperatures, an increase in the coefficient of friction is observed. However, changing the test temperature in the range from 500 to 550°C has practically no effect on the coefficient of friction. Figure 11 shows the curves of the coefficient of friction, the depth of penetration of the counterbodies, depending

Figure 11. Graphs of friction coefficient t, counterbody penetration depth h, sample temperatures t1 and furnace t2 versus friction time τ during testing at a temperature of 600°C of R6M5 steel specimens before (a) and after (b) nitriding

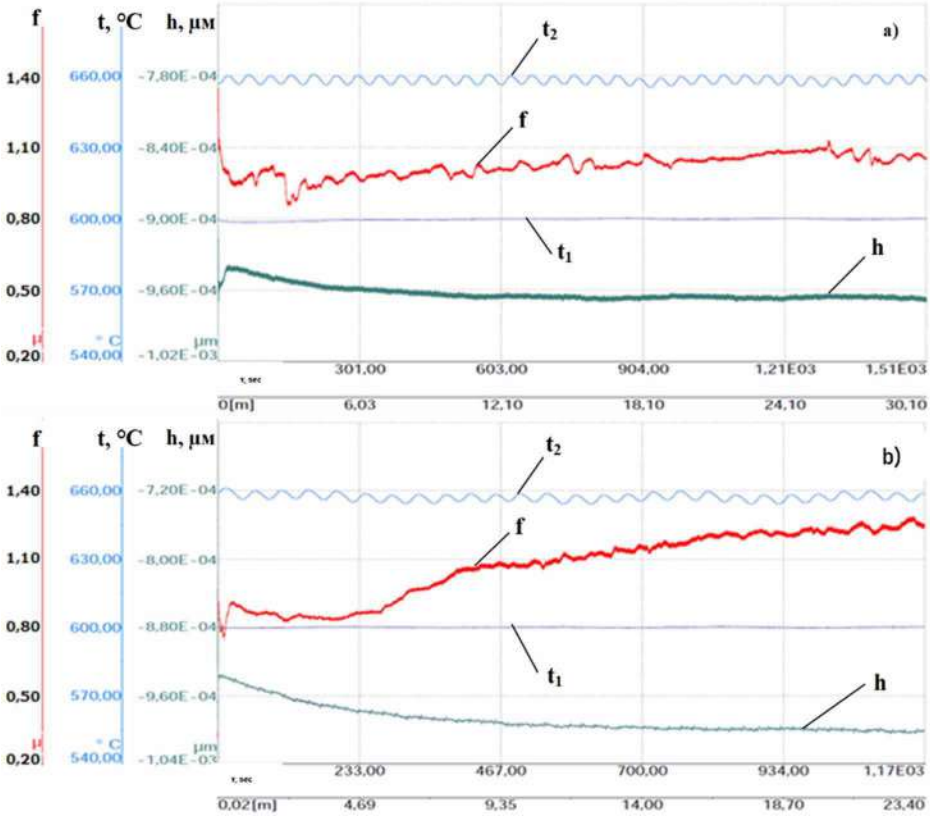

Didar Yeskermessov (diko090@gmail.com)
IGI Global Platform
Downloaded: 10/3/2023 3:42:03 AM
IP Address: 91.185.25.163

on the time of friction during tests at a temperature of 600°C of samples of steel R6M5 before and after nitriding. Increasing the test temperature to 600°C leads to a significant increase in the coefficient of friction of the original and nitrided samples compared to the samples tested at room temperature and at 500,550°C. At the same time, the coefficient of friction is of great importance during the entire testing process, remaining insufficiently high in magnitude. A decrease in wear resistance, as well as an increase in the friction coefficient at a test temperature of 600°C, may be associated with processes similar to the processes of coagulation or diffusion growth of coherent particles of the nitride phase. Thus, it is known from (Gol'dshmidt, 1971) that at temperatures above 550°C, diffusion processes develop on the surface layer of high-speed steel, as a result of which special carbides coagulate, which reduce hardness, as well as surface oxidation and decarburization.

Comparison of the wear intensity and wear coefficient of nitrided layers for different test temperatures (500°C, 550°C and 600°C) gives grounds to conclude that the wear resistance of nitrided steel varies depending on the ambient temperature, i.e. operating temperature, and the nitrided layer is more stable up to a temperature of 550°C.

3.3 Resistance of High-Speed Steels to Abrasive Wear Before and After Electrolytic-Plasma Nitriding

The mechanism of tool wear when cutting metals is complex and includes abrasive, adhesive and diffusion wear. The specific influence of each of them depends on the properties of the material, tool, workpiece, and processing conditions (Belotskiy et al., 1973). However, the material of the cutting tool during operation is more characterized by abrasive wear. In this regard, nitrided high-speed steels were tested for resistance to abrasive wear according to the "flat surface – rotating disk" scheme. Samples from high-speed steels were tested by abrasion of their surface with a rubber roller. The results of testing the samples for abrasive wear were characterized by the weight loss of the samples after the test. Figure 12 shows the dependences of the weight loss value of R6M5 steel samples before and after nitriding on the abrasion time. In order to investigate the wear resistance throughout the depth of the modified layer, the wear was evaluated every minute. In this case, after each minute, the sample was removed and weighed. It can be seen that the wear intensity of the nitrided samples is less than that of the original sample in the first and second minutes. And in the third minute, the wear intensity of nitrided and non-nitrided samples is equal. Further, the wear of all samples is almost the same, since the modified layer wears out after the 3rd minute, as experience has shown.

Thus, it is determined that in the surface modified layer, abrasive wear resistance is greater than in the base. It has been established that the surface modified layer of the nitrided sample has high wear resistance, and it decreases with the depth of the sample. Based on the studies of wear resistance in depth (every minute), it was determined that for nitrided steel samples, the optimal time for testing for abrasive wear is 3 minutes. Figure 13 shows the dependence of the mass loss value of R6M5 steel samples on the nitriding temperature. The tests were carried out for 3 minutes. It can be seen that the weight loss of the samples after nitriding at 500°C and 550°C is low compared to the samples nitrided at 450°C. Since after nitriding at 450°C, a modified layer with a small thickness is formed on the surface of R6M5 steel and Fe_4N nitrides are not formed, which provide high wear resistance. And the mass loss of steel samples nitrided at 500°C and 550°C is close, lies within the error. In this case, it can be seen that fine nitrides of alloying elements, which are formed only after nitriding at 550°C, do not play a special role in this

Didar Yeskermessov (diko090@gmail.com)
IGI Global Platform
Downloaded: 10/3/2023 3:42:03 AM
IP Address: 91.185.25.163

Figure 12. Dependence of the value of weight loss on the test time for samples of R6M5 steel nitrided at 550°C for 3, 5, and 7 min

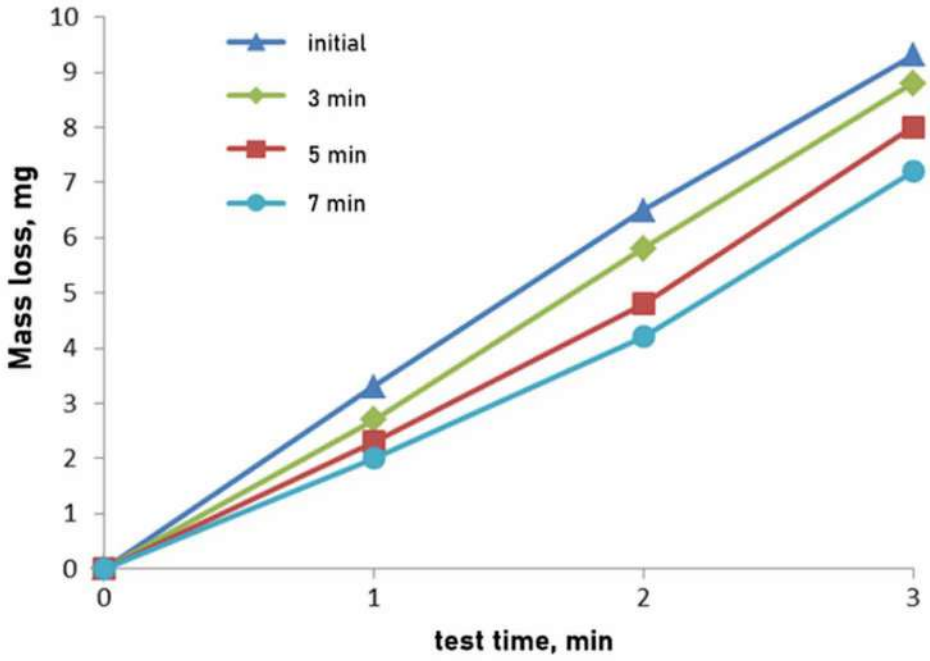

Figure 13. Dependence of the mass loss value of R6M5 steel samples on the nitriding temperature (nitriding was carried out for 7 min)

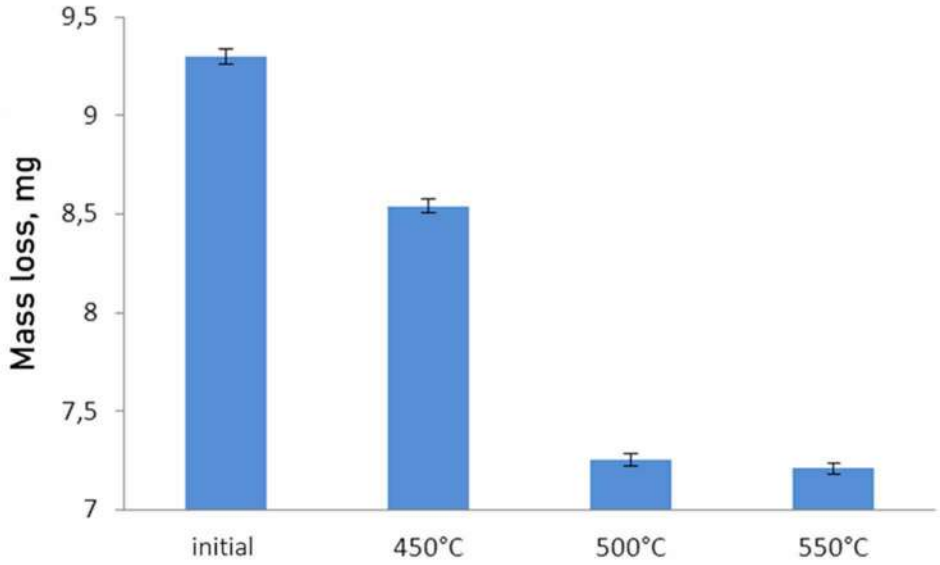

Didar Yeskermessov (diko090@gmail.com)
IGI Global Platform
Downloaded: 10/3/2023 3:42:03 AM
IP Address: 91.185.25.163

Figure 14. Resistance of samples of high-speed steels to abrasive wear

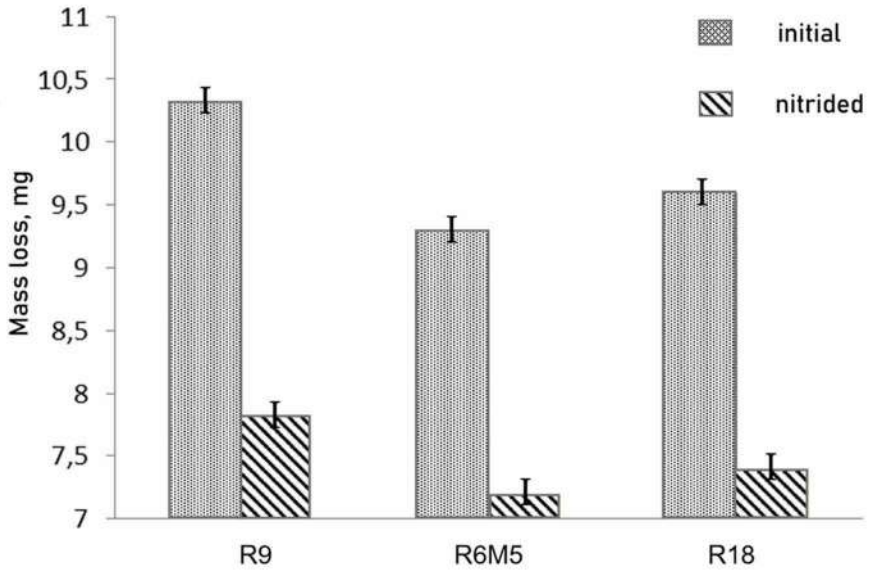

case. Perhaps this is due to the fact that the sizes of these nitrides are very small compared to abrasive particles, also due to their small formation depth.

Figure 14 shows the values of weight loss for samples of steels R9, R6M5 and R18 before and after nitriding at a temperature of 550^0C, lasting 7 minutes. It can be seen that the mass loss of nitrided samples is less than that of non-nitrided samples, which indicates an increase in the abrasive wear resistance of high-speed steels after nitriding. According to the weight loss, the relative wear resistance of samples of high-speed steels was determined (Table 4).

Table 4 also shows that the abrasive wear resistance of nitrided high-speed steels turned out to be 1.3 times higher than the wear resistance of the same steels in the initial state. At the same time, the relative wear resistance of R6M5 and R18 steels is higher compared to R9 steel before and after nitriding. This is due to the fact that R9 steel is characterized by a smaller amount of hard carbides. It is known (Grigor'yev, 2004; Badisch and Mitterer, 2003; Gnyusov et al., 2008) that the nature, amount, distribution pattern, and size of carbides have a significant effect on the wear resistance of high-speed steels. Thus, it was found that the surface layer of the nitrided sample has a high resistance to abrasive wear.

Conclusions for Section 3

Thus, based on the analysis of the results of mechanical and tribological tests of high-speed steel samples that have undergone electrolytic-plasma nitriding, we can draw the following conclusions:

1. As a result of electrolytic-plasma nitriding at 550°C, samples of high-speed steels, there was an increase in surface microhardness by 1.6 times.

Didar Yeskermessov (diko090@gmail.com)
IGI Global Platform
Downloaded: 10/3/2023 3:42:03 AM
IP Address: 91.185.25.163

Table 4. Abrasion test results

Nº	Sample	Relative Wear Resistance K_{wr}
1	R9, initial	1,84
2	R9, nitrided	2,43
3	R6M5, initial	2,04
4	R6M5, nitrided	2,64
5	R18, initial	1,98
6	R18, nitrided	2,57

2. It was determined that the wear intensity of nitrided samples of high speed steels R9, R6M5 and R18 is reduced by 77%, 81% and 83%, respectively, which indicates a significant increase in the wear resistance of high speed steels after electrolytic-plasma nitriding;
3. Scratch testing showed that after nitriding, the friction coefficient decreases, and the depth of the scar of the surface of the high-speed steel specimen formed during friction decreases, which shows a significant increase in the hardness and wear resistance of the steel surface after nitriding. Based on the pin-disk test, it was found that the coefficient of friction after nitriding decreases depending on the nitriding temperature. At the same time, there is a significant decrease in the coefficient of friction of samples nitrided at 550°C.
4. 4. It has been established that the wear resistance of nitrided steel varies depending on the ambient temperature, i.e. operating temperature, and the nitrided layer is more resistant to wear up to temperatures of 550°C, and an increase in temperature to 600°C leads to a decrease in wear resistance, as well as an increase in the coefficient of friction.
5. It has been established that after electrolytic-plasma nitriding, the resistance of high-speed steels to abrasive wear increases. The relative wear resistance of samples of high-speed steels after nitriding increases up to 1.3 times compared to the original samples

4. CHANGES IN THE STRUCTURAL-PHASE STATE OF HIGH-SPEED STEELS AS A RESULT OF ELECTROLYTE-PLASMA NITRIDING

This section is devoted to the study of changes in the structure, phase composition of the surface layers of high-speed steels R6M5, R9 and R18 as a result of electrolytic-plasma nitriding. As is known (Bakovets, Polyakov, & Dolgovesova, 1991; Parfenov et al., 2007; Petukhov, 2001), in the process of treatment with an electrolytic-plasma effect, significant changes occur in the structural-phase states of the material in thin surface layers due to the physical effect of low-temperature plasma ions and electric discharge. The processes of structural rearrangement developing in this case, structural phase transformations occur under conditions far from thermodynamically equilibrium states, and they make it possible to obtain modified surface layers with a unique set of physical and mechanical properties (Gupta, Tenhundfeld, Daigle, & Ryabkov, 2007). In this regard, the study of changes in the structural-phase state of high-speed steels as a result of electrolytic-plasma nitriding is of scientific and practical interest.

Didar Yeskermessov (diko090@gmail.com)
IGI Global Platform
Downloaded: 10/3/2023 3:42:03 AM
IP Address: 91.185.25.163

4.1 Structural-Phase States of High-Speed Steels in the Initial State

High cutting properties of high-speed steels (high heat resistance in the presence of high hardness and wear resistance) are achieved through special alloying and complex heat treatment, providing a certain phase composition (Suminov et al., 2005). The main alloying elements of high speed steels are carbon, tungsten, molybdenum, vanadium and chromium. These elements under certain temperature-time conditions form particles of the carbide phase in steel, which are the strengthening phase of the material. As a rule, in high-speed steels, the main carbide phase is a complexly alloyed carbide of the composition $(Fe,M)_6C$, where "M" are the elements that form the metal base of the carbide (W, Cr, Mo, V). According to the temperature range of formation, carbide particles are divided into a) primary, formed during the crystallization of steel from the melt; b) secondary, released during crystallization from austenite and c) tertiary, formed during the decomposition of martensite. The volume fraction of carbides is quite large and can reach up to 30% in high-speed steels, according to (Geller,, 1983). In addition, as the cutting speed increases, the requirements for the heat resistance of steel increase. The heat resistance of high-speed steels is due to alloying them with carbide-forming elements: tungsten, vanadium, molybdenum and chromium. These elements under certain temperature and time conditions form particles of the carbide phase in steel, which are the strengthening phase of the material (Moiseyev & Grigor'yev, n.d.). A high-temperature tool made of high-speed steels acquires high heat resistance after hardening and repeated tempering. Tempering after quenching within the temperature limits established for cutting tools leads to a decrease in the carbon content in martensite and the formation of ultramicroscopic carbides (Schastlivtsev et al., 1994). These carbides play an important role in the mechanical properties of steel, including hardness, wear resistance, and heat resistance (Liu, et al., n.d.).

In this regard, in this work, as the initial state of high-speed steels, we chose the state that the studied steels acquire after standard heat treatment, i.e. after quenching and three times tempering. As is known, the analysis of the microstructure and phase composition of steel after quenching followed by tempering makes it possible to evaluate its properties under operating conditions. At present, a large number of concepts have been developed, a number of patterns have been identified that relate the microstructure of a material to its physical and mechanical properties. However, the features of carbide phases, which play an important role in the mechanical properties of high speed steels, have been little studied. In this regard, in order to establish the main regularities of structural-phase transformations in high-speed steels during electrolytic-plasma nitriding, the structural-phase states of samples of high-speed steels R6M5, R9 and R18 in the initial state were previously studied. Figure 15 shows the microstructures of steels R6M5, R9 and R18 in the initial state, i.e. after standard heat treatment. The heat treatment mode is described in detail in the second section. It can be seen from the figure that the microstructures of steels R6M5, R9 and R18 are very similar to each other and consist of tempered martensite and special carbides (Figure 15). Previously, in (Maksakova et al.,2016; Skakov Rakhadilov, and Karipbaeva, 2013; Skakov and Rkhadilove, 2012), we found that martensite and special carbides are present in the steel structure after standard heat treatment. No residual austenite was observed in the matrix. The preliminary estimate was confirmed by X-ray diffraction phase analysis.

Figure 16 shows SEM images of the surface of steels R6M5, R9 and R18. The structure of steels consists of martensite and carbides. Carbide particles are evenly distributed in the matrix and are close to regular spherical shape. In the structure of high-speed steels R6M5 and R9, two types of carbides are observed: light and gray carbides (Figure 16 a, b, d). And in the structure of steel R18 there are only light carbides (Figure16 c). Figure 16d shows the microstructure of R6M5 steel obtained using a semi-

Didar Yeskermessov (diko090@gmail.com)
IGI Global Platform
Downloaded: 10/3/2023 3:42:03 AM
IP Address: 91.185.25.163

Figure 15. Microstructure of steels R6M5 (a), R9 (b), and R18 (c) in the initial state after standard heat treatment obtained using an optical microscope

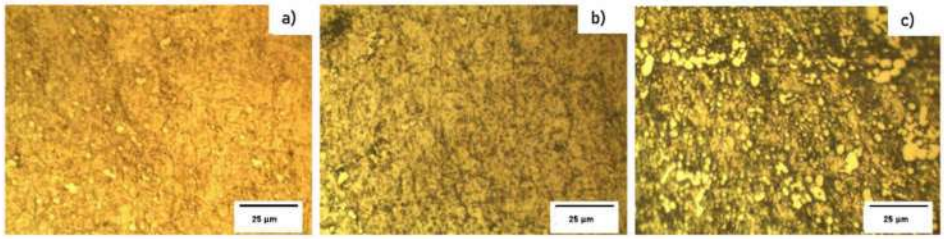

Figure 16. Surface microstructure of high-speed steels R6M5(a, d), R9 (b), R18 (c)

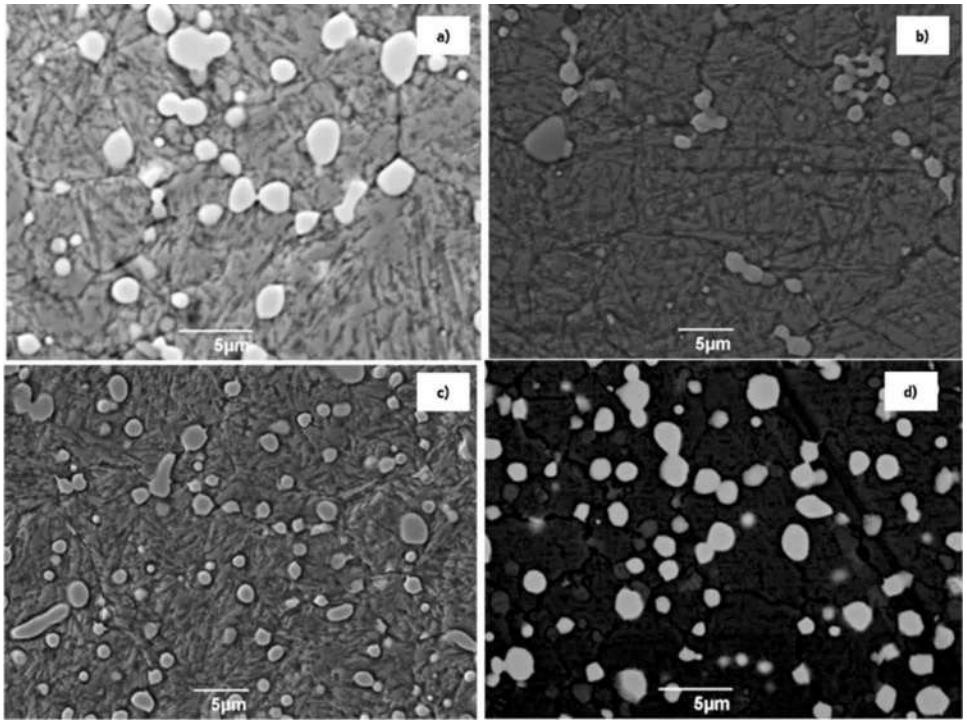

Table 5. Quantitative parameters of the structure of steels R6M5, R9, and R18

Nº	Steel	Carbides	Volume Fraction	Average Particle Size
1	R6M5	Light colored carbides	10.4±0.6%	2,1 μm
		Dark carbides	2,3±0.4%	0,8 μm
2	R9	Light colored carbides	3.1±0.6%	1,6 μm
		Dark carbides	1,7±0.4%	1,8 μm
3	R18	Light colored carbides	13.4±0.6%	1,9 μm

Didar Yeskermessov (diko090@gmail.com)
IGI Global Platform
Downloaded: 10/3/2023 3:42:03 AM
IP Address: 91.185.25.163

conductor backscattered electron detector, giving surface patterns with chemical contrast display with high spatial resolution. Gray carbides are clearly visible from this image. Thus, it can be established that after standard heat treatment, two types of carbides are present in the structure of R6M5 and R9 steels: very bright colors of carbides (light carbides) containing elements above the atomic number and gray carbides containing elements below the atomic number, and in the steel structure R18 contains only light carbides. The volume fraction of each fraction was estimated. The sizes of carbide particles in the studied steels are also determined. The results of the quantitative parameters of the steel structure are shown in Table 5.

To reveal the composition of carbides and their distribution, a map of the distribution of alloying elements in the steel structure was obtained. The general nature of the distribution of alloying elements in the structure of steels R6M5, R9 and R18 is shown in Figures 17, 18 and 19, respectively. It can be seen from the figures that light spherical carbides are enriched in tungsten and molybdenum, and gray ones are enriched in vanadium. The obtained maps of the distribution of alloying elements confirmed that in the structure of steels R6M5 and R9 there are two types of carbides - light and dark, and in the structure of steel R18 only light. The absence of gray carbides, which are enriched with vanadium in the structure of steel R18, is possibly due to the fact that the content of vanadium in the composition of steel R18 is low compared to steels R6M5 and R9. In addition, Figure 19 shows that the bulk of vanadium is in light carbides in the structure of R18 steel. It should be kept in mind that V, W, Mo and Cr are carbide-forming elements. In other words, the carbides of these metals have a high binding energy and stability (Skakov & Rakhadilov, 2012; Skakov, Rakhadilov, Karipbayeva et al, 2014). That is why most of the alloying elements are in carbides, and not in solid solution.

To determine the elemental composition of particles of precipitated carbides and matrix (martensite), microprobe analysis was carried out (Figure 20). Table 6 shows the content of alloying elements in carbides and matrix for steels R6M5, R9 and R18.Tungsten, molybdenum, vanadium and chromium form special carbides in steel: M_6C based on tungsten and molybdenum, MC based on vanadium and $M_{23}C_6$ based on chromium. The results of mapping and microprobe analysis show that the structure of R6M5 steel after

Figure 17. Surface microstructure and distribution map of alloying elements of R6M5 steel in initial states

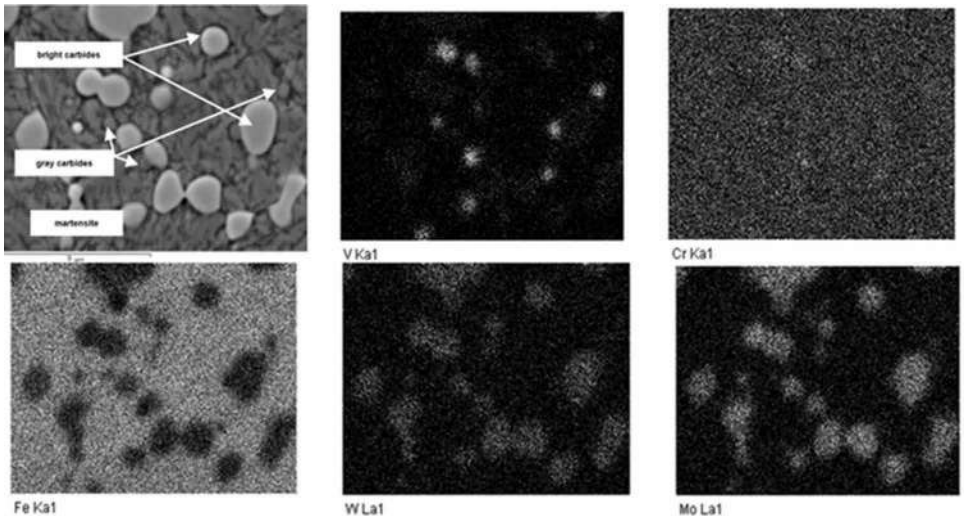

Didar Yeskermessov (diko090@gmail.com)
IGI Global Platform
Downloaded: 10/3/2023 3:42:03 AM
IP Address: 91.185.25.163

Figure 18. Surface microstructure and distribution map of alloying elements of R9 steel in initial states

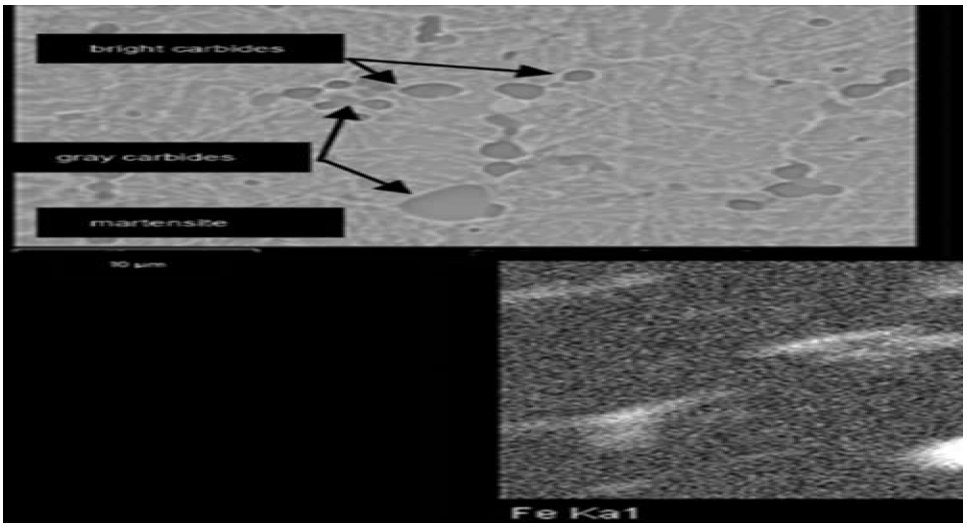

standard heat treatment contains M_6C and MC carbides and no $M_{23}C_6$ carbides, which is in good agreement with the literature data (Kremnev, 2008; Skakov, Rakhadilov, Karipbayeva et al, 2014). However, in some works (Guenzel et al., 2000; Vorob'yeva & Skladnova, 2003) it is stated that after standard heat treatment in the structure of R6M5 steel there are only particles of M_6C type carbide. Apparently, this is due to the small volume fraction of particles of MC type carbides and the similarity of these particles with the matrix, which makes it impossible to detect them. In addition, the methods used in these works have limitations in the detection of carbide particles with a low concentration. Therefore, in this work, along with X-ray diffraction phase analysis, special methods of scanning electron microscopy are used.

Figure 19. Surface microstructure and distribution map of alloying elements of steel R18 in initial states

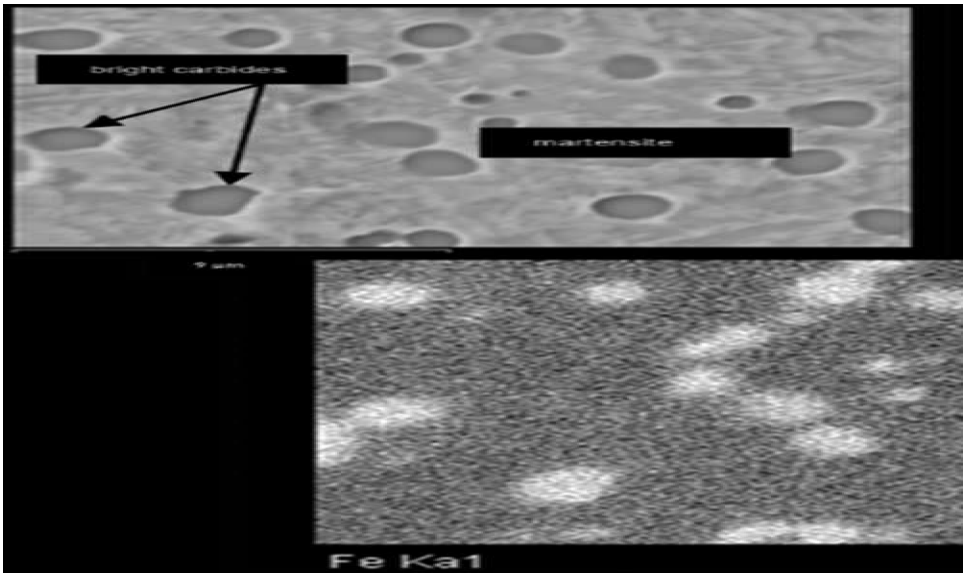

Didar Yeskermessov (diko090@gmail.com)
IGI Global Platform
Downloaded: 10/3/2023 3:42:03 AM
IP Address: 91.185.25.163

Table 6. The content of alloying elements in the structural components of high speed steels

Structural Components	Content of Elements, % (wt.)				
	V	Cr	Fe	Mo	W
R6M5					
Light colored carbides	3.42	3.31	30.85	26.05	36.37
Dark carbides	26.47	4.45	30.82	16.62	21.64
Martensite	1.33	4.62	84.50	4.25	5.30
R9					
Light colored carbides	3.15	3.52	28.83	3.10	61.4
Dark carbides	28.64	4.55	40.99	-	25.82
Martensite	3.11	4.95	80.78	-	11.16
R18					
Light colored carbides	3.50	3.80	34.77	2.70	55.23
Martensite	1.07	4.64	84.39	-	9.90

The proposed configuration of M_6C carbide is between the formulas $Fe_3(W,Mo)_3C$ - $Fe_3(W,Mo)_2C$ (Ivanov et al., 2002). In other words, along with tungsten and molybdenum atoms, M_6C carbide can contain up to 2/3 iron atoms of the total number of metal atoms. In addition, chromium and vanadium atoms can be dissolved, which replace iron atoms. According to the results of microprobe analysis, it can be assumed that gray carbide particles are vanadium-based MC carbides.

Figure 20 shows the diffraction patterns of steels R6M5, R9 and R18. X-ray diffraction analysis showed that in the initial state, i.e. after heat treatment, in the structure of steels R6M5 and R9 there is an α-phase and carbides M_6C, MC, and in the structure of steel R18 only M_6C carbides.

Thus, X-ray diffraction analysis confirmed that the main carbides in the studied steel are M_6C and MC carbides. It has been determined that M_6C type carbides, which have a complex FCC crystal lattice and Fd_3m space group, correspond to the Fe_3W_3C composition, and MC type carbides, which have a cubic crystal lattice and Fm_3m space group, correspond to the VC composition. In this case, it should be borne in mind that the M_6C type carbide can have the form of both Fe_3W_3C and Fe_3Mo_3C. As is known, one of the advantages of X-ray diffraction analysis (XRD) is that the peak position and lattice parameters can be determined quite accurately. Nevertheless, in this case, when studying individual carbides, it is advisable to apply the EBSD analysis. Therefore, to confirm the obtained results of X-ray diffraction analysis, the crystal structure of M_6C and MC carbides was studied by EBSD analysis using a reflected electron detector on a scanning microscope (system) with electron and focused ion beams. Figure 21 shows the results of an EBSD analysis of the surface of R6M5 steel. The EBSD analysis showed that tungsten-rich M_6C carbides are most optimally combined with the Fe_3W_3C cubic phase, while MC-type carbides correspond to the VC phase. However, it is worth noting that in this case Fe_3W_3C may also mean that other carbide-forming elements are present in the form of M_6C carbides.

Thus, we have characterized the structures and carbide phases of R6M5, R9, and R18 high-speed steels in the initial state, i.e., after standard heat treatment. The study of structural-phase states before a certain treatment is necessary in terms of identifying patterns of structure changes and its effect on

Didar Yeskermessov (diko090@gmail.com)
IGI Global Platform
Downloaded: 10/3/2023 3:42:03 AM
IP Address: 91.185.25.163

Figure 20. X-ray diffraction patterns of high-speed steels in the initial state (after heat treatment)

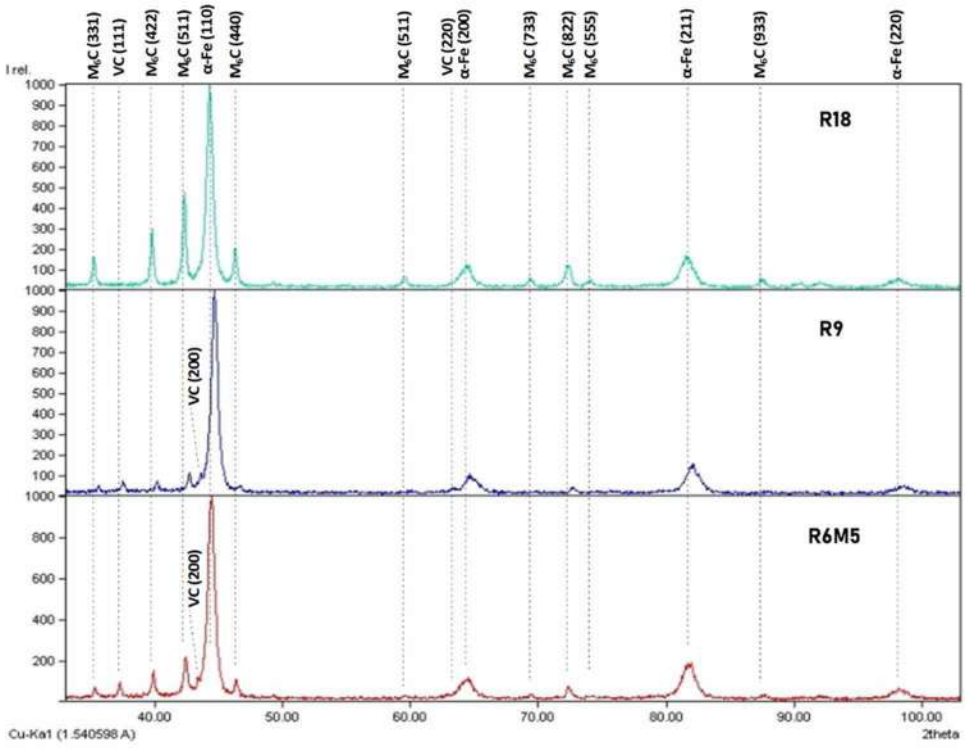

Figure 21. Results of EBSD analysis of steel R6M5

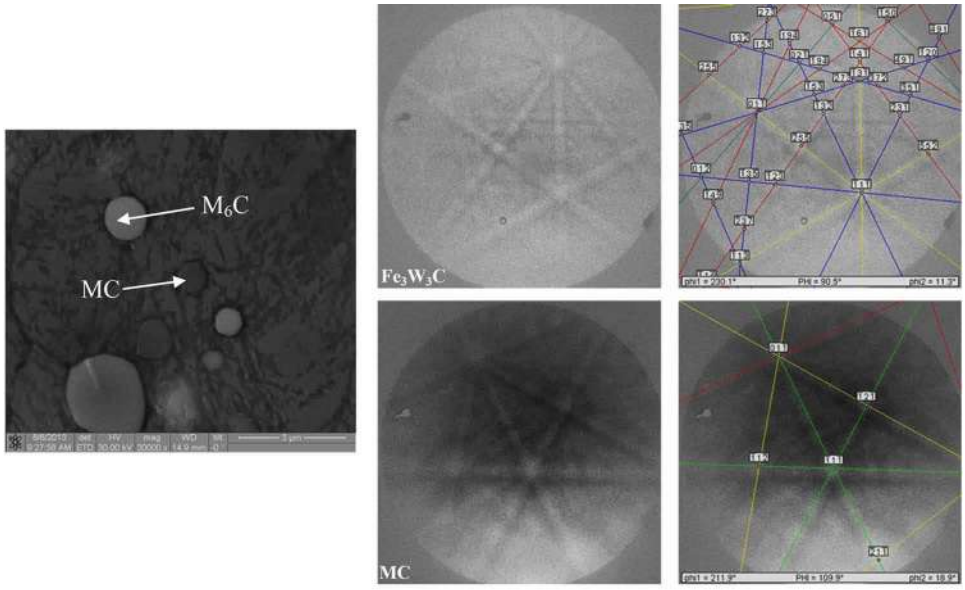

Didar Yeskermessov (diko090@gmail.com)
IGI Global Platform
Downloaded: 10/3/2023 3:42:03 AM
IP Address: 91.185.25.163

properties. Since the physical and mechanical properties of high-speed steel are largely determined by the structure and state of the carbide phases and their shape, size, distribution in volume.

4.2 Study of the Influence of Electrolytic-Plasma Nitriding on the Microstructure of High-Speed Steels

Figure 22 shows the microstructures of the modified surface layer of samples of high-speed steels R6M5, R9 and R18, nitrided for 7 minutes. It can be seen that after nitriding, a dark-etched nitrided layer is observed on the surface, which is a zone of internal nitriding. At the same time, the dark-etched zone smoothly transitions into the base. After nitriding at temperatures of 450°C, 500°C and 550°C, the thickness of the nitrided layer of R6M5 steel is 25–40 μm and increases with increasing nitriding temperature. And the thickness of the nitrided layer of steels R9 and R18 is on average 45 μm, 35 μm, respectively, after nitriding at 550°C. The thickness of the diffusion layer depends on: the composition of the treated metal (alloy), saturation temperature, duration of the process, the concentration of the diffusing element on the surface, and the nature of the formed solid solution. The higher the concentration of the diffusing element on the surface, the greater the layer thickness at a given temperature and the duration of the saturation process.

Thus, by metallographic analysis it has been established that during nitriding by electrolytic-plasma action, the process of diffusion saturation of steel with nitrogen proceeds with accelerated formation of a modified layer, consisting only of a well-developed zone of internal nitriding, i.e. diffusion layer. In this case, the diffusion layer is nitrogenous martensite, since the initial structure of the steel consisted of tempered martensite. The formation of a diffusion layer without a continuous nitride layer on high-speed steels makes it possible, on the one hand, to increase the hardness and wear resistance of the tool, and, on the other hand, to avoid high stresses leading to increased brittleness of the surface layer. Since it is known (Gol'dshmidt, 1971) that the formation of a nitride zone and an internal nitriding zone on the surface of nitrided steel, which have a larger specific volume than the core, leads to the appearance of large residual compressive stresses in the diffusion layer, and tensile stresses in the core. The dependence

Figure 22. Microstructure of the modified layer of high-speed steels after nitriding a) R6M5, at 450°C; b) R6M5, at 500°C; c) R6M5, at 550°C; d) R9, at 550°C; e) R18, at 550°C

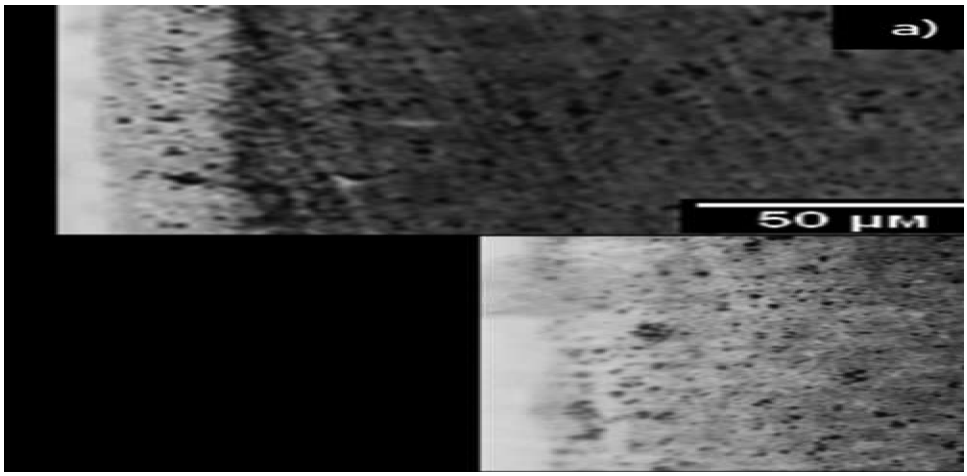

Didar Yeskermessov (diko090@gmail.com)
IGI Global Platform
Downloaded: 10/3/2023 3:42:03 AM
IP Address: 91.185.25.163

Figure 23. Growth kinetics of nitrided layers of R6M5 steel at different temperatures depending on the holding time, 1 -450°C; 2 -500°C; 3 -550°C

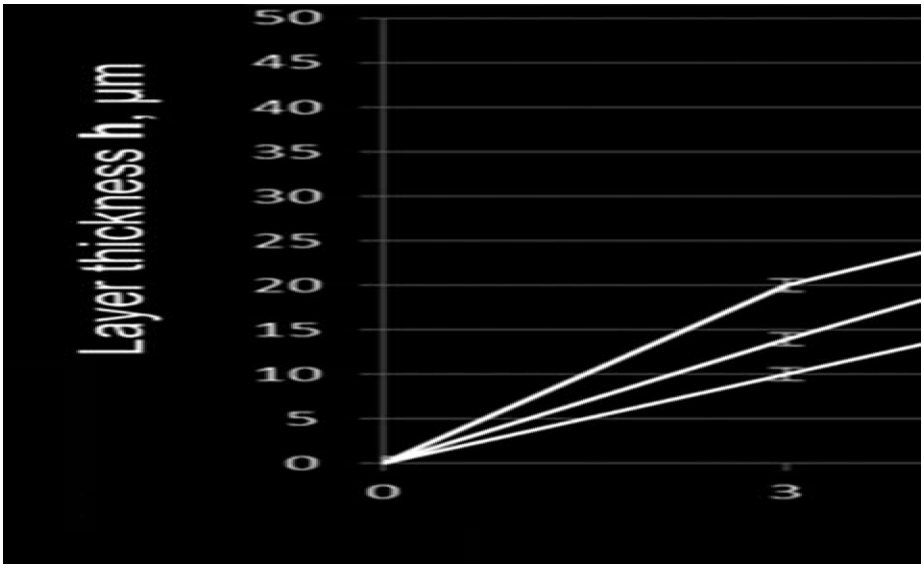

Figure 24. Microstructure of R6M5 high-speed steel before (a) and after electrolytic-plasma nitriding at temperatures of 450°C (b), 500°C (c), 550°C (d)

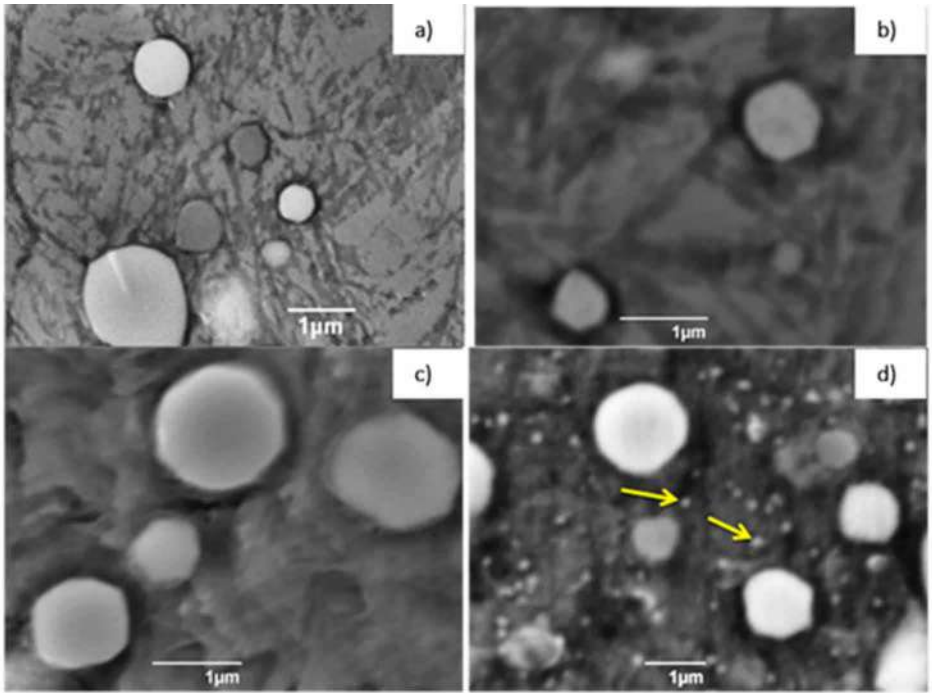

Didar Yeskermessov (diko090@gmail.com)
IGI Global Platform
Downloaded: 10/3/2023 3:42:03 AM
IP Address: 91.185.25.163

Figure 25. Microstructure of high-speed steel R9 before (a) and after (b) electrolytic-plasma nitriding at temperatures of 550°C

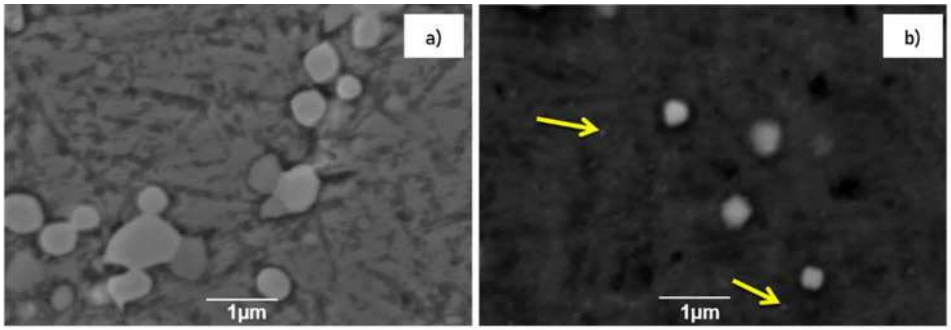

of the thickness of the diffusion layer h of the R6M5 steel on the time of its exposure at various nitriding temperatures was obtained (Figure 23). Figure 23 shows that the thickness of the modified layer increases with increasing nitriding temperature and holding time, which makes it possible to obtain a modified layer of a given thickness by varying the temperature and nitriding time. According to literature sources (Goldshmidt, 1971; Artinger, 1982; Lakhtin, 2009), for a cutting tool, the value of h should not exceed 50–60 μm. Therefore, the considered modes of nitriding are quite suitable for hardening cutting tools. It has been determined that the optimal time for electrolytic-plasma nitriding for high-speed steel is 7 minutes. In this regard, only samples nitrided with a duration of 7 minutes were studied further.

Figures 24, 25, 26 show SEM images of the surface of steels R6M5, R9 and R18 before and after nitriding with a duration of 7 minutes. The results of scanning electron microscopy showed that after electrolytic-plasma nitriding at 550°C, fine particles are formed on the surface of R6M5 steel (Figure 24 d, fine particles are marked by arrows). And when nitriding at 450°C and 500°C, they are not observed (Figure 24 b, c).

In the structure of steels R9 and R18 after nitriding at 550°C, fine particles are also observed (Figures 25 b, 26 b, fine particles are indicated by arrows). It is assumed that these particles are finely dispersed nitrides of alloying elements, in particular, chromium. Since alloying elements, such as tungsten, molybdenum and vanadium, which are part of high-speed steels, are 95% bound into carbides, it can be assumed that the main share of the formed nitrides of alloying elements falls on chromium nitrides. Since in all grades of high-speed steels considered in this work, the chromium content is the same and amounts to ~ 4%. The formation of fine nitrides of alloying elements at a temperature of 550°C is possible due to the fact that this temperature corresponds to the tempering temperature of this steel. Since, during the tempering of R6M5 steel at a temperature of 550–560°C, precipitation hardening occurs as a result of the partial decomposition of martensite and the precipitation of finely dispersed inclusions of strengthening phases (Arshinger,, 1982).

Figures 27, 28 and 29 show the results of surface mapping of R6M5 steel after nitriding at 450°C, 500°C and 550°C. The mapping results showed that after nitriding, the surface of R6M5 steel is saturated with nitrogen. In this case, after nitriding at 500°C and 550°C, areas are observed in the surface where the nitrogen content is higher. These areas are most consistent with the matrix. However, mapping does not allow one to accurately determine which structural component is more saturated with nitrogen, i.e. where the nitrides are located. Therefore, to identify the nitrogen content in the structural components and

Didar Yeskermessov (diko090@gmail.com)
IGI Global Platform
Downloaded: 10/3/2023 3:42:03 AM
IP Address: 91.185.25.163

Figure 26. Microstructure of high-speed steel R18 before (a) and after (b) electrolytic-plasma nitriding at temperatures of 550°C

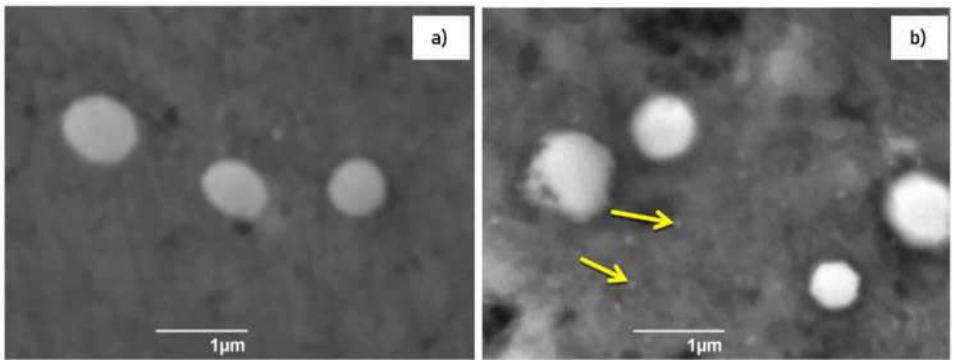

Figure 27. Surface microstructure and distribution map of alloying elements of R6M5 steel after nitriding at 450°C

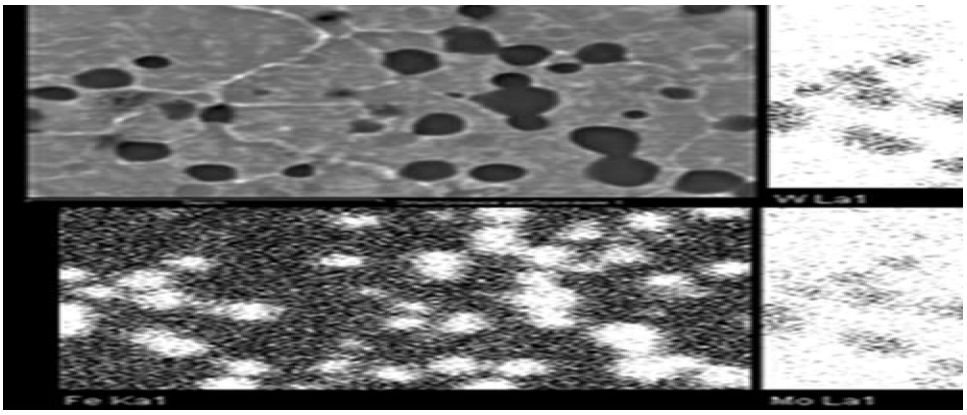

Figure 28. Surface microstructure and distribution map of alloying elements of R6M5 steel after nitriding at 500°C

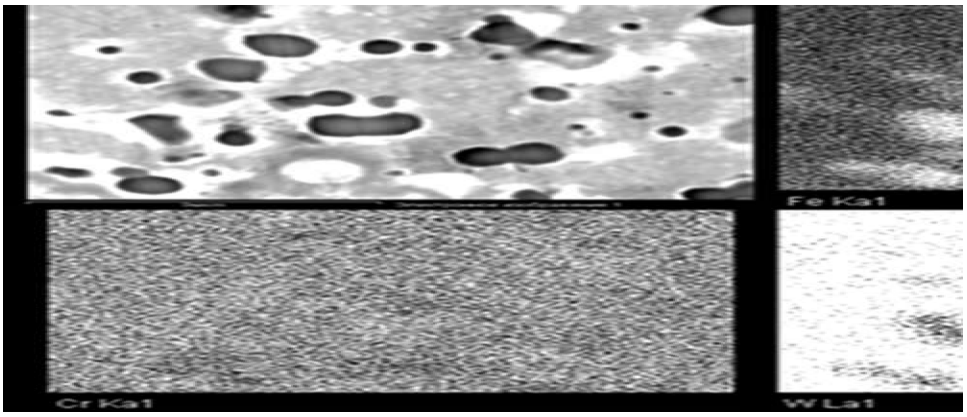

Didar Yeskermessov (diko090@gmail.com)
IGI Global Platform
Downloaded: 10/3/2023 3:42:03 AM
IP Address: 91.185.25.163

Figure 29. Surface microstructure and distribution map of alloying elements of R6M5 steel after nitriding at 550°C

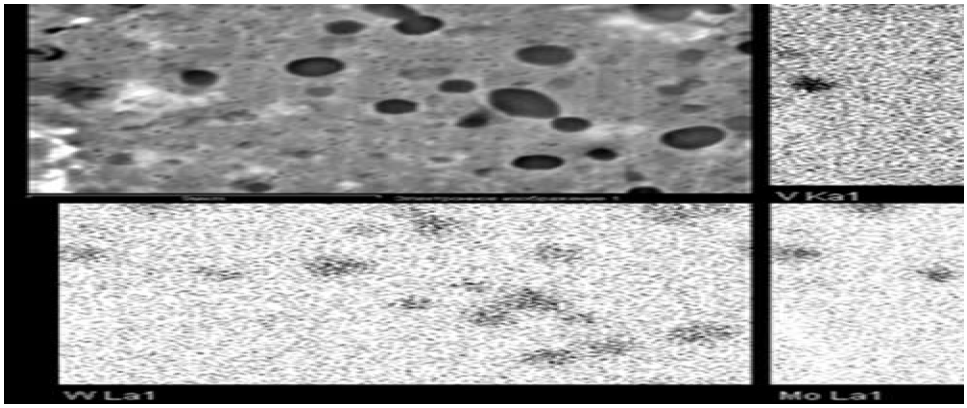

changes in the chemical composition of the surface as a whole, it is necessary to conduct a quantitative energy dispersive analysis of the surface. In order to identify changes in the elemental composition of the surface after nitriding, an energy dispersive analysis of the surface of R6M5 steel samples nitrided at 450°C, 500°C, and 550°C was carried out. Figures 30, 31 and 32 show the results of the energy dispersive analysis.

The analysis showed that nitrogen is observed only in the matrix, as expected from the mapping results. The nitrogen content in the surface of R6M5 steel reaches up to 7% (in weight%). The results of mapping and energy dispersive analysis showed a more uniform distribution of nitrogen over the matrix of the nitrided layer. The observed phenomenon of uniform adsorption and uniform growth of the nitrided layer should be explained by the appearance of a special defect substructure in the grain volume (dislocation-disclination structure of grains in the near-surface zone). The resulting defectiveness, apparently, approaches the defectiveness of the grain boundaries. Since, electrolytic-plasma nitriding is carried out under conditions of excessive excitation of the metal surface and subsurface layers. An

Figure 30. SEM image of R6M5 steel after nitriding at 450°C (a), characteristic radiation spectra (b), and microanalysis results, at% (c)

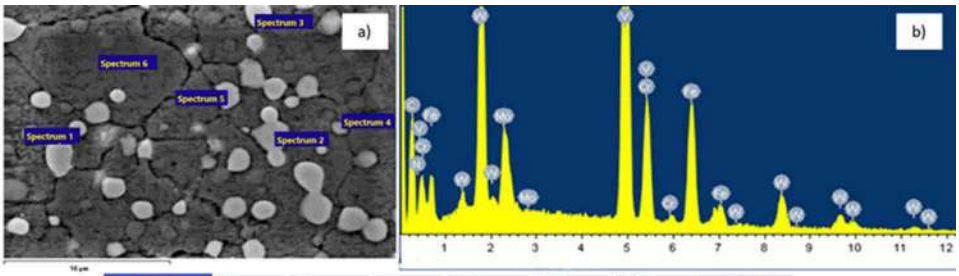

Spectrum	N	V	Cr	Fe	Mo	W	Total
Spectrum 1	0.00	39.66	5.78	17.06	9.87	27.63	100.00
Spectrum 2	0.00	2.31	3.40	26.73	13.74	53.82	100.00
Spectrum 3	0.00	2.42	3.25	26.60	13.55	54.18	100.00
Spectrum 4	0.06	4.06	4.69	78.71	3.33	9.15	100.00
Spectrum 5	0.12	12.33	5.05	65.71	3.91	12.88	100.00
Spectrum 6	0.40	1.03	4.44	85.09	1.97	7.07	100.00

c)

Didar Yeskermessov (diko090@gmail.com)
IGI Global Platform
Downloaded: 10/3/2023 3:42:03 AM
IP Address: 91.185.25.163

Figure 31. SEM image of R6M5 steel after nitriding at 500°C (a), characteristic radiation spectra (b), and microanalysis results at% (c)

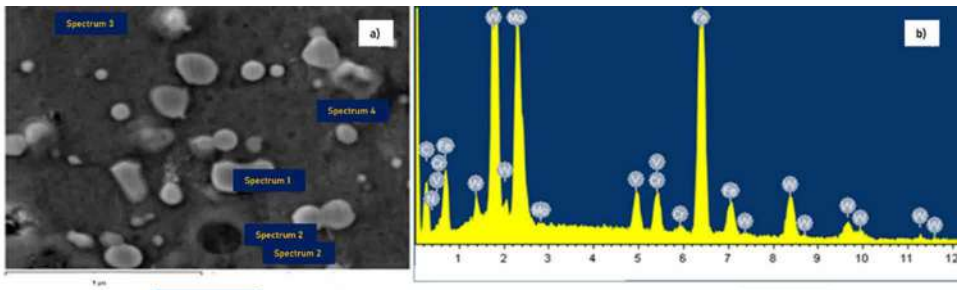

Spectrum	N	V	Cr	Fe	Mo	W	Total
Spectrum 1	0.00	3.25	3.51	32.04	25.91	35.29	100.00
Spectrum 2	6.36	9.86	6.14	62.59	7.12	7.93	100.00
Spectrum 3	5.87	1.45	4.70	80.41	3.60	3.97	100.00
Spectrum 4	6.00	1.56	4.91	78.45	3.97	5.11	100.00

c)

Figure 32. SEM image of R6M5 steel after nitriding at 550°C (a), characteristic radiation spectra (b), and microanalysis results (c) at% (c)

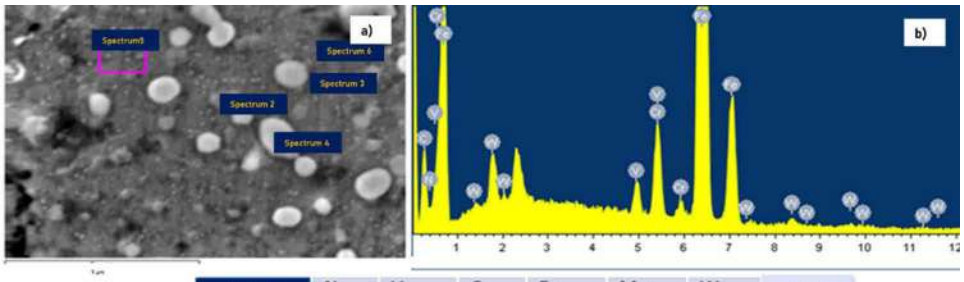

Spectrum	N	V	Cr	Fe	Mo	W	Total
Spectrum 2	0.14	10.46	5.19	72.12	5.29	6.80	100.00
Spectrum 3	7.08	1.82	5.12	77.05	4.47	4.46	100.00
Spectrum 4	0.00	1.47	4.53	33.93	24.26	35.81	100.00
Spectrum 5	5.91	2.47	5.12	78.02	3.94	4.54	100.00
Spectrum 6	3.58	2.59	4.78	81.23	3.21	4.61	100.00

c)

important factor influencing the growth rate of the nitrided layer and its structure during this process is the exclusion of the predominant role of boundary diffusion. Plasma, accelerating the directed mass transfer of ions to the surface of the sample, creates conditions for the uniform adsorption of nitrogen atoms over the entire surface of the metal, and not selectively along the grain boundaries, as is observed during conventional nitriding by traditional methods. Thus, the conducted studies have shown that after electrolytic-plasma nitriding, a modified layer is formed on the surface layer of high-speed steels, consisting of a diffusion layer, which is nitrogenous martensite with finely dispersed nitrides of alloying elements. It is determined that the surface is saturated with nitrogen up to 7% (in weight%). Nevertheless, in order to verify the results obtained and to establish the regularities of the formation of the modified layer, it is necessary to study the phase transformations in the surface layers of high-speed steel during nitriding by the X-ray diffraction analysis.

Didar Yeskermessov (diko090@gmail.com)
IGI Global Platform
Downloaded: 10/3/2023 3:42:03 AM
IP Address: 91.185.25.163

4.3 Phase Transformations in the Surface Layers of High-Speed Steels During Electrolytic-Plasma Nitriding

One of the most effective ways to improve the physical and mechanical properties of the surface layer of high-speed steels is the development of optimal nitriding modes. It is practically impossible to choose the necessary nitriding regimes without a detailed study of phase transformations in the material during nitriding. Figure 33 shows X-ray diffraction patterns of R6M5 steel before and after nitriding. X-ray diffraction analysis showed that in the initial state, that is, after standard heat treatment, the R6M5 steel structure contains martensite (α-phase) and M_6C, MC carbides. After nitriding, broadening, a decrease in intensity, and a shift towards smaller Bragg angles of the interference line (110) of the α-phase are observed, which indicates the formation of a solid solution of nitrogen in iron, i.e. internal nitriding zone. On the diffraction patterns of R6M5 steel samples nitrided at 500°C and 550°C, interference lines of the Fe_4N phase were found.

Figures 34 and 35 show X-ray diffraction patterns of R9 and R18 high-speed steels. X-ray diffraction analysis showed that in the initial state, that is, after standard heat treatment, the structure of R9 steel contains martensite (α-phase) and carbides M_6C, MC. And in the structure of steel R18 there are - martensite (α-phase) and M_6C carbides. After nitriding, interference lines of the Fe_4N phase were found on the diffraction patterns (Figure 34 b, 35 b). Thus, it can be established that the diffusion layer of high-speed steels R6M5, R9 and R18 consists of an α-phase with excess nitrides - Fe_4N, formed during cooling in the surface layer. Since metallographic analysis showed that after nitriding, a modified layer is formed on the surface of high-speed steels, consisting only of a diffusion layer. The results of X-ray diffraction analysis are shown in Table 7. The analysis showed that the main carbides in the studied steels are M_6C and MC carbides. It has been determined that M_6C type carbides are most optimally combined with the Fe_3W_3C phase, and MC type carbides correspond to the VC phase. Quantitative analysis showed that after nitriding, there is no noticeable change in the content of carbide phases. At the same time, it was determined that the content of the γ'-phase (Fe_4N) in steels R9, R6M5 and R18 is 5.5%, 3.9% and 3.7%, respectively.

Using the method of scanning electron microscopy, it was found that finely dispersed nitrides of alloying elements are formed in the surface layer of steels after nitriding. However, X-ray diffraction studies did not reveal nitride phases of alloying elements, possibly due to their low concentration and small size. Perhaps this is also due to the formation of finely dispersed nitrides, the distribution of which over the layer does not ensure their detection with the existing sensitivity of X-ray diffraction phase analysis. In this case, to study these particles, it is necessary to apply the method of transmission electron microscopy. Thus, the main advantage of nitriding by electrolytic-plasma action is the possibility of obtaining a diffusion hardened layer from the α-phase with excess Fe_4N nitrides (γ'-phase), in contrast to gas nitriding in ammonia, where a nitride layer is formed, consisting of two γ'- and ε-phases, which is a source of internal stresses at the phase boundary and causes brittleness and flaking of the hardened layer of cutting tools during operation (Arzamasova, & Mukhina,, 2001; Kuksenova et al., 2004; Skakov, Rakhadilov, & Scheffler, 2013; Skakov, Rakhadilov, & Rakhadilov, 2014). The formation of a diffusion layer of nitrogenous martensite in the surface layers will have a positive effect on the performance properties of a cutting tool made of R6M5 high-speed steel. For example, iron nitrides have a higher heat capacity than iron (Skakov, Rakhadilov, Batyrbekov, & Manapbayeva, 2014). This creates favorable conditions for preventing temperature flashes on the surface of the cutting tool.

Didar Yeskermessov (diko090@gmail.com)
IGI Global Platform
Downloaded: 10/3/2023 3:42:03 AM
IP Address: 91.185.25.163

Figure 33. XRD patterns of samples of R6M5 high-speed steel before (a) and after nitriding at temperatures of 450°C (b), 500°C (c), and 550°C (d)

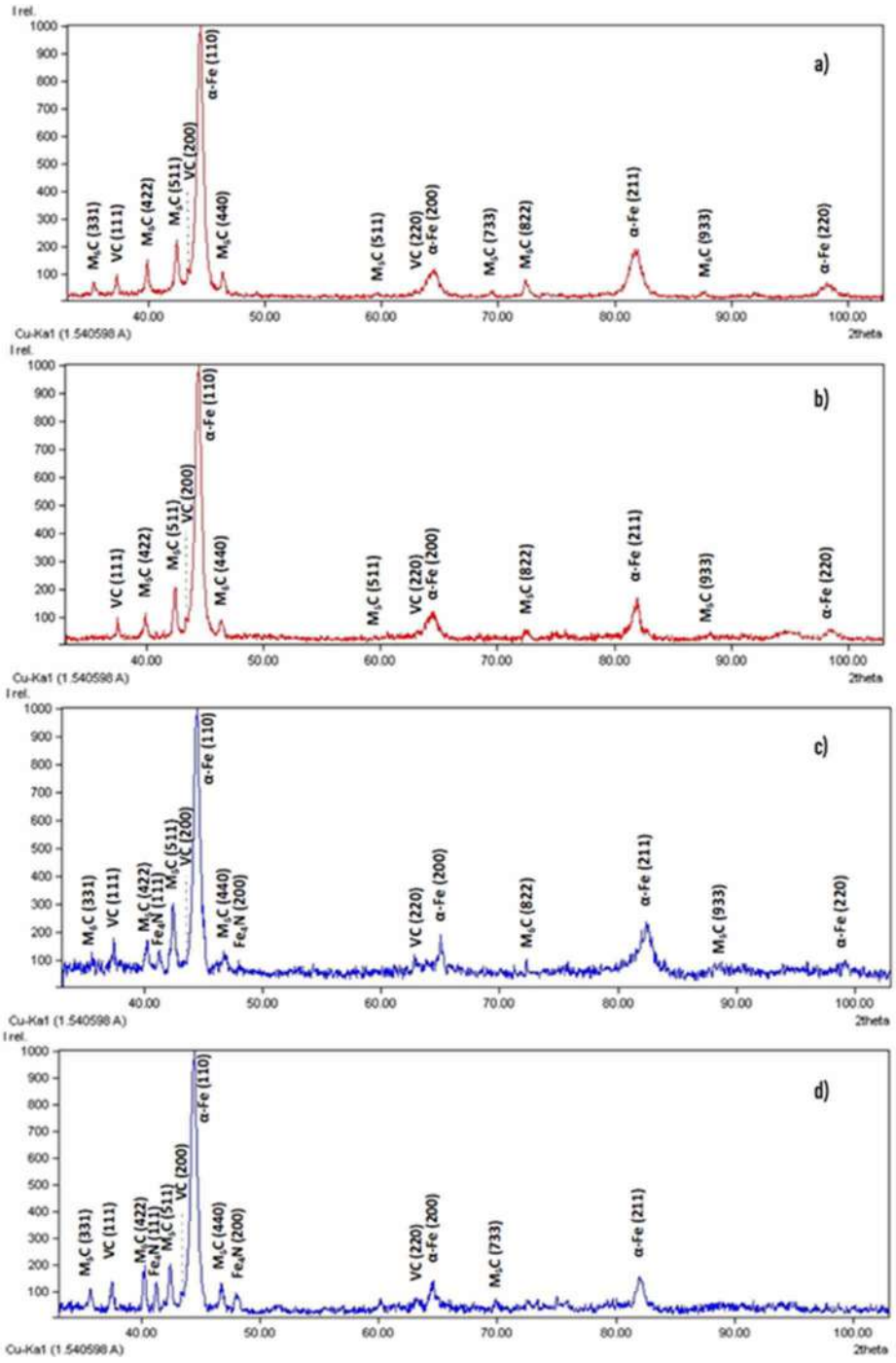

Didar Yeskermessov (diko090@gmail.com)
IGI Global Platform
Downloaded: 10/3/2023 3:42:03 AM
IP Address: 91.185.25.163

Figure 34. X-ray diffraction patterns of high-speed steel R9 before (a) and after (b) nitriding at a temperature of 550°C

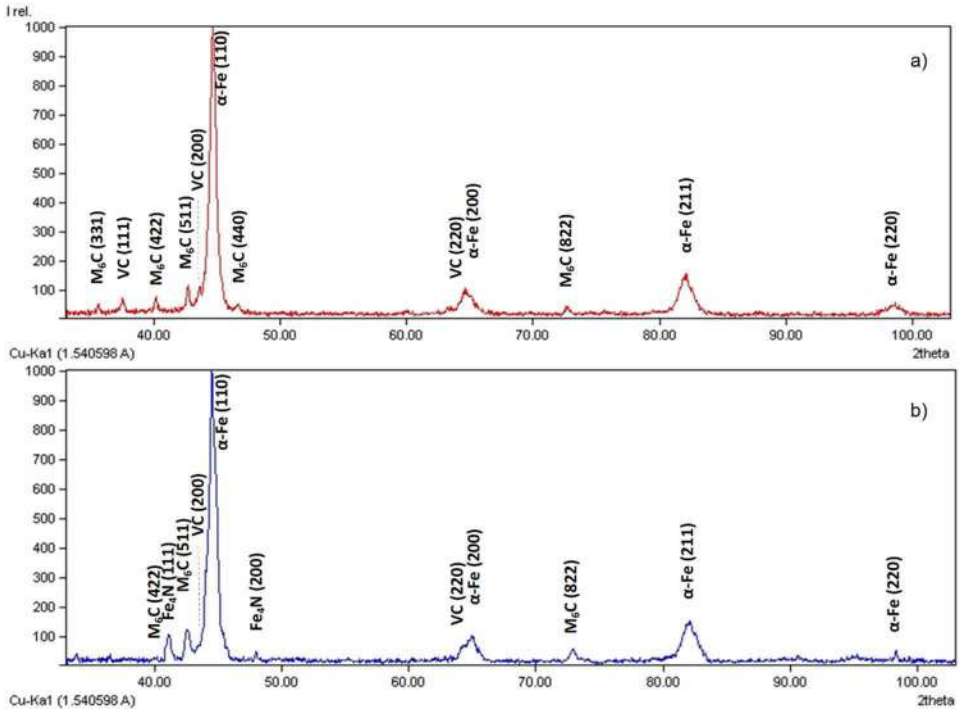

Figure 35. X-ray diffraction patterns of high-speed steel R18 before (a) and after (b) nitriding at a temperature of 550°C

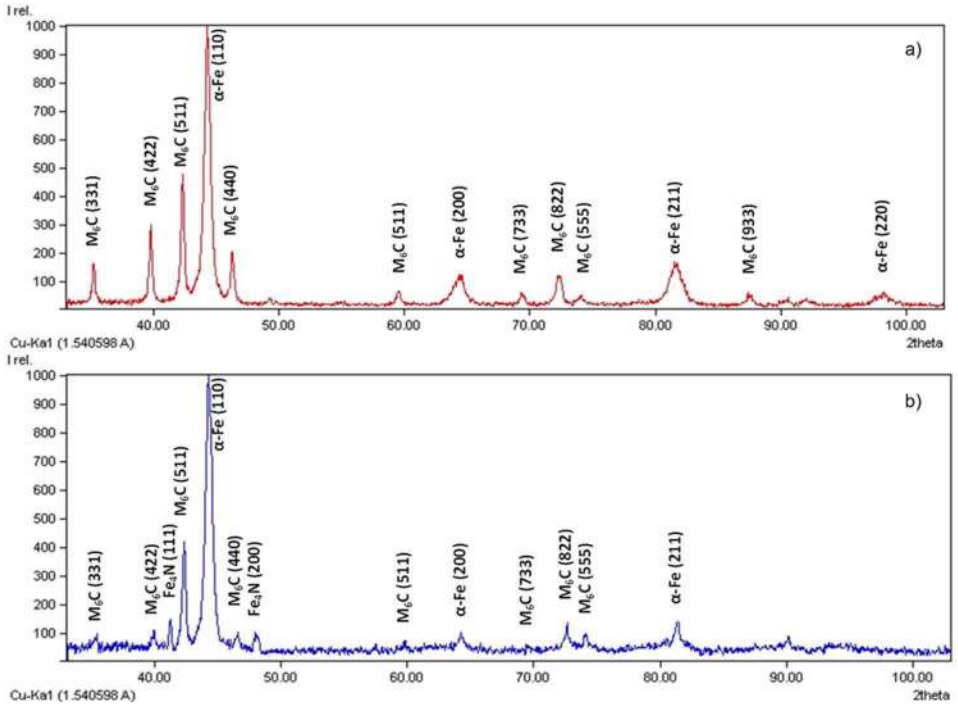

Didar Yeskermessov (diko090@gmail.com)
IGI Global Platform
Downloaded: 10/3/2023 3:42:03 AM
IP Address: 91.185.25.163

4.4 Studies of the Fine Structure and Second Phases of High-Speed Steel After Electrolytic-Plasma Nitriding

Intensive progress in the physical materials science of steels created the foundations of the science of their strength, which continue to be intensively developed at the present time. At the same time, a number of important issues in the physical materials science of steels have not been adequately developed. In this regard, it is necessary to note the clearly insufficient attention to the fine structure of steels and its evolution during chemical-thermal treatment. This is especially true for high speed steels. Of particular interest is the formation of secondary phases in the surface layers of high-speed steels during plasma nitriding. As already noted, the structure of high-speed steel in the initial (heat-treated) state is tempered martensite with hard carbides. X-ray diffraction analysis established that Fe_4N nitride is formed in the surface layer after nitriding. Also, by scanning electron microscopy, it was determined that after nitriding at 550°C, fine nitrides of alloying elements are formed in the surface layer of high-speed steel. However, X-ray diffraction analysis did not show the presence of nitrides of alloying elements, possibly due to the low concentration and shallow depth of their formation (Skakov, & Rakhadilov,, 2013; Usmanov & Yakunin, 1984). In this regard, in order to reveal the crystal structures of the second phases formed during nitriding, this section examines the fine structure of R6M5 steel samples before and after nitriding at 550°C for 7 min using transmission electron microscopy.

Previously, X-ray diffraction studies, the results of which are discussed in (Maksakova et al., 2016; Skakov, Rakhadilov, and Karipbaeva, 2013; Skakov and Rakhadilov, 2012), showed that the structure of R6M5 steel in the initial state, i.e. after standard heat treatment, it consists of an α'-phase based on iron with special carbides M_6C and MC. The results of TEM studies confirm these data. The fine structure of R6M5 steel, observed by electron microscopy, is shown in Figure 36 It is clearly seen that the main phase is the α'-phase (martensite) and that carbide particles of globular morphology occupy a significant part of the volume. Morphologically, the carbide phases are more clearly faceted. It should be noted that the α'-phase has a body-centered cubic lattice, a crystal lattice, and can be solid solutions based on iron of interstitial (C, N, B, S, P, etc.) and substitution atoms (Si, Mn, Ni, Cr, Mo, V, W, etc.) at the same time. In the case of the steel under study, the α'-phase is possibly a substitutional solid solution of Cr, W and Mo and an interstitial solid solution of carbon. After nitriding, the martensite structure is more fragmented and is characterized by a defective substructure. The resulting imperfection, apparently, approaches the defectiveness of the grain boundaries. The possibility of forming such a substructure of grains during electrolytic-plasma nitriding is provided by the increased energy state of the surface and subsurface layers, which are bombarded with ions and neutral atoms of low-temperature plasma throughout the treatment.

Figure 37 shows electron microscopic images of the fine structure of R6M5 steel before nitriding and their microdiffraction patterns obtained from the matrix and M_6C and MC carbides and their indexing schemes. Microdiffraction studies have confirmed that the main carbides in steel are M_6C carbide, which has a complex FCC crystal lattice and Fd_3m space group, and MC carbide, which has an FCC NaCl-type lattice and Fm_3m space group.

Figure 38 shows electron microscopic images of the fine structure of R6M5 steel after nitriding at 550^0C. It was found that after nitriding, particles are formed in the surface layer in the form of thin layers (Figure 4.24 a, indicated by arrows) and finely dispersed precipitates of irregular shape (Figure 4.24 b, indicated by arrows), randomly located in the martensitic matrix. Thus, the formation of fine precipitates of secondary phases in the surface layer after nitriding was confirmed by the electron microscopic method.

Didar Yeskermessov (diko090@gmail.com)
IGI Global Platform
Downloaded: 10/3/2023 3:42:03 AM
IP Address: 91.185.25.163

Table 7. Results of X-ray diffraction analysis of steel samples before and after electrolytic-plasma nitriding

Sample	Detected Phases	Volume Fraction of Phases, %	Lattice Parameters, nm	Size Coherent Scattering Region, nm
R9, initial	α-Fe	81	0,28680	23,30 (all ref)
	M_6C	11,8	1,10543	26,14 (100)
	MC	7,2	0,41566	25,01 (100)
R9, nitrided	α-Fe	76,6	0,28712	34,90 (all ref)
	M_6C	11.4	1,10804	32.79 (100)
	MC	6,5	0,41625	17.43 (100)
	γ'-Fe_4N	5.5	0.37945	27.43 (100)
R6M5, initial	α-Fe	75,2	0,28781	19,20 (all ref)
	M_6C	13,7	1,10867	38,77 (all ref)
	MC	11,	0,41663	18,72 (100)
R6M5, nitrided	α-Fe	73,2	0,28784	26,53 (all ref)
	M_6C	13,1	1,10818	40,98 (100)
	MC	9,8	0,41576	16,61 (100)
	γ'-Fe_4N	3,9	0.37923	40,22 (100)
R18, initial	α-Fe	72,2	0,28720	50,36 (all ref)
	M_6C	27,8	1,10429	39,43 (100)
R18, nitrided	α-Fe	70,5	0,28822	41,68 (all ref)
	Fe_3W_3C	25,8	1,10472	106,98 (100)
	γ'-Fe_4N	3,7	0.37756	97,44 (100)

Figure 36. Electron microscopic image of the fine structure of R6M5 steel before (a) and after (b) nitriding at 550^{0}C

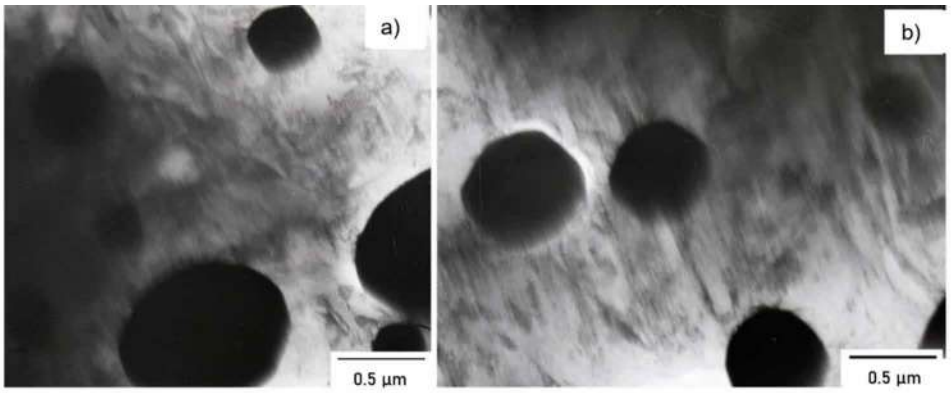

Didar Yeskermessov (diko090@gmail.com)
IGI Global Platform
Downloaded: 10/3/2023 3:42:03 AM
IP Address: 91.185.25.163

Figure 37. Electron microscopic images of the fine structure of R6M5 steel before nitriding and their microdiffraction patterns obtained from the matrix (a) and M_6C (b) and MC (c) carbides and their indexing scheme

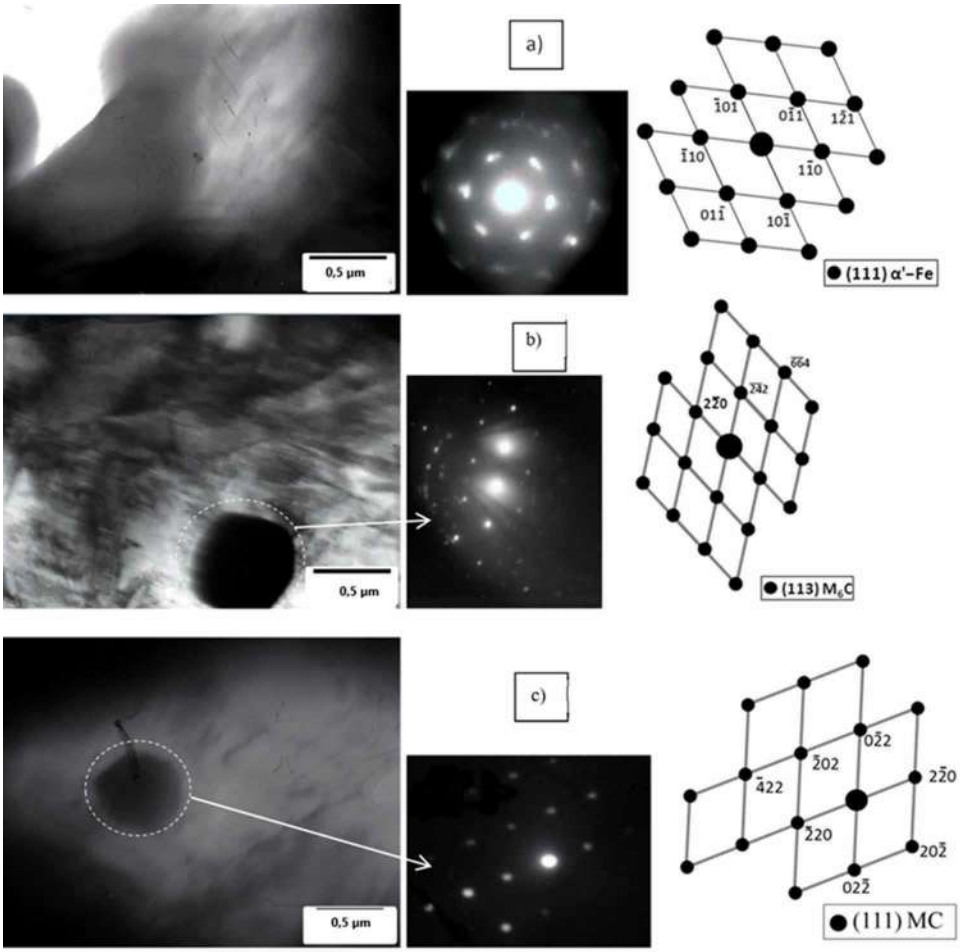

Figure 38. Electron microscopic images of the fine structure of R6M5 steel after nitriding at 550^{0}C (arrows mark particles of the γ/-phase (a) and fine precipitates of secondary phases (b))

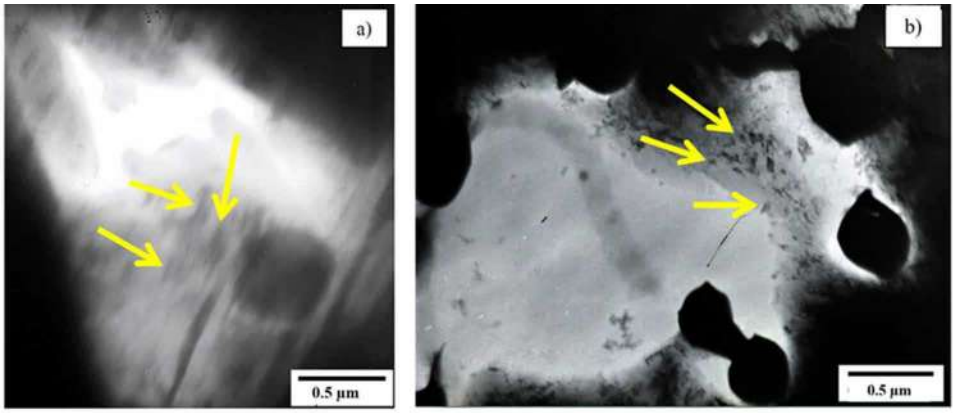

Didar Yeskermessov (diko090@gmail.com)
IGI Global Platform
Downloaded: 10/3/2023 3:42:03 AM
IP Address: 91.185.25.163

Electron microscopic images of the fine structure of R6M5 steel after nitriding and their microdiffraction patterns obtained from carbide, matrix and fine nitrides and their indexing schemes are shown in Figure 39. X-ray diffraction analysis determined that after nitriding at 500 and 550^{0}C, γ'-nitride is formed in the structure of high-speed steels. From the electron microscopic image obtained from the surface of R6M5 steel nitrided at 550°C, one can see particles of γ'-nitrides in the form of thin layers. The indexing of the microelectron diffraction pattern shown in Figure 39 showed that the formed thin layers (plate-shaped particles) are iron nitrides of the composition Fe_4N (γ'-phase). Iron nitrides of composition Fe_4N (γ'-phase) are formed upon cooling. Thus, in the process of cooling to room temperature, due to the low solubility of nitrogen in the α-phase at low temperatures, a strongly supersaturated solid solution appears. And this leads to the precipitation, preferably on dislocations, of α''-nitride particles of a lamellar shape with a certain orientation, which are subsequently transformed into γ'-nitrides (Pastukh,, 2006). The mechanism corresponds to the release of carbon and the formation of carbides during the tempering of hardened steel. Electron microscopic studies have shown that after nitriding, fine precipitates with a size of 50–100 nm are formed on the surface of R6M5 steel, which are in a nanocrystalline state.

Microdiffraction analysis also showed that the crystal structure of these finely dispersed precipitates corresponds to chromium nitride of the co imposition CrN, which has a FCC lattice of the NaCl type and space group Fm3m. The formation of such CrN nitrides in the surface layers of R6M5 and X210Cr12 tool steels after nitriding was observed earlier in (Rakhadilov et al., 2011; Shestopalova, 2011). The formation of CrN nitride in high-speed steels is possible in the presence of fluctuations with a sufficiently high concentration (Ramazanov & Vafin, 2011). The presence of concentration fluctuations in solutions in general and in solid solutions in particular is beyond doubt and has been confirmed experimentally in many systems. Under conditions when fluctuations of chromium occur in a medium supersaturated with carbon, they are stabilized at the initial stage due to interaction with carbon (Permyakov et al., 1972). This is all the more likely that chromium is a carbide-forming element. Stabilization of fluctuations by carbon creates prerequisites during nitriding for the transformation of the chromocarbon cluster into the nitride phase. The latter is natural in connection with the higher affinity of chromium for nitrogen compared with the affinity for carbon. Thus, we have characterized all secondary phases formed after nitriding in the surface layers of R6M5 high-speed steel. These studies are practically significant, because the mechanical properties of high-speed steel are largely determined by the structure and composition of the secondary phases (Ivanov et al., 2002). It is assumed that the formation of the γ'-phase (Fe_4N) and finely dispersed CrN nitride leads to an increase in the hardness and wear resistance of R6M5 steel.

4.5 Mechanisms That Provide High Wear Resistance of the Nitrided Layer of High-Speed Steels

In the previous subsections of this section, it was shown that high-speed steels R6M5, R9 and R18 after electrolytic-plasma nitriding have high wear resistance and increased microhardness. As is known (Barabash et al., 1974), the main criterion for the wear resistance of nitrided steels is their high hardness. However, the surface layer structure corresponding to maximum wear resistance and the structure corresponding to maximum hardness are not always the same. Wear resistance is a structurally sensitive characteristic. Therefore, it is not always necessary to strive to achieve the maximum hardness of steel during nitriding. In the process of friction, the structure and properties of the material of the surface plastic deformation zone change, and a friction structure is created that controls the degree of wear. In turn, the structure of the deformation zone during friction depends on the initial structure of the nitrided layer. Therefore,

Didar Yeskermessov (diko090@gmail.com)
IGI Global Platform
Downloaded: 10/3/2023 3:42:03 AM
IP Address: 91.185.25.163

Figure 39. Electron microscopic images of the fine structure of the surface layer of R6M5 steel formed after nitriding and their microdiffraction patterns obtained from carbide (a), matrix (b), and fine nitrides (c) and schemes for their indexing

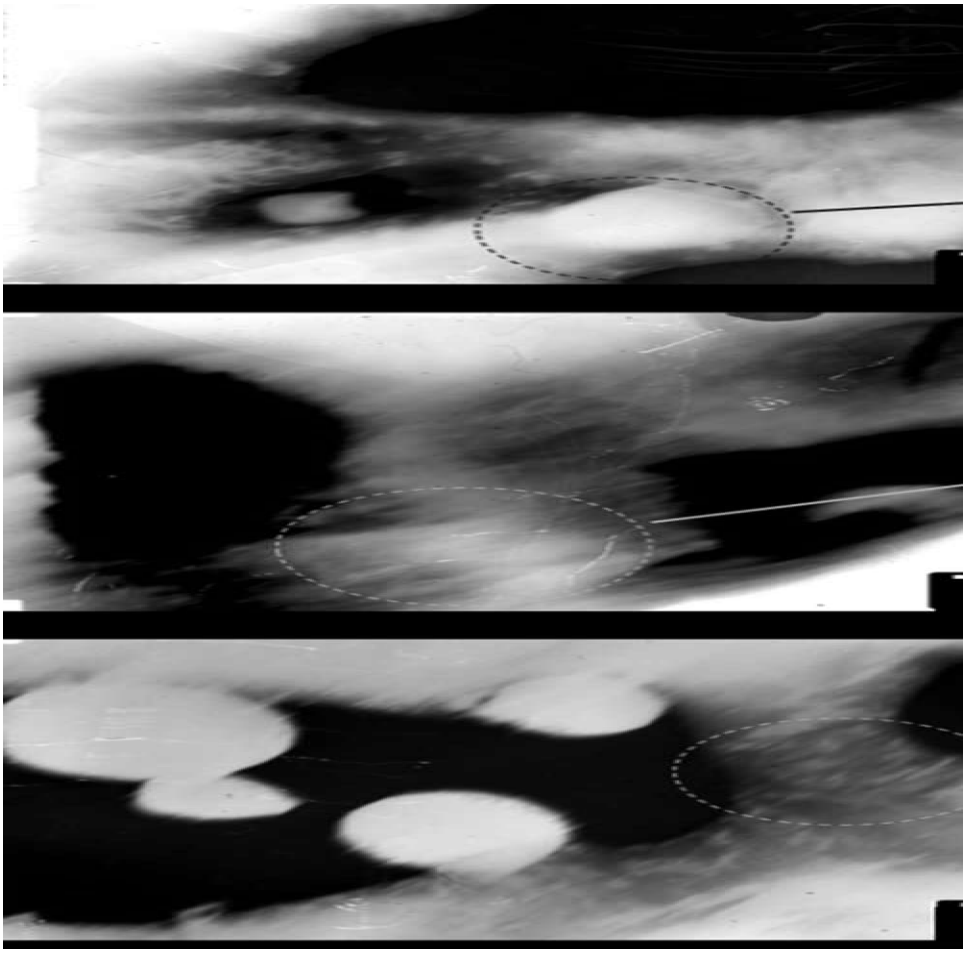

Table 8. Experimental data on the structure and tribological characteristics of the nitrided layer of R6M5 steel

$t_{azot.}$,°C	Characteristics					
	h, μm	Phase Composition	Hμ, MPa	f	j, 10^4 mm^3/Hm	K_{wr}
initial	-	αc', M6C, MC	7,7	6,8±0,4	6,52	2,04
450°C, 7 min	25	αN', M6C, MC	11,75	5,5±0,5	4,85	2,24
500°C 7 min	35	αN', γ', M6C, MC	12,15	5,3±0,2	2,23	2,58
550°C 7 min	40	αN', γ', NC, M6C, MC	12,4	4,1±0,2	1,21	2,64

Didar Yeskermessov (diko090@gmail.com)
IGI Global Platform
Downloaded: 10/3/2023 3:42:03 AM
IP Address: 91.185.25.163

there is a connection between the conditions of pre-treatment of steel, which forms a certain structural state of the surface layer, the conditions of nitriding, which create the structural state of the nitrided layer characteristic of them, and the tribotechnical characteristics of the structural state of the deformation zone during friction. Determining this relationship is the key to solving the problem of optimizing the technological process of nitriding for processing materials for tribotechnical products. In addition, there is no consensus in the literature on the structure and causes of a sharp change in the properties of the nitrided layer on high-alloy steels of various compositions. A correct understanding of the mechanisms of formation and hardening of the nitrided layer makes it possible to assume the structure of the layer and to foresee the changes that can occur with it depending on the nature of the alloying. In this regard, it is necessary to find out the main mechanisms that ensure high wear resistance of the nitrided layer of high-speed steels. The properties are determined by the nature of the structure formed during nitriding and by the transformations that take place in the layer upon cooling. We have carried out a systematic study of the change in tribological characteristics (wear intensity and friction coefficient) of the nitrided layer of high-speed steels depending on the nitriding temperature and holding time during nitriding, as well as on the test temperature. The paper shows that by varying the nitriding temperature, it is possible to obtain different structural states and different phase composition of the surface modified layer. Table 8 shows data on the structure and tribological characteristics of the nitrided layer obtained at nitriding temperatures of 450, 500 and 550°C. The experimental data clearly illustrate the correlation between the structural and tribological characteristics of the nitrided layer.

Note - h is the thickness of the nitrided layer; Hμ - microhardness; f - is the coefficient of friction; j - is the wear rate; K_{wr} - relative wear resistance to abrasive wear. From the generalized data given in the table, the dependence of the wear intensity of the modified layers on the structural-phase states is clearly traced. The wear of the modified layer consisting of the nitrided α'-phase (nitrogenous martensite) obtained after nitriding at 450°C is significantly lower than that of the layer consisting of the nitrided α'-phase with excess γ'-phase particles obtained after nitriding at 500°C. Particularly noteworthy are the results on the wear resistance of the modified layer obtained after nitriding at 550°C. This layer, consisting of a nitrided α'-phase with γ'-phase particles and fine particles of secondary phases, showed increased wear resistance when tested both at room temperature and at high test temperatures. It is known from (Barabash et al., 1974; Du et al., 2002) that the effects of an increase in hardness and wear resistance are directly related to the size and number of dispersed inclusions that are formed during the saturation of the steel surface with nitrogen. In this case, a special role is given to finely dispersed particles of secondary phases of CrN composition, which are in the nanocrystalline (ultrafinely crystalline) state. Under such states, the CrN particles turn out to be coherently bound to the matrix. Similar results were obtained in (Permyakov et al., 1972; Ramazanov & Vafin, 2011), where a significant amount of dispersed CrN particles coherently bonded to the matrix was found on chromium-alloyed steels.

Thus, the totality of experimental results on the evaluation of the parameters of the structural state and wear resistance suggests that in ensuring high wear resistance of nitrided high-speed steel under sliding friction, an important role belongs under the surface layer with dispersed nitrides and the change in its substructure, in general, has three main components: fineness particles, the level of microdeformation of the crystal lattice, a component of microdiffusion processes. Therefore, on the basis of experimental data, it can be said that a special role in the processes of surface hardening is assigned to finely dispersed particles of secondary phases of the CrN composition. Since, according to modern concepts of the dislocation nature of plastic deformation (Chaus & Hudakova, 2009), dispersed precipitates of secondary phases are effective barriers to moving dislocations and contribute to metal strengthening. The high wear

Didar Yeskermessov (diko090@gmail.com)
IGI Global Platform
Downloaded: 10/3/2023 3:42:03 AM
IP Address: 91.185.25.163

resistance of the nitrided layer was also confirmed by fractographic analysis, which showed that in the initial state, crumbling particles of special M6C carbide are observed on the friction surface, which have an abrasive effect on the surface of the mating sample, the wear of which is significant. However, such particles are not observed on nitrided friction surfaces, which may be due to the formation of a nitrogenous α'-phase, as well as excess particles of the γ'-phase and finely dispersed particles of secondary phases. Thus, summarizing the data available in the literature and the results obtained in this study, we can formulate the following conclusions:

- a modified layer consisting of a nitrided α'-phase with a fragmented substructure, M_6C and MC carbides, excess particles of the γ'-phase (Fe_4N) and finely dispersed chromium nitride CrN, obtained after nitriding at 550°C, is wear-resistant, hard, antifriction and has the effect of extremely high wear resistance at high temperatures;
- the main mechanisms that ensure high wear resistance of the nitrided layer of high-speed steels obtained by electrolytic-plasma nitriding are, firstly, the formation of a modified layer consisting only of a diffusion zone (i.e., an internal nitriding zone), and secondly, precipitation during cooling in diffusion layer, preferably on dislocations of γ'-nitrides of lamellar shape; thirdly, the formation of fine particles of chromium nitride composition CrN in the diffusion layer due to fluctuations of chromium.

Conclusions for Section 4

Thus, based on the analysis of the research results obtained in the section, the following conclusions can be drawn:

1. It has been established that the structure of high-speed steels R6M5, R9 and R18 in the initial state, i.e. after standard heat treatment, consists of α'-phase and special carbides. At the same time, carbides of the M_6C and MC types are present in the structure of steels R6M5 and R9, and only carbides of the M_6C type are present in the structure of steel R18. Using X-ray diffraction analysis and EBSD analysis, it was found that carbides of the M_6C type, which have a complex FCC crystal lattice and space group Fd_3m, correspond to the Fe_3W_3C composition, and MC-type carbides, which have a cubic crystal lattice and space group Fm3m, correspond to the VC composition.
2. Metallographic analysis has established that during electrolytic-plasma nitriding, the process of diffusion saturation of steel with nitrogen occurs with accelerated formation of a modified layer, consisting only of a well-developed zone of internal nitriding, i.e. diffusion layer.
3. X-ray diffraction analysis has established that on the surface of steels R9, R6M5 and R18 after electrolytic-plasma nitriding at a temperature of 450°C, a diffusion layer is formed, consisting of the α'-phase ($Fe_{\alpha(N)}$), and at temperatures of 500°C and 550 °C along with the α'-phase, the γ'-phase (Fe_4N) is formed.
4. It was found that after electrolytic-plasma nitriding at a temperature of 550°C for 7 minutes, fine precipitates form on the surface of high-speed steels R 9, R6M5 and R18. By microdiffraction analysis, it was found that these fine precipitates are particles of chromium nitride of composition CrN with an FCC lattice NaCl type.

Didar Yeskermessov (diko090@gmail.com)
IGI Global Platform
Downloaded: 10/3/2023 3:42:03 AM
IP Address: 91.185.25.163

5. It has been established that after electrolytic-plasma nitriding at a temperature of 550°C for 7 minutes, the structure of R6M5 steel consists of nitrogenous martensite with a fragmented substructure, carbides (M_6C and MC), Fe4N nitride, and finely dispersed CrN nitride.
6. It has been established that the main structural factors affecting the increase in the tribological properties of high-speed steels during electrolytic-plasma nitriding are, firstly, the formation of a modified layer consisting only of a diffusion zone (i.e., an internal nitriding zone), and secondly, the formation of diffusion layer of excess particles of the γ'-phase, thirdly, the formation in the diffusion layer of fine particles of chromium nitride composition CrN;
7. It was determined that the modified layer, consisting of a nitrided α'-phase with a fragmented substructure, M_6C and MC carbides, excess particles of the γ'-phase (Fe_4N) and finely dispersed CrN chromium nitride, obtained after nitriding at 550°C, are wear-resistant, hard, antifriction and have the effect of extremely high wear resistance at high temperatures. The main mechanisms that ensure high wear resistance of the nitrided layer of high-speed steels obtained by electrolytic-plasma nitriding are, firstly, the formation of a modified layer consisting only of a diffusion zone (i.e., an internal nitriding zone), and secondly, precipitation during cooling in a diffusion layer, preferably on dislocations of plate-like γ'-nitrides.

CONCLUSION

Based on the results of this study, the following conclusions can be drawn:

1. It has been established that during electrolytic-plasma nitriding of high-speed steels, the process of diffusion saturation of steel with nitrogen occurs with accelerated formation of a modified layer, consisting only of a well-developed zone of internal nitriding, i.e. diffusion layer. It was found that after electrolytic-plasma nitriding at a temperature of 450°C, a modified layer is formed on the surface of high-speed steel, consisting of α'-phase ($Fe_{\alpha(N))}$ and carbides (M_6C and MC), with an increase in the nitriding temperature from 450^0C to 500^0C in the modified layer particles of the γ′-phase (Fe_4N) are formed, and at a nitriding temperature of 550^0C, finely dispersed particles of chromium nitride of composition CrN with an FCC lattice of the NaCl type are formed.
2. As a result of electrolytic-plasma nitriding at 550°C, samples of high-speed steels, there was an increase in surface microhardness by 1.6 times. It has been experimentally established that the main increase in the hardness of the diffusion layer occurs after nitriding at 550°C, which is the result of the precipitation of finely dispersed nitrides in the supersaturated α-phase, which distort the crystal α-lattice. It has been determined that the main factors influencing the increase in the microhardness of R6M5 steel are the formation of a diffusion layer of nitrogenous martensite, as well as the formation of fine particles of chromium nitride with the composition CrN in the surface layers;
3. It has been established that after electrolytic-plasma nitriding, the microhardness, wear resistance and resistance to abrasive wear of high-speed steels increase, depending on the nitriding mode. After electrolytic-plasma nitriding at a temperature of 550°C for 7 minutes, microhardness increases by 1.6 times, wear resistance increases by 2 times, and abrasive wear resistance increases by 1.3 times.

Didar Yeskermessov (diko090@gmail.com)
IGI Global Platform
Downloaded: 10/3/2023 3:42:03 AM
IP Address: 91.185.25.163

4. It has been established that the main mechanisms that ensure high wear resistance of the nitrided layer of high-speed steels obtained by electrolytic-plasma nitriding are, firstly, the formation of a modified layer consisting only of a diffusion zone (i.e., an internal nitriding zone), and secondly, precipitation in diffusion layer, preferably on dislocations of plate-like γ'-nitrides; thirdly, the formation of fine particles of chromium nitride with the composition CrN in the diffusion layer. It has been determined that the modified layer, consisting of a nitrided α'-phase with a fragmented substructure, M_6C and MC carbides, excess particles of the γ'-phase (Fe_4N) and finely dispersed chromium nitride, obtained after electrolytic-plasma nitriding at 550°C, is wear-resistant, hard, antifriction and has the property of extremely high wear resistance at high temperatures.

REFERENCES

Anel'nik, D.Ye. Polevoy, S.N., & Yevdokimov, V.D. (1981). Remont, vosstanovleniye i ispytaniye instrumenta i tekhnologicheskoy proverki: spravochnik. *Tekhnika*, 200. Kiyev.

Arshinger, I. (1982). Instrumental'nyye stali i ikh termicheskaya obrabotka: spravochnik. *Metallurgiya, 313*.

Artinger, I. (1982). Instrumental'nyye stali i ikh khimiko-termicheskaya obrabotka. *Spravochnik*, 312.

Arzamasov, B.N., Bratukhin, A.G., Yeliseyev, YU.S., & Panayoti, T.A. (1999). Ionnaya khimiko-termicheskaya obrabotka splavov. *MGTU im. Baumana*, 400.

Arzamasova, B.N., Mukhina, G.G. (2001). Materialovedeniye: uchebnik dlya vuzov. N.E. Baumana, (ed.) *Izd-vo MGTU im*. 648.

Astaf'yev A.A. (1997). Nekotoryye zakonomernosti vodorodnogo okhrupchivaniya konstruktsionnykh staley. *Metallovedeniye i termicheskaya obrabotka metallov*, (2), 5 -8.

Badisch, E., & Mitterer, C. (2003). Abrasive wear of high speed steels: Influence of abrasive particles and primary carbides on wear resistance. *Tribology International*, *36*(10), 765–770. doi:10.1016/S0301-679X(03)00058-6

Bakovets, V. V., Polyakov, O. V., & Dolgovesova, I. P. (1991). Plazmenno-elektroliticheskaya anodnaya obrabotka metallov. Novosibirsk, Nauka. Sib. otd.

Barabash R.I., Belobashskiy A.V., & Permyakov V.G. (1974). Tonkaya struktura i uprochneniye azotirovannykh volokon zheleza, legirovannogo khromom. Izvestiya vuzov. *Chernaya metallurgiya,* (10), 118–120.

Baranchikov V.I., Zharikov A.B., Yudina N.D., & Sadykhov A.I. (1990). Progressivnyye otvety i rezhimy rezaniya metallov, 400. *Mashinostroyeniye*.

Baranova L.V., & Demina E.L. (1986). Metallograficheskoye travleniye metallov i splavov: spravochnik, 256. *Metallurgiya*.

Belkin P.N. (2010). Anodnaya elektrokhimiko-termicheskaya modifikatsiya metallov i splavov. *Elektronnaya obrabotka materialov, 46*(6), 29–41.

Didar Yeskermessov (diko090@gmail.com)
IGI Global Platform
Downloaded: 10/3/2023 3:42:03 AM
IP Address: 91.185.25.163

Belkin P.N., Ganchar V.I., & Tovarkov A.K. (1986). Teploobmen mezhdu anodom i parogazovoy obolochkoy pri elektrolitnom nagreve. *Inzhenerno-fizicheskiy zhurnal. T. 51*(1), 154-155.

Belkin P.N., & Pasinkovskiy Ye.A. (1989). Termicheskaya i khimiko-termicheskaya obrabotka staley pri nagreve v rastvorakh elektrolitov. *Metallovedeniye i termicheskaya obrabotka metallov*, (5), 12 - 17.

Belkin P.P. (1997). Anodnyy nagrev v vodnykh rastvorakh. *Vestnik Kostromskogo gosudarstvennogo pedagogicheskogo universiteta*, (4), 55-58.

Belkin P.P., & Ganchar V.I. (1988). Prokhozhdeniye toka cherez parogazovuyu obolochku pri elektrolitnom elektrolitnom nagreve. *Elektronnaya obrabotka materialov*, (5), 59-62.

Belotskiy, A. V., Marchevskaya, E. I., & Permyakov, V. G. (1973). Osobennosti obrazovaniya azotistykh faz v sisteme Fe–V–N. Izv. AN SSSR. *Metally*, (3), 116–119.

Belotskiy A.V., & Permyakov V.G. (1972). O prirode vysokoprochnogo azotirovannogo sostoyaniya sloyev na legirovannom zheleze. *Zashchitnyye pokrytiya na metallakh*, (6), 83-86.

Belyy A.V., Karpenko G.D., & Myshkin N.K. (1991). *Struktura i metody formirovaniya iznosostoykikh sloyev,* 209. Mashinostroyeniye.

Boyarskaya YU.S., Grabko D.Z., & Kats M.S. (1986). *Fizika protsessov mikroidentirovaniya*, 295. Kishinev, Shtiinitsa.

Braun, E. D., Bushe, N. A., & Buyanovsky, I. A. (2001). Fundamentals of tribology (friction, wear, lubrication). In A.V. Chichinadze (ed.) Textbook for technical schools, 2nd edition. Center “Science and technology”, 778.

Braun E.D., Bushe N.A., Chichinadze A.V., & Buyanovskiy I.A. (2001). Osnovy tribologii (treniye, iznos, smazka). *Uchebnik dlya tekhnicheskikh VUZov*, 2-ye izdaniye, 778. Tsentr «Nauka i tekhnika».

Budilov V.V., Agzamov R.D., & Ramazanov K.N. (2004). Sposobnost’ vzryvnogo uprochneniya detaley. *Patent na izobreteniye Nº 2275433*, MPK 7, C21D1/09, C21D1/38. 3.

Budilov V.V., Agzamov R.D., & Ramazanov K.N. (2004). *Sposob azotirovaniya izdeliy v tleyushchem razryade s effektom pologo katoda.* Patent for invention No. 2276201, IPC 7, C23C8/36, C23C8/80.

Budilov, V. V., Agzamov, R. D., & Ramazanov, K. N. (2007). Tekhnologiya ionnogo azotirovaniya v tleyushchem razryade s polym katodom. *MiTOM*, (7), 25–29.

Chatterjee-Fisher, R., & Supova, A.B. (1990). Azotirovaniye i karbonitrirovaniye. 12. *Metallurgiya*.

Chaus, A. S. (2008). On the wear resistance of high-speed steels. *Journal of Friction and Wear*, *29*(1), 24–34. doi:10.3103/S1068366608010054

Chaus, A. S., & Hudakova, M. (2009). Wear resistance of high-speed steels and cutting performance of tool related to structural factors. In *17th International Conference on Wear of materials*. Las Vegas, USA. 10.1016/j.wear.2008.12.101

Chernyavskiy, K.S. (1977). Stereologiya v metallovedenii. 240. *Metallurgiya*.

Didar Yeskermessov (diko090@gmail.com)
IGI Global Platform
Downloaded: 10/3/2023 3:42:03 AM
IP Address: 91.185.25.163

Du, E. H., Marchie, V. V., Boerma, D. O., & Chechenin, N. C. (2002). Low-temperature extension of the Lehrer diagramand the iron-nitrogenp has ediagram. *Metallurgical and Materials Transactions*, (33), 34–39.

Duradzhi V. N., & Bryantsev I.V. (1979). O nekotorykh osobennostyakh issledovaniya magnitnogo polya na anodnyy i katodnyy protsessy. *Elektronnaya obrabotka materialov*, (5), 15 - 19.

Duradzhi V. N., & Parsadanyan A. S. (1988). *Nagrev metallov v elektrolitnoy plazme*. Kishinev, Shtiintsa.

Endryus K., Dayson D., & Kioun S. (1971). Elektronogrammy i ikh interpretatsiya. *Mir*, 56.

Fillipov, M. A., Fillipenkov, A. A., & Plotnikov, G. N. (2009). *Iznosostoykiye stali dlya otlivok*.

Geller, Y.A. (1983). *Instrumental'nyye stali,* 527. Metallurgiya.

Gerasimov, S.A., Kuksenova, L.I., & Lapteva, V.G. (2012). *Struktura i iznosostoykost' azotirovannykh staley i splavov*, 518.

Gnyusov S.F., Khazanov I.O., & Sovetchenko B.F. (2008). Primeneniye effekta sverkhplastichnosti staley v instrumental'nom proizvodstve. *Tomsk: Izd-vo nauch.-tekhn. lit*., 237.

Gol'dshmidt KH.Dzh. (1971). Splavy potrebleniya. *Mir*, 424.

Gol'dshteyn M.I., Grachev S.V., & Veksler YU.G. (1985). Spetsial'nyye stali, 408. Metallurgiya.

Gorelik S.S., Skakov YU.A., & Rastorguyev L.N. (2002). Rentgenograficheskiy i elektronno-opticheskiy analiz. *MISIS*, 360.

GOST 9450-76. (n.d.). *Measurement of microhardness by intrusion of diamond tips* [Data set].

Grigor'yev, S. (2004). Kak povysit' nadezhnost' obnaruzheniya instrumenta. *TekhnoMIR.*, *21*(3), 53–57.

Grigorevich, V. K. (1976). Tverdost' i mikrotverdost' metallov. Nauka, 230.

Grigoriev, S. N., Tabakov, V. P., & Volosova, M. A. (2011). *Tekhnologicheskiye metody povysheniya iznosostoykosti kontaktnykh ploshchadok rezhushchego instrumenta*.

Guenzel, R., Matz, W., Ivanov, Yu. F., & Rothtein, V. P. (2000). *Pulsedelectron-beamtreatmentofhigh-speedsteelcurrenttools: struchire-phase transformation and wear resistance*. 1st International Congress on Radiation Physics, high current electronics, and modification of materials, Tomsk, Russia.

Gupta, P., Tenhundfeld, G., Daigle, E. O., & Ryabkov, D. (2007). Electrolytic plasma technology: Science and engineering – an overview. *Surface and Coatings Technology*, *201*(25), 87–96. doi:10.1016/j.surfcoat.2006.11.023

Guriev A. M., Ivanov S. G., Lygdenov B. D., Zemlyakov S. A., Vlasova O. A., Kosheleva E. A., & Guriev M.A. (2009). *MPK Sposob uprochneniya detaley iz konstruktsionnykh i instrumental'nykh staley.* Patent. 2345175 Russian Federation, Nº 2007112368/02, (3), 9.

Guryev, A. M., Kozlov, E. V., & Popova, N. A. (2001). Izmeneniye fazovogo sostava i mekhanizm formirovaniya struktury perekhodnoy zony pri termotsiklicheskom borirovanii ferritno-perlitnoy stali. *Izv. Vuzov. Fizika*, (2), 58–63.

Didar Yeskermessov (diko090@gmail.com)
IGI Global Platform
Downloaded: 10/3/2023 3:42:03 AM
IP Address: 91.185.25.163

Guryev, A. M., Vlasova, O. A., & Lygdenov, B. D. (2007). Povysheniye prochnosti instrumental'nykh staley metodom termotsiklicheskogo borirovani. XVII Petersburg readings on the problems of strength, St. Petersburg, Russia.

Ivanov, Yu., Matz, W., Rotshtein, V., Günzel, R., & Shevchenko, N. (2002). Pulsed electronbeams melting of high-speed steel: Structural phase transformations and wear resistance. *Surface and Coatings Technology*, *150*(2-3), 188–198. doi:10.1016/S0257-8972(01)01542-0

Kardonina, N. I., Yurovskikh, A. S., & Kolpakov, A. S. (2010). Prevrashcheniya v sisteme Fe – N. *MiTOM*, (10), 5–15.

Kheyker D.M., & Zevin A.S. (1963). *Rentgenovskaya difraktometriya*. 540. M.:Fizmatgiz,

Khrushchov, M. M., & Babichev, M. A. (1970). *Abrazivnoye iznashivaniye*. Nauka.

Kittel, C. (1976). *Introduction to Solid State Physics*. John Wiley & Sons.

Kremnev L.S. (1985). Zaevtektoidnyye bystrorezhushchiye stali. *Metallovedeniye i termicheskaya obrabotka metallov*, (8), 24 – 25.

Kremnev, L. S. (2008). Teoriya legirovaniya i sozdaniya na yeye osnove teplostoykikh instrumental'nykh staley i splavov razlichnogo sostava. *Metallovedeniye i termicheskaya obrabotka metallov*, (11), 18–28.

Kuksenova, L. I., Lapteva, V. G., & Berezina, Ye. V. (2004). Struktura i iznosostoykost' azotirovannoy stali. *MiTOM*, (1), 31–34.

Lakhtin, Y. U. M. (1993). Sovremennoye sostoyaniye protsessa azotirovaniya. *Metallovedeniye i termicheskaya obrabotka metallov*, (JV27), 6–11.

Lakhtin, Y. U. M. (1995). Diffuzionnyye osnovy protsessa azotirovaniya. *MiTOM*, (7), 14–17.

Lakhtin, Y.M. (1995). Diffuzionnyye osnovy protsessa azotirovaniya. *Metallovedeniye termicheskaya obrabotka metallov*, (7),14-17.

Lakhtin, Y.M. (2009). *Materialovedeniye i termicheskaya obrabotka metallov: uchebnik dlya vuzov. 5-ye izd., pererab,* 448. TID Az – kniga.

Lakhtin, YU. M., & Arzamasov, B. N. (1985). Khimiko-termicheskaya obrabotka metallov: ucheb. posobiye dlya vuzov po spets. "Metallovedeniye, oborud. i tekhnologiya term, obrab. metallov. Metallurgiya, 256.

Lakhtin, YU.M., & Kogan, YA.D. (1982). Gazovoye azotirovaniye detaley mashin i instrumenta. Mashinostroyeniye, 60.

Lakhtin, Y.M., Kogan, YA.D., Shpis, G.Y., & Bemer, Z. (1991). Teoriya i tekhnologiya azotirovaniya. Metallurgiya, 320.

Lakhtin, Y.M., Neustroyev, G.N., & Ivanov, YU.P. (1973). Nizkotemperaturnoye tsianirovaniye instrumental'nykh staley. *Metallovedeniye i termicheskaya obrabotka metallov*, (12), 27-31.

Lakhtin, Y.M. & Silina, N.V. (1977). Kharakter vysokoy tverdosti legirovannogo ferrita posle azotirovaniya. *MiTOM*, 23-29.

Didar Yeskermessov (diko090@gmail.com)
IGI Global Platform
Downloaded: 10/3/2023 3:42:03 AM
IP Address: 91.185.25.163

Lazarenko, B.R., Duradzhi, V.N., & Bryantsev, I.V. (1979). O vliyanii povysheniya induktivnosti na kharakteristiki anodnogo i katodnogo protsessov. *Elektronnaya obrabotka materialov*, (5), 8 - 13.

Liu, Z.Y., Loh NH, Khor KA, & Tor S.B. Microstructure evolution during sintering of injection molded M2 high speed steel. *Mater SciEng*, -P. 46–55.

Loladze T.N. (1982). Prochnost' i iznosostoykost' rezhushchego instrumenta. *Mashinostroyeniye*, 320.

Maksakova, O. V., Plotnikov, S. V., Eskermesov, D. K., & Yurchenko, D. (2016). The effect of Si additions and deposition conditions on the structure and properties of the (Zr-Ti-Cr-Nb-Si)N coatings fabricated by vacuum-arc deposition. *Proceedings of the 6th International Conference Nanomaterials: Applications and Properties.* NAP.

Minkevich, A.N., & Suchevyanu, G. (1968). Khimiko-termicheskaya obrabotka staley v smesyakh soley, soderzhashchikh mochevinu. *Metallovedeniye i termicheskaya obrabotka metallov*, (10), 11-16.

Mirkin L.I. (1961). Spravochnik po rentgenostrukturnomu analizu polikristallov. *Gosizdat. Fiz. mat. literatury*, 863.

Moiseyev V.F., & Grigor'yev S.N. Instrumental'nyye materialy. *Izd. 2-ye*, 248. MGTUStankin.

Muras, V. S. (1955). *O svyazi mezhdu temperaturoy i napryazheniyem toka pri elektrolitnom nagreve metallov. Mashinostroitel' Belorussii*. Gosizdat BSSR.

Neustroyev G.P., Bogdanov V.V., & Ivanov YU.P. (1972). Nizkotemperaturnoye tsianirovaniye instrumental'nykh staley. *Progressivnyye metody termicheskoy i khimiko-termicheskoy obrabotki*, 89-91. Mashinostroyeniye.

Novikov, I. I. (1986). Teoriya termicheskoy obrabotki metallov. *Metallurgiya*, 480.

Parfenov, E. V., Yerokhin, A. L., & Mattews, A. (2007). Frequency response studies for the plasma electrolytic oxidation process. Surface and coatings technology. Science Direct. doi:10.1016/j.surfcoat.2007.04.044

Pastukh, I.M. (2006). *Teoriya i praktika bezvodorodnogo azotirovaniya v tleyushchem razryade*. Khar'kov, NNTS KHFTI, 364.

Pastukh, I. M., & Zdybel', A. S. (2008). Kharakteristiki obrazovaniya nitridov v stalyakh pri azotirovanii v tleyushchem razryade. OTTOM - 9: materialy mezhdunarodnoy konferentsii. Khar'kov, 62-68.

Permyakov V.G., Belotskiy A.V., & Barabash R.I. (1972). Struktura i svoystva diffuzionnoy zony pri azotirovanii khromistogo zheleza. Izvestiya vuzov. *Chernaya metallurgiya*, (40), 129–131.

Petrova L.G. (2001). Vnutrenneye azotirovaniye zharoprochnykh staley i splavov *MiTOM9*, (1), 10-17.

Petrova L.G. (2004). *Vysokotemperaturnoye azotirovaniye zharoprochnykh splavov*, (1), 18-24.

Petrova, L. G., Aleksandrov, V. A., & Zyuzin, D. M. (2003). Reguliruyemyye protsessy azotirovaniya korrozionnostoykikh staley. *Vestnik MADI*, (1), 20–26.

Petrova L.G. & Zyuzin D.M. (2005). Vysokotemperaturnoye azotirovaniye austenitnoy stali. *Uprochnyayushchiye tekhnologii pokrytiy*, (3), 29−36.

Didar Yeskermessov (diko090@gmail.com)
IGI Global Platform
Downloaded: 10/3/2023 3:42:03 AM
IP Address: 91.185.25.163

Petukhov, B. V. (2001). Statisticheskaya teoriya dvizheniya dislokatsiy pri nalichii spontannykh protsessov blokirovki-deblokirovki. *FTT*, *43*(5), 813–817.

Plotnikov, S. V., Pogrebnjak, A. D., Yerokhina, L. N., Yeskermessov, D. K., & Erdybaeva, N. K. (2016). Study of nanostructured (Ti-Zr-Nb)N coatings' physical- mechanical properties obtained by vacuum arc evaporation. *IOP Conference Series. Materials Science and Engineering*, *110*(1), 12–31. doi:10.1088/1757-899X/110/1/012031

Popilov L.YA., & Zaytseva L.P. (1963). Elektropolirovaniye i elektrotravleniye metallograficheskikh shlifov. *Metallurgiya*, 125.

Poznyak, L. A. (1996). Instrumental'nyye stali, 488. Kiyev: Naukova dumka.

Poznyak, L.A., Tishayev, S.I., & Skrynchenko, Y.M. (1977). Instrumental'nyye stali: spravochnik. *Metallurgiya*, 167.

Prokoshkin D.A. (1984). *Khimiko-termicheskaya obrabotka metallov karbonitratsiya*, Metallurgiya, mashinostroyeniye, 204.

Przhenosil B. (1969). Nitrotsementatsiya. *Mashinostroyeniye*, 212.

Rakhadilov, B. K., & Skakov, M. K. (2012). Issledovaniye tribologicheskikh svoystv stali bystrorezhushchey R6M5, uprochnennoy vysokoenergeticheskoy otsenki. *Vestnik VKGTU*, (4), 43–48.

Rakhadilov, B. K., & Skakov, M. K. (2014). Vysokoeffektivnaya tekhnologiya elektrolitno-plazmennogo azotirovaniya bystrorezhushchikh staley. *Vestnik VKGTU*, (1), 50–55.

Rakhadilov B.K., Skakov M.K., & Karipbayeva G.S. (2011). Elektrolitno-plazmennoye azotirovaniye bystrorezhushchey stali Sbornik trudov IV mezhdunarodnoy nauchno-prakticheskoy konferentsii s ispol'zovaniyem nauchnykh shkol dlya molodykh uchenykh *Innovatsionnyye tekhnologii i ekonomika mashinostroyeniya*, 151-155. Yurginskiy tekhnologicheskiy institut. Izd-vo Tomskogo politekhnicheskogo universiteta.

Rakhshtadt A.G., Bernshteyn L.M., Kurdyumov G.V., & Mes'kin V.S. (2005). Metallovedeniye i termicheskaya obrabotka stali i chuguna: spravochnik v 3 t.. *Intermet Inzhiniring,(*T.2), 528.

Ramazanov K.N., Budilov V.V., & Vafin R.K. (2010). Azotirovaniye stalirezhushchey R6M5 v tleyushchem razryade s nalozheniyem magnitnogo polya. *Uprochnyayushchiye bystrodeystvuyushchiye tekhnologii i pokrytiya*, (5), 39-42.

Ramazanov, K. N., & Vafin, R. K. (2011). Razrabotka khorosho ionno-stal'nogo azotirovaniya instrumental'noy KH12 v skreshchennykh elektricheskikh i magnitnykh polyakh. *Vestnik UGATU*, (41), 101–104.

Sablev, L. P., Andreyev, A. A., & Kunchenko, V. V. (2000). Plazmennoye azotirovaniye rezhushchego instrumenta iz bystrorezhushchey stali, 133-137. Trudy simpoziuma OTTOM, Khar'kov.

Sal'nikova S.S., & Rudman V.A. (1987). Opyt primeneniya ionnogo azotirovaniya v mashinostroyenii. *LDNTP, 20*.

Didar Yeskermessov (diko090@gmail.com)
IGI Global Platform
Downloaded: 10/3/2023 3:42:03 AM
IP Address: 91.185.25.163

Schastlivtsev V.M., Mirzayev D.A., & Yakovleva I.L. (1994). Struktura termicheski obrabotannoy stali. *Metallurgiya*, 288.

Shestopalova, L. P. (2011). Issledovaniye khimicheskogo sostava i sostava nitrid-oksidnoy zony oksiazotirovannogo sloya legirovannykh konstruktsionnykh staley. *Vestnik KHNADU*, (54), 78–81.

Skakov, M., Rakhadilov, B., & Scheffler, M. (2013). Wear-resistance increase of high speed steel surface layer. 5 World Tribological Congress. *Tribology of materials. –Wroclaw*, (3), 491.

Skakov, M. K., & Rakhadilov, B. K. (2012). Change of structure and wear-resistance of P6M5 steel for processing in electrolyte plasma. *32th All-Polish Tribology conference Autumnal school of Tribology 2012*. Wroclaw University of Technology Institute of Machine Design and Operation, Wroclaw, Poland.

Skakov, M. K., & Rakhadilov, B. K. (2013a). *Ustroystvo dlya nagrevaniya detaley v elektrolite: Patent na poleznuyu model' Respubliki Kazakhstan: MPK6 S21D 1/44 - Nº 912*. Zayavl, Byul.

Skakov, M.K., & Rakhadilov, B.K. (2013b). Modifikatsiya poverkhnosti obnaruzheniya stali instrumentom iz bystrorezhushchey al'ternativno-plazmennoy obrabotki. *Sbornik tezisov V konferentsii Sovremennyye metody v teoreticheskoy i eksperimental'noy elektrokhimii i IV konferentsii Elektrokhimicheskiye i elektrolitno-plazmennyye metody obrabotki metallov*. Ples: Izd-vo Institut khimii rastvorov im. G.A. Krestova RAN – Ivanovo.

Skakov, M. K., Rakhadilov, B. K., Batyrbekov, E. G., & Manapbayeva, A. B. (2014). Povysheniye iznosostoykosti bystrorezhushchikh staleyel ektrolitno-plazmennym azotirovaniyem. *Vestnik KazNU*, (48), 44–52.

Skakov, M. K., Rakhadilov, B. K., Batyrbekov, E. G., Sheffler, M., Manapbayeva, A. B., Ayapbergenova, G. T., & Karipbayeva, G. S. (2014). Izmeneniye rezhimov elektrolitno-plazmennogo azotirovaniya na strukturno-fazovoye sostoyaniye i iznosostoykost' stali R6M5. *Vestnik KazNTU*, *103*(3), 65–71.

Skakov, M. K., Rakhadilov, B. K., & Karipbaeva, G. S. (2013). Specifics of microstructure and phase composition of high-speed steel R6M5. *Applied Mechanics and Materials*, *404*, 20–24. doi:10.4028/www.scientific.net/AMM.404.20

Skakov, M. K., Rakhadilov, B. K., Karipbayeva, G. S., & Manapbayeva, A. B. (2014). Strukturno-fazovoye sostoyaniye bystrorezhushchey stali R6M5 posle termicheskoy obrabotki. *Vestnik KazNU*, *48*(1), 53–59.

Skakov, M. K., Rakhadilov, B. K., & Rakhadilov, M. K. (2014). Wear-resistance of nitrided W-Mo-high speed steel in abrasive wear conditions. *Key Engineering Materials*, 1117–1121.

Slovetskiy, D. I. (1991). Mekhanizmy neravnovesnykh plazmokhimicheskikh reaktsiy, Novosibirsk, Nauka. Khimiya plazmy. T.3. Nizkotemperaturnaya plazma, (3), 94-100.

Slovetskiy D.I., Terent'yev S.D., & Plekhanov V.G. (1986). Mekhanizm plazmenno-elektrolitnogo nagreva. *Teplofizika vysokoy temperatury*, (2), 353-363.

Solntseva Yu.P. (1988). Metallovedeniye i tekhnologiya metallov. *Metallurgiya*, 491.

Suminov I.V., Belkin P.N., & Epel'fel'd A.V. (2011). Plazmenno-elektrolitnoye modifitsirovaniye poverkhnosti metallov i splavov. *Tekhnosfera*, (T.1), 464.

Didar Yeskermessov (diko090@gmail.com)
IGI Global Platform
Downloaded: 10/3/2023 3:42:03 AM
IP Address: 91.185.25.163

Suminov I.V., Epel'fel'd A.V., Lyudin V.B., Krit B.L., & Borisov A.M. (2005). Mikrodugovoye oksidirovaniye, teoriya tekhnologii, oborudovaniye. *EKOMET*, 368.

Seriya. (1975). Tekhnologicheskiy protsess poverkhnostnogo uprochneniya rezhushchego instrumenta. *Informatsionnyy listok*, 10-09.

Tomilov A.P. (1968). Elektrokhimiya pishchevykh soyedineniy. Izd-vo *Khimiya*, 115.

Usmanov, K. B., & Yakunin, G. I. (1984). Vliyaniye vneshney sredy na iznos i stoykost' obnaruzheniya instrumentov. Tashkent, 158.

Ustinovshchikov, Y. U. I. (1988). *Vydeleniye vtoroy fazy v tverdykh rastvorakh.* Nauka, 172.

Utevskiy L.M. (1973). Difraktsionnaya elektronnaya mikroskopiya v metallosoderzhanii. *Metallurgiya*, 584.

Vanin, V. S. (1967). Nagrev metallov v elektrolite. *Elektrotermiya*, (55), 18–19.

Veynberga F. (1973). Pribory i metody fizicheskogo metallovedeniya, (1), 427.

Vorob'yeva, G. A., & Skladnova, Ye. Ye. (2003). Instrumental'nyye stal'nyye materialy: Instrumental'nyye i splavy. *SPb.*, (1), 100.

Yasnorodskiy I.Z. (1971). Elektrolitnyy nagrev metallov. Elektrokhimicheskaya i elektromekhanicheskaya obrabotka metallov. *Mashinostroyeniye*, 117-168.

Yelyutina O.P. (1979). Prakticheskiye voprosy ispytaniy metallov. *Metallurgiya*, 280.

Yerokhin, A. L., Nie, X., Leyland, A., Matthews, A., & Dowey, S. J. (1999). Plasma electrolysis for surface engineering. *Surface and Coatings Technology*, *122*(2-3), 73–93. doi:10.1016/S0257-8972(99)00441-7

Younesi, Y., Bahrololoom, M. E., & Fooladfar, H. (2010). Development of Wear Resistant NFSS-HA Novel Biocomposites and Study of their Tribological Properties for Orthopedic Applications. *Journal of the Mechanical Behavior of Biomedical Materials*, *3*(3), 178–188. doi:10.1016/j.jmbbm.2009.08.003 PMID:20129417

Zubtsov M.E., & Korsakov V.D. (1971). Stoykost' shtampov. *Mashinostroenie*, 200.